

UNIVERSITAT POLITÈCNICA DE CATALUNYA

Doctoral Thesis

**DECOLOURIZATION OF TEXTILE
WASTEWATER BY MANGANESE-
ALUMINIUM METALLIC PARTICLES**

by

MITRA ABOLIGHASEMABADI

Supervisors:

Eloi Pineda Soler (Universitat Politècnica de Catalunya)

Juan José Suñol Martínez (Universitat de Girona)

A thesis submitted for the degree of Doctor of Philosophy in the

PhD programme in Computational and Applied Physics

Department of Physics

BARCELONA, MAY 2019

Dedicated to the Sanchi Oil Tanker heroes.

Acknowledgments

I have a great deal of thanks for the many people who have helped me and encouraged me over these past four years during my work on this dissertation.

This dissertation is the outcome of a collaboration between the Polytechnic University of Catalonia and the University of Girona; a research effort that I feel fortunate to have been a part of.

I want to express my many thanks to Dr. Eloi Pineda for providing me with this opportunity and his unending support throughout my dissertation work. His endless efforts of monitoring myself and his tremendous contributions are highly appreciated. I was in fact introduced to this interesting area of work by Eloi. My knowledge about metastable metallic particles was garnered over time through his patient explanation. I am of course indebted to him for lending his precious time on alleviating all of my concerns on the experimental details. Aside from the research, his affirmative and cheerful character also positively influenced me.

I am thankful for the guidance of Dr. Juan Jose Suñol from the University of Girona for his support, patience, understanding, and for giving me direction. He helped me overcome many difficult problems when designing experiments, provided much support for putting many thoughts into practice, and taught me many things.

I would like to thank Dra. Luisa Escoda from the University of Girona for her help on the HPLC experiments and chemical reactions. I am also thankful to Dra. Francisca Blázquez Cano from Autonomous University of Barcelona for Toxicity experiments and also grateful to Dr. Trifon Trifonov from Centre de Recerca en Nanoenginyeria for the X-Ray diffraction, SEM and EDX experiments.

Many thanks are given to Dr. Daniel Crespo, the head of the department, who has given a lot of support and suggestions, not only in scientific research but also in my life.

I would like to thank the SUNY College of Environmental Science and Forestry and Dr. Klaus Doelle, who was an excellent host, for giving me the opportunity to do my doctoral project there. I would also like to express my deep gratitude to Dr. Siddharth G. Chatterjee. Many of the things that I learned while in Syracuse have aided me greatly in writing this thesis.

I feel rich because I have colleagues and friends in the physics department that love me and take care of me. I would like to thank Fuqiang and Wael for our discussions on the research topic. I'm also indebted to Oriol, Helena and Andrea for working on some of the

experiments. I would like to thank Ruxandra and Enrique for their organization of many experiences which made my life more interesting. I am deeply grateful to the people that I shared all of this time with in our department: Siddharth, Xieng, Leila, Miguel, Nura, Charlie, Milad and Anna.

I don't know if you can tell everything about a person from looking at his or her friends, but I know that I do have great friends. In Spain, I met many wonderful people: Joaquim, Pablo, Cristina, Alireza, Golshid, Baran, Shiva, Eve, Carlo, David, Edneide, and Zahra. And my life-long friends Helia, Neda, and Mahtab from back home are simply amazing, they have made 6,000 km and at times 10,000 km seem much less than it had any right to be.

I would like to thank my family for their constant support and love. My parents, who taught me right from wrong, and then always allowed me to choose. My brother Mohammad for his belief and faith in me, he has supported me ever since I decided to go adventuring out into the world. When my self-doubts would exceed my curiosity, my brother Ehsan carried me through with effortless grace, and I'd like to thank my sister for all her tireless support. I would also like to thank the person that has been my side, holding my hands and weathering my persian personality for two years now, Joseph.

If I have forgotten somebody, I am truly sorry, but please do not hold it against me. I know that a PhD experience is very much influenced by the people you meet and interact with. If anybody else decides to embark on such as adventure, I wish them to be at least as fortunate as I was.

Contents

Acknowledgments	i
Contents	iii
List of Figures	v
List of Tables.....	vii
Outline and research target	1
1. Introduction.....	3
1.1 The textile industry and the dyeing process.....	3
1.2 Environmental problem of textile industrial effluents linked to dyes	3
1.2.1 Relocation of the problem to emerging countries	4
1.3 Dyes.....	6
1.3.1 Dyes and pigments	6
1.3.2 Colour and constitution of the dyes	7
1.3.3 Classification of dyes	7
1.4 Dyed water treatments	13
1.4.1 Physicochemical treatments	13
1.5 Biological treatments.....	16
1.6 Metallic nanocrystalline and glassy materials	17
1.6.1 Treatment with MPs	19
1.6.2 Metallic particles to degrade the azo link	19
2. Objectives.....	23
3. Methods and materials	25
3.1 Obtaining the alloy	25
3.2 Dyes	27
3.3 Decolourization treatment.....	29
3.3.1 Preparation of the solutions	29
3.3.2 Colour analysis	30
3.4 Kinetics	34
3.5 Toxicity	35
3.6 Chemical analysis of the decolourized water	35
3.7 Analysis of the Mn-Al particles	36
3.8 Analysis of particle reusability	38
3.8.1 Recovery of particles	39
3.8.2 Particle washing	39
3.9 Biological method	40
4. Results and discussion	43
4.1 Decolourization tests of Orange II by Mn₇₀Al₃₀-30h particles.....	43
4.1.1 Effect of temperature.....	44
4.1.2 Effect of the particle dosage.....	46
4.1.3 Effect of pH.....	47
4.2 Decolourization tests of Orange II by different types of Mn-Al particles.....	49
4.2.1 Effect of the milling time	49
4.2.2 Effect of the particle composition	52
4.2.3 Comparison with Iron particles.....	61
4.3 Analysis of the decolourized water solutions	61
4.3.1 Chemical analysis of the decolourized water solutions	61
4.3.2 Toxicity of the decolourized water solutions	66
4.4 Analysis of the metallic particles after decolourization of Orange II solutions.....	67

4.5 Efficiency of Mn-Al particles on the degradation of other dye molecules	72
4.5.1 Degradation tests of Acid Black 58 dye.....	72
4.5.2 Degradation of the Orange G dye	79
4.6 Study of the reusability of the Mn-Al particles.....	83
4.6.1 Decolourization tests of Orange II with reused particles	84
4.6.2 Analysis of the reused Mn-Al particles.....	86
4.7 Comparison with bacterial treatment	93
4.8 Discussion of the decolourization reactions	96
5. Conclusions.....	99
References.....	103

List of Figures

Figure 1-2-1. Industrial wastewater pipes emerging on the beaches of the Yellow Sea	5
Figure 1-2-2. Industrial water spill with metals.....	5
Figure 1-2-3. Many of the more than 100 factories in the city of Jiangsu.....	5
Figure 1-3-1. Structure of the Mauveine dye.....	6
Figure 1-3-2. Structure of the Aniline Yellow dye.....	8
Figure 1-3-3. Structure of the Biebrich Scarlet dye.....	9
Figure 1-3-4. Structure of Phthalocyanine dye.....	10
Figure 1-3-5. Structure of Malachite Green Triarylmethane.....	10
Figure 1-3-6. Structure of sulphur dyes.....	11
Figure 1-3-7. Structure of Pigment Violet 23.....	12
Figure 1-3-8. Structure of nitro dyes.....	12
Figure 1-6-1. Diagram of degradation of the azo link of the Acid Orange II dye.....	21
Figure 3-1-1. Mechanical mill Mixer.....	26
Figure 3-3-1. Filter Titan.....	30
Figure 3-3-2. Absorbance analysis of non-decolourized solutions before adding MPs.....	31
Figure 3-3-3. Calibration straight line.....	32
Figure 3-3-4. Acid Black 58 calibration line.....	33
Figure 3-3-5. Sample of the solution with Orange II dye.....	33
Figure 3-6-1. High resolution liquid chromatograph (HPLC).....	36
Figure 3-6-2. Mass spectrometer (MS).....	36
Figure 3-6-3. Calibration Rings of Al and Mn for atomic absorption.....	36
Figure 3-7-1. Samples of MP attached on carbon stickers, prepared for the SEM analysis.....	37
Figure 3-7-2. Summary of the basic steps of the decolourizing experiments.....	38
Figure 3-8-1. MP analysed with the SEM.....	40
Figure 3-9-1. Schematic diagram depicting the pilot scale trickling filter.....	41
Figure 4-1-1. Orange II colourant absorbance spectrum at a concentration of 40 mg L ⁻¹	43
Figure 4-1-2. Absorbance change of the Orange II dyed solution.....	44
Figure 4-1-3. Kinetics of the reaction at different temperatures.....	45
Figure 4-1-4. Arrhenius Equation.....	45
Figure 4-1-5. Absorbance changes of the Orange II dye.....	46
Figure 4-1-6 : Kinetics of the reaction with a different amount of MPs.....	47
Figure 4-1-7. Absorbance changes of Orange II dyed solutions.....	48
Figure 4-1-8. Kinetics of the reaction with different pH.....	49
Figure 4-2-1. Absorbance change of the Orange II dye.....	49
Figure 4-2-2. SEM images of different Mn ₇₀ Al ₃₀ MPs produced by milling s.....	50
Figure 4-2-3. X-ray diffraction pattern.....	51
Figure 4-2-4. Kinetics of the reaction with different Mn ₇₀ Al ₃₀ MPs produced.....	52
Figure 4-2-5. Degradation of the Orange II dye with MP Mn ₅₀ Al ₅₀ 30h.....	52
Figure 4-2-6. Degradation of the Orange II dye with MP Mn ₇₀ Al ₃₀ 30h.....	52
Figure 4-2-7. Degradation of Orange II dye with Mn 30h.....	53
Figure 4-2-8. Degradation of Orange II dye with Al 30h.....	53
Figure 4-2-9. Experimentally obtained decolourization kinetics.....	53
Figure 4-2-10. Saturation concentration.....	54
Figure 4-2-11. SEM of the Mn ₇₀ Al ₃₀ particles.....	55
Figure 4-2-12. SEM of the Mn ₅₀ Al ₅₀ particles at three different magnification.....	55
Figure 4-2-13. SEM of the Mn particles at three different magnifications.....	55
Figure 4-2-14. SEM of the Al particles at three different magnifications.....	55
Figure 4-2-15. Compositional analysis of MP Mn ₇₀ Al ₃₀	56
Figure 4-2-16. Mean and error of the atomic percentage of C, Al, Mn and O.....	56
Figure 4-2-17. Compositional analysis of MP Mn ₅₀ Al ₅₀	57
Figure 4-2-18. Compositional analysis of MP Mn.....	57
Figure 4-2-19. Compositional analysis of MP Al.....	58
Figure 4-2-20. Normalized reaction time as function of the percentage of manganese MP.....	59
Figure 4-2-21 Kinetics of the reactions.....	60
Figure 4-2-22 Kinetics of the reactions.....	60
Figure 4-3-1. Ellipse profile of the HPLC.....	62
Figure 4-3-2. HPLC eluate profile of the solution with Orange II.....	63
Figure 4-3-3. The mass spectra.....	64

Figure 4-3-4. Scheme of the degradation of azo bonds using metallic particles of Mn-Al.....	65
Figure 4-3-5. Amount of Mn or Al.....	65
Figure 4-4-2. Particle surface morphology.....	67
Figure 4-4-3. Image of the liquid used for the washing of particles.....	68
Figure 4-4-4. Morphology of the Mn ₅₀ Al ₅₀ -60h particles.....	69
Figure 4-4-5. Morphology of the Mn ₅₀ Al ₅₀ -60h particle.....	69
Figure 4-4-6. Chemical compositions of Mn ₅₀ Al ₅₀ -60h.....	70
Figure 4-4-7. Morphology of the Mn ₇₀ Al ₃₀ -60h particles.....	71
Figure 4-4-8. Morphology of the Mn ₇₀ Al ₃₀ -60h particles.....	71
Figure 4-4-9. Chemical compositions of Mn ₅₀ Al ₅₀ -60h powder.....	72
Figure 4-5-1. Absorbance spectrum of a solution with 150 mg / L of Acid Black 58 colourant.....	73
Figure 4-5-2. Coloured water with 150mg / L of Black Acid 58.....	73
Figure 4-5-3. Coloured water with 150mg / L of Black Acid 58 once treated with MPs of Mn ₇₀ Al ₃₀	73
Figure 4-5-4. Degradation of Acid Black 58 by particles Mn ₇₀ Al ₃₀ at 25 °C and 45 °C.....	74
Figure 4-5-5. Acid black 58 degradation applying 100 mg and 500 mg of Mn ₇₀ Al ₃₀ particles.....	74
Figure 4-5-6. Degradation of Acid black 58 at initial pH 4, 7 and 10 with Mn ₇₀ Al ₃₀ particles.....	75
Figure 4-5-7. Degradation of the solution with Acid black 58.....	76
Figure 4-5-8. Decolourization of the solution with Acid black 58 by Mn ₇₀ Al ₃₀ particles.....	76
Figure 4-5-9. Decolourization of the solution with Acid black 58 rs.....	77
Figure 4-5-10. Complete decolourization after a centrifugation process.....	77
Figure 4-5-11. Morphology of the surface of the as produced MPs.....	78
Figure 4-5-12. Image of the the washing solution (water and ethanol).....	78
Figure 4-5-13. Absorption spectrum of a solution with 40 mg / L of orange G colourant.....	79
Figure 4-5-14. Decolourization of the Orange G solution.....	80
Figure 4-5-16. Decolourization of the Orange G solutions.....	82
Figure 4-5-17. Decolourization of the Orange G solutions.....	83
Figure 4-6-1. Kinetics of decolourization obtained experimentally.....	84
Figure 4-6-2. Kinetics of degradation of Orange II using Mn-Al MPs.....	84
Figure 4-6-3. Kinetics of degradation of Orange II using Mn-Al MPs.....	85
Figure 4-6-4. Kinetics of degradation of Orange II using Mn-Al MPs.....	85
Figure 4-6-5. Colour degradation percentage after 60 minutes of treatment.....	86
Figure 4-6-6. Morphology of MP Mn ₇₀ Al ₃₀	87
Figure 4-6-7. Morphology of MP Mn ₇₀ Al ₃₀	87
Figure 4-6-8. Morphology of MP Mn ₇₀ Al ₃₀	87
Figure 4-6-9. Morphology of MP Mn ₇₀ Al ₃₀	87
Figure 4-6-10. Morphology of MP Mn ₇₀ Al ₃₀	88
Figure 4-6-11. Morphology of MP Mn ₇₀ Al ₃₀	88
Figure 4-6-12. Morphology of MP Mn ₇₀ Al ₃₀	88
Figure 4-6-13. Morphology of MP Mn ₇₀ Al ₃₀	88
Figure 4-6-14. MPs after the third cycle and washed with distilled water with pH 3.....	89
Figure 4-6-15. Morphology of the Mn ₇₀ Al ₃₀ particles.....	89
Figure 4-6-16. Morphology of the Mn ₇₀ Al ₃₀ particles.....	90
Figure 4-6-17. Morphology of the Mn ₇₀ Al ₃₀ particles.....	90
Figure 4-6-18. Morphology of the Mn ₇₀ Al ₃₀ particles.....	90
Figure 4-6-19. Atomic percentage of the elements.....	91
Figure 4-6-20. Atomic percentage of the elements.....	91
Figure 4-6-21. Atomic percentage of the elements.....	92
Figure 4-6-22. Atomic percentage of the elements.....	92
Figure 4-8-1. Representation of the extraction.....	96

List of Tables

Table 3-1: Amount of Mn and Al	25
Table 3-2-1: The basic data for the identification of the Orange II dye.....	27
Table 3-2-3: The basic data for the identification of the Orange G dye	27
Table 3-2-4: The basic data for the identification of the Brilliant Green.....	28
Table 3-2-5: The basic data for the identification of the Acid Black 58.....	28
Table 4-1: Surface area of particles $Mn_{70}Al_{30}$, Al and Mn.....	58
Table 4-2: Table results of toxicity analysis.....	66
Table 4-3: Comparison of biological treatment with <i>T. versicolour</i> and treatment with MP.....	67

Outline and research target

Waste treatment is an important aspect of an industry. Organic dyes are used in many fields, such as textile, paper, leather, etc. Residual dye compounds from these industries are one of the most critical sources of environmental pollution because of their visibility and potential carcinogenic properties. It is essential to remove these organic dyes from wastewater before being released into environment. Unfortunately, many organic dyes are not degradable in conventional wastewater treatment processes due to complex molecular structures.

Azo compounds are one of the most common families of dyes used in textile and leather treatments. An important step during the treatment of water polluted by these compounds is the degradation of the compounds by decomposition of the -N=N- bonds, producing the decolourization of the water. Modern dyes are often intended to resist the long-term exposure to sunlight, water, and other conditions, thus making them more resistant to decomposition and so hindering the treatment of wastewater. Different physical, chemical and biological approaches are employed for the removal of azo dyes from aqueous solutions.

Among these approaches, the reduction with zero-valent metals (ZVM), like iron, magnesium or aluminium has been studied as a promising route because of its merits of low cost and rapid degradation efficiency.

Recently, it has been discovered that the use of metallic particles in a metastable state (amorphous or nanocrystalline) multiplies significantly the efficiency of the decolourization water treatment step. Amorphous metallic phases in the shape of porous structures have shown an excellent performance in degradation of azo dyes. Indeed, it is known that the metastable structures generated during rapid solidification or mechanical alloying tend to increase the chemical activity of the alloys.

In this thesis we study the use of Mn-Al metallic particles to provide a rapid degradation of these dye compounds. We first studied the use of a ball-milling process, under an argon gas atmosphere, to produce the Mn-Al powder. Different types of powders, obtained by different milling protocols were characterized. The morphology, particle size distribution and chemical composition of the Mn-Al powders were analysed by different techniques such as Scanning Electron Microscopy (SEM) and Energy Dispersive X-ray microanalysis system (EDX).

The decolourization process of aqueous solutions coloured with various types of dyes, triggered by the Mn-Al powders, was monitored by ultraviolet-visible (UV)

spectrophotometry. The activation energy was determined and various parameters such as pH, initial dye concentration, dosage and different temperatures were studied in terms of their effect on the reaction progress.

Next, we analysed the efficacy of the metallic particles (MP) mediated degradation of Orange II dye using four different alloys with different proportions of Mn and Al, it was determined that $Mn_{70}Al_{30}$ was the composition that showed highest efficacy and reproducibility decolourizing Orange II solutions.

The changes in the solvent water produced by the MP-mediated reaction were also analysed with high performance liquid chromatography (HPLC), Mass Spectrometry (MS) and Atomic Absorption flame spectrometry (AA). The analysis of the treated water identified several intermediary components and two amines, as well as liberation of Mn ions. We also analysed the kinetics of the degradation of other colourants such as Acid Black 58 and Orange G dyes by using $Mn_{70}Al_{30}$ particles. The results also showed efficacy of the intervention on Acid Black 58 dye, but only partial decolourization was observed in the solution with Orange G.

Moreover, the chance to reuse the particles in successive processes of decolourization has a big interest from both environmental and economic point of view. The results showed that each cycle of decolourization reduce the efficiency of the particles and that the best results are obtained without using any washing method.

Lastly, this work analyses the efficiency of Mn-Al metallic powders for degrading azo dyes and compares the results with the ones obtained in a pilot scale trickling filter. The bacterial microorganisms selected in the trickling filter presented the ability to remove dye under aerobic conditions at pH values between 6 and 7.5 but with low efficiency. Note though that lower rates of dye removal were observed with the bacterial approach as compared to the Mn-Al metallic powder approach. A discussion on possible combinations of these two processes to increase efficiency on a wide range of temperature and pH conditions will be also given in this work.

1. Introduction

The textile industry, in its various stages of production, emits a wide variety of organic chemicals contaminants - such as organic dyes and colourants - being added to the water supply. The increasing demand for dyes by the textile industry has shown a high pollutant potential. Such dye contaminated wastewater is considered to be a highly toxic liquid harmful to both aquatic and human Life. Such dye contaminated wastewater also has resistance to bio-degradation which is also of great concern.

1.1 The textile industry and the dyeing process

The textile industries involved in paper processing, resizing, cosmetic, bleaching, colouring, leather, and wrapping have greatly expanded and involve many different stages of production and processing of materials for the subsequent transformation to fabric and industrial items. The most important environmental impact of the textile industry is derived from the wet processes where the dyeing stage stands out. In this stage colour is given to the tissues and large volumes of water and energy are used. Dyeing processes can use up to 170 L of water, 1.1kW of electrical energy and 16 MJ of thermal energy per kilogram of finished product[1][2]. By using different techniques and equipment, dyeing processes can be performed discontinuously or continuously. In discontinuous staining, a certain amount of tissue is placed on a dyeing machine and is brought to balance with a solution that contains the dyeing compound; the dye is fixed to the fibre using heat and chemical products and finally the fabric is washed to eliminate the non-fixed dye content and other chemical products. In continuous dyeing processes, the fabrics are continuously fed to a bath where the colour is applied, fixing products and heat are added in proportion to the incoming fabric. The textile wastewater therefore contains complex mixtures of products such as metals, salts, acids and dyes.

1.2 Environmental problem of textile industrial effluents linked to dyes

More than 100,000 commercially available dyes are known in the market and around 10,000 are obtained on an industrial scale giving rise to more than 7×10^5 tonnes of production per year [3]. It is estimated that two thirds of all existing dyes are used in the textile market [4]. Around 10-15% of the textile dyes are lost in wastewater stream during the dyeing processes [5][6], although the percentages can reduce by 2% in basic dyes, or increase up to 50% with reactive dyes [7]. Even in the case of a low concentration of these chemical compounds, their presence results in a great visual effect [8]. Textile dyes are characterized by having a great staining power and a great persistence in the environment. They are designed to be highly stable against light, temperature, oxidizing agents and the attacks of microorganisms. Molecules responsible for colour have complex

chemical structures and in many cases contain one or several aromatic rings. They are difficult to degrade and usually are not eliminated from the water by conventional effluent treatment with active sludge.

The contamination potential of some textile dyes, apart from colour, is due to its toxicity and carcinogenesis [9], since some of them come from carcinogens known as benzidine and other aromatic compounds. Moreover, although many dyes may be non-toxic for microorganisms, a strong colouration of the receptor medium can eliminate the photosynthetic processes thus inhibiting the biological activity [10]. On the other hand, the effect of the dyes is enhanced in the process of dyeing by products such as oxidizing agents, reducing agents, dispersive agents or emulsifiers, that help to increase the effect on the parameters of water quality such as Biochemical Oxygen Demand (BOD), Chemical Oxygen Demand (COD), Total Organic Carbon (COT), and total solids [11].

Taken into account that each type of dye has its own characteristics and the existence of a great structural variety of dyes, together with the fact that the textile industry is characterized by using different dyes for short periods of time in the same factory, and extremely variable composition of effluents can be generated, making it difficult to find a single treatment for this type of wastewater. The presence of this type of pollution must be controlled and the legislation is becoming increasingly stricter in developed countries. In the EU, the directives 91 / 271CEE, 98/15 / CE and 2002/61 / CE are applied which oblige to eliminate the colour of wastewater before pouring them, and even prohibits the commercialization and use of certain dyes, especially azo dyes that can release aromatic amines. The growth of social sensitivity towards the environment that has occurred in recent years has had an important influence on the industry (including textiles), which has to comply with stricter measures not only to satisfy the legislation but also the public perception.

1.2.1 Relocation of the problem to emerging countries

In recent decades, the textile industry has moved to countries such as China or India, where legislative pressure and labour costs are lower than those existing in more developed countries such as those in the European Union. In countries like China or India water pollution has become one of the greatest environmental challenges in their struggle to be among the main industrialized countries in the world. The textile industry in China is a great business, in 2010 it represented 7.6% of the total commercial volume of the country. China, however, has one of the worst levels of water pollution in the world, up to 70% of rivers, lakes and marshes are affected by pollution, 20% of which is organic and comes from industrial spills. In order to maintain low prices, many industries,

including textiles, build pipes that pour industrial waste either underground or directly into surface water (Figures 1-2-1, 1-2-2 and 1-2-3).



Figure 1-2-1. Industrial wastewater pipes emerging on the beaches of the Yellow Sea (April 28, 2008) [website: Eugene Smith, 2009].



Figure 1-2-2. Industrial water spill with metals less than 1000 meters downstream from the capture of water by the city of Danyang (June 10 2009) [website: Eugene Smith, 2009].



Figure 1-2-3. Many of the more than 100 factories in the city of Jiangsu discharge highly polluted water directly into the sea. Other industries store them in pools, where they are finally spilled into the sea with high tides each month (June 2, 2008) [website: Eugene Smith, 2009].

1.3 Dyes

Colour is present in everything that surrounds us and has fascinated humans since prehistoric times, where pigments of natural origin originated from plants, trees, molluscs and insects were already used. Synthetic textile dyestuffs, however, are mostly organic compounds and their origin is much more recent since they were not used until mid-nineteenth century. Until then natural dyes were used, although the process of fixing the dye to the fabric had been improved.

It is believed that the first synthetic dye was picric acid, first prepared in 1771. The beginning of the synthetic dye industry, however, is attributed to William Henry Perkin, who discovered in 1856 the dye Synthetic Aniline Purple (now called Mauveine)[12]. Figure 1-3-1 shows its structure.

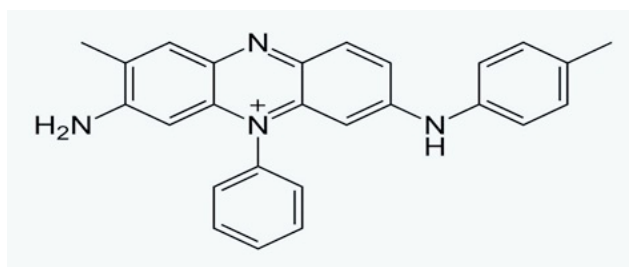


Figure 1-3-1. Structure of the Mauveine dye.

Subsequently, one of the most important discoveries in this field was carried out by Peters Griens, who developed Azo Dyes Chemistry, the most important group of dyes in terms of use, an example of which is shown in Figure 1-3-2. Since then, the dyeing industry has risen, and today, at the beginning of the 21st century, the production of new types of dyes and pigments for textile applications, pellets, paints, plastics, etc. is widely investigated. At the moment, in addition, the colouring field has opened up to new applications, with the so-called "functional colours" that are characterized to fulfil other functions besides giving colour. It is the case, for example, of the dyes applied to fields such as electronics, lasers, liquid-crystal displays, electrophotography and medicine (Fluorimetry, photodynamic therapies against cancer, etc.) [13].

1.3.1 Dyes and pigments

The colouring term is commonly used to refer to two types of compounds: dyes and pigments. Both are used in the colouration of materials and even become chemically similar substances, but it is necessary to distinguish the differences in their properties and especially in their use. Dyes and pigments differ mainly in their solubility: if the dyes are soluble, the pigments are insoluble. The traditional use of dyes is in the textile industry, where it is usually required to be soluble in aqueous media and in new applications such

as electronics, where they are required to be soluble in organic solvents. On the contrary, the pigments are completely insoluble in the colouring medium and their main applications are found in paints, plastics, colouring of materials such as cement, ceramic materials, glass, etc. A more accurate distinction between these two materials would be that, while the dyes are designed to be strongly bound to polymeric molecules to carry out the colouration process, pigments are not attracted to the environment but to each other, to form a structure in the form of a crystalline network and thus to withstand any dissolution [13]. In the following sections the main characteristics and existing classifications for dyes and pigments are described, both groups referring to the term "colourants" will be discussed.

1.3.2 Colour and constitution of the dyes

One of the simplest methods, but currently used to explain the origin of colour, was proposed by Witt in 1876. His theory postulates the existence of two main groups (chromophore and auxochrome) as responsible for the appearance of colour. According to this theory, the first group called chromophore is defined as the group of atoms responsible for colour. Secondly, the auxochrome group is seen as a colour enhancer. Later, it has been seen that in order to explain the presence of colour it is necessary that the chromophore group be in a conjugated structure (alternating simple double bonds). This terminology is still used today to give a simple explanation of the colour, although Witt's initial suggestions that auxochrome groups are as essential as chromophore groups to guarantee the properties of the dyes have proved to be invalid. This essential element is the existence of conjugation within the molecule. The most important chromophore groups are: azo ($-N=N-$) followed by the carbonyl group ($-C=O$), methylene ($=CH_2$) and nitro ($-NO_2$). As primary auxochrome is common to found carboxyl ($-COOH$) and amino groups ($-NR_2$). Some theories also associate the auxochrome group with the ionization state of the molecule, so groups such as COO^- and HSO_2^- give acidity to the molecule while the amino group gives the molecule a positive ionization state, therefore basic character.

1.3.3 Classification of dyes

The Colour Index is the most important and complete reference work in the field of dyes. It grants each colour or pigment, either natural or synthetic, two references: the first based on its industrial designation and the second according to its chemical structure. Knowing this numerical index allows you to obtain very useful information for each colour on its properties and the application methods. The dyes can be classified in two main forms, depending on their chemical structure or according to their application. There is a third

form of classification, but only important at a theoretical level and which is based on the mechanism of electronic excitement [13].

1.3.3.1 Chemical classification

The chemical classification, most important for dyes, is based on the common structural characteristics of dyes. According to this, the classes of colourants and pigments in order of decreasing importance are: Azoic, Carbonyl (including anthraquinone), Phthalocyanine Quinone imine, Sulphur, Polyenes, Dioxazines and Nitro. It should be said that there are other groups of dyes that have not been mentioned in this chemical classification, either because they have not been sufficiently investigated or because they have no commercial usage [13].

Azoic Dyes (Azo)

Azoic dyes (also called "azo") are the most important class of organic dyes. They include 60-70% of the entire colourant market used in textile applications as they have the best cost-effectiveness relationship. They are able to give twice as much colour intensity as many other dyes and at the same time they are manufactured at a lower cost. The reason is in its chemical structure; which can be prepared in large quantities according to application requirements and with few energy requirements. Azo dyes are very important in colours such as yellows, oranges and reds.

The common structure for azo dyes is determined by the link $-N=N-$. Normally, although not exclusively, the azo groups are linked to two systems of aromatic rings. Most azo dyes contain a single link $-N=N-$, and they are called mono azo dyes. Figure 1-3-2 presents the structure of the mono azo dye Aniline Yellow.

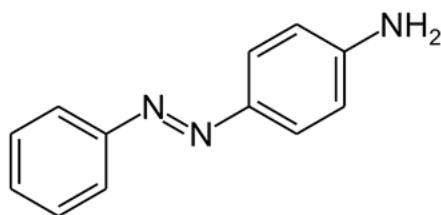


Figure 1-3-2. Structure of the Aniline Yellow dye.

Although they are also found, in lesser quantity, with two or more links, such as the structure of the Diazo Biebrich Scarlet colour that is shown in Figure 1-3-3.

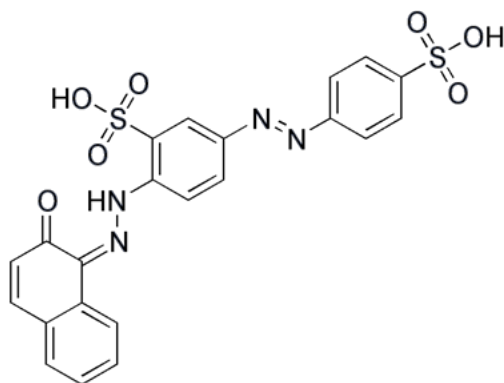


Figure 1-3-3. Structure of the Biebrich Scarlet dye.

One of the subgroups in the azo class that is of significant importance is that of the metallic complex azo dyes. Azo dyes have been combined with metals (especially transition metals) in order to improve the speed of the dyeing process and the brightness of the finished product. This is what is called the fixation process. These dyes are still used today, but their use has been restricted basically to the dyeing of wool[14].

Carbonyl dyes

It is the second most important group after azo dyes, and is characterized by the presence of the carbonyl group ($-C=O$) as a chromophore group. The carbonyl dyes have a great structural range, and therefore of colours, wider than the azo dye group. Within this group, special mention should be made to the subgroup of anthraquinone dyes. Also, commercially relevant are other subgroups such as benzophenones, coumarins, naphthalimides. The anthraquinone dyes contain a characteristic system of three rings of six atoms, in which the carbonyl group is in the central ring and the two outer rings are aromatic.

Regarding the properties of firmness and rapidity in dyeing, these dyes are usually superior to Azo dyes and are used (especially anthraquinone dyes) in dyeing of fabrics such as cotton. Today, around 200 different types of anthraquinone dyes exist, and their use has so far been based on the application of green, blue and violet colours. However, the production of carbonyl dyes, compared with that of azo, is much less versatile and much more elaborate, involving multiple intermediate stages and the use of intermediaries[15].

Phthalocyanine dyes

Phthalocyanines undoubtedly represent the most important chromophore group developed during the 20th century. After its discovery, the industry begins to rapidly exploit its unique properties with regard to intense colours and high brightness; being the colouring class that has been most extensively studied. The basic structure of

Phthalocyanine is flat and consists of four "isoindole" units connected by four nitrogen atoms. Most Phthalocyanine contain a central metallic atom, as shown in Figure 1-3-4. This class of compounds is very important in the field of pigments, especially in plastic applications of the blue and green colours, as they are structurally very stable, even at high temperatures.

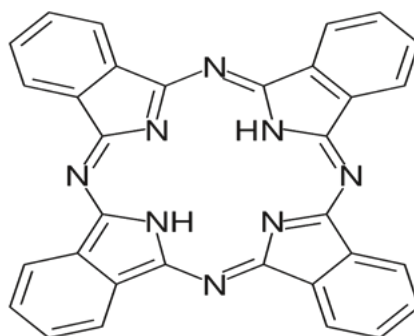


Figure 1-3-4. Structure of Phthalocyanine dye.

Aryl carbine dyes

They are the first textile dyes that were synthetically developed since Mauveine, the first synthetic organic dye, belongs to this group. Most of these dyes were developed throughout the 19th and 20th centuries. Although its importance has been diminishing considerably, they still retain some weight in the textile industry (used in dyeing acrylic fabrics). Although in the dyeing process, they give very vivid and extremely intense colours in a wide range of tones, for the textile industry, technically, they are well below the azo and carbonyl dyes. The basic structure of these dyes is based on a central carbon surrounded by three aromatic rings, this form has given them the common name of triarylmethane or triphenylmethane[16]. An example of the structure of these dyes is presented in Figure 1-3-5.

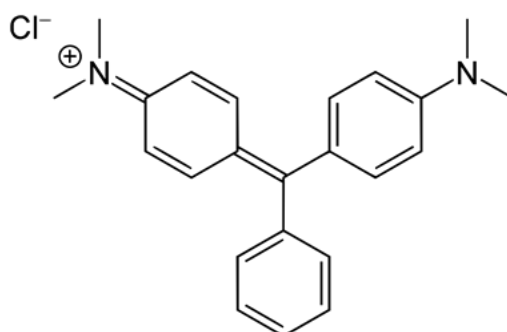


Figure 1-3-5. Structure of Malachite Green Triarylmethane.

Sulphur dyes

This group consists of a small amount of dyes. Individually however, they occur in large quantities, especially in terms of colours such as blacks. They are mixtures of polymeric

structures that have a large number of sulphide in the form of sulphite (-S⁻), disulphide (-S-S-) and polysulphide (-S_n-). Figure 1-3-6 shows the basic structure that constitutes sulphur-type dyes. They are traditionally products that are not soluble in water, and once solubilized, although produced at low cost, they cause environmental problems that are so serious that their use has decreased in a very important way in recent years[17].

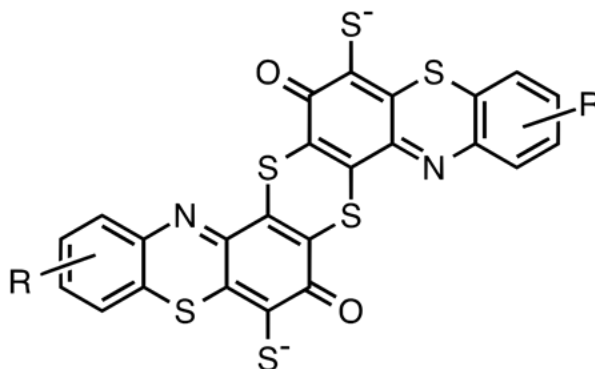


Figure 1-3-6. Structure of sulphur dyes.

Polyenes and Polyethylene Dyes

Polyene and polymethylene dyes have structures that have one or more than one methylene group (-CH=). They are structures that contain a series of double conjugated bonds that give colour to the molecule. These chains usually end up with aliphatic and alicyclic groups. The most well-known and used group is β -carotene (of natural origin), although its application is not in the textile industry but in biochemistry. The dyes of this group are characterized by having a wide structural variety. Where donor groups and acceptor groups give the character: anionic, cationic or neutral. Although this last group is able to give a great intensity of colour, with regard to its staining rate, it is so poor that they are practically not used in the textile industry (only in dyed polyester fabric)[18].

Dioxazine dyes

They are colourants that are characterized by containing two oxazine groups as a chromophore group. They have an angular structure, as shown in Figure 1-3-7. There are relatively few dyes of this class. They basically give violet colours. Many of them are pigments and have a high resistance at high temperatures.

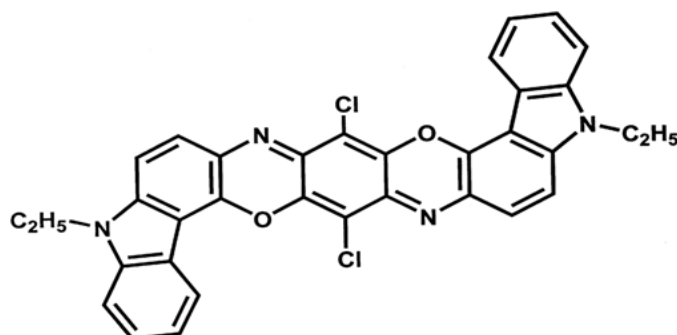


Figure 1-3-7. Structure of Pigment Violet 23.

Nitro dyes

This small group of dyes have in their structure the chromophore group (-NO₂), as shown in Figure 1-3-8. Although the synthesis of these dyes is relatively simple and to a certain extent the cost of their production is low. The vast majority of these dyes have not been applied commercially, since their staining properties are poor. They have high toxicity and special measures must be taken during their handling due to their high explosiveness[19].

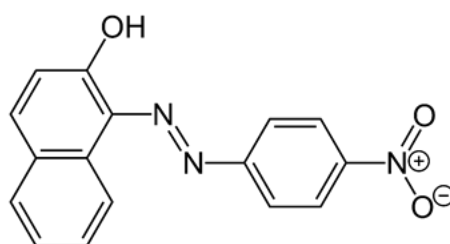


Figure 1-3-8. Structure of nitro dyes.

1.3.3.2 Classification of dyes according to their application

The classification according to application is used mainly when it is spoken of pigments and basically is based on the utility that has a dye to dye a certain type of fabric. According to this classification it is distinguished between fixing dyes used in dyeing of fabrics, direct dyes for cellulose fabrics, disperse dyes for polyester, etc. Each class has a certain mechanism of fixation in the tissue. For example, direct dyes use Van der Waals forces to adhere to cotton [13].

According to this classification, a very important group is the group of reactive dyes. The development of reactive dyes has meant one of the most important innovations in the textile sector. They are the colours that behave better during and after the dyeing process, and if until now its application was basically in the dyeing of cellulose fabrics, studies have already been made to apply them to synthetic fabrics. The importance of reactive dyes lies in the fact that these dyes do not use different binding forces but are capable of reacting chemically with the reactive groups of the fabrics. So for example, these dyes

perform a nucleophilic attack on cellulose fabric by taking advantage of the -OH groups that it has. Although reactive dyes can be prepared with almost any of the different chemical classes, those that are most important are those prepared from the azo group[20].

Generally, for the selective removal or decomposition of dye contaminants from wastewater various methods such as physical, biological, or chemical techniques are the adopted approaches. Nanocomposite adsorption, ozonation, nano-filtration, flocculation and ion exchange belong to the family of physical techniques. Meanwhile bacteria and fungi approaches belong to the biological techniques family. And chemical methods include Fenton reaction and the use of NaClO and ozone. Azo dyes can be treated by both physical and biological techniques as a relatively new and very promising processes for clarifying water. Each family, physical and biological, has its own set of disadvantages. For example, physical techniques can produce large amounts of sludge which requires safe disposal. Meanwhile biological techniques often require relatively severe degradation conditions and also exhibit strong selectivity and lead to secondary waste stream which need further treatment. Chemical techniques are however considered fast and efficient.

1.4 Dyed water treatments

Considering that the presence of very low concentrations of dyes in effluents is very visible and undesirable [8], that the chemical structure of the dyes makes them resistant to external agents such as light, water and chemical agents [21] and the large diversity of commercially used dyes, a universal process for the treatment of textile sewage has not yet been developed. The following sections show a summary of the most widely used dye elimination methods.

1.4.1 Physicochemical treatments

The physicochemical processes for the elimination of the colour of the residual water can be classified into two main categories: the methods of transformation of the component of the colour and the methods of elimination of the component of the colour.

1.4.1.1 Methods of transformation of the colour component

These treatments are characterized by the decomposition of the colouring structure and the formation of intermediate products. Below is a brief summary of the colour transformation processes most commonly used to eliminate dyes.

Oxidative processes: Oxidative processes are based on the use of oxidizing agents such as hydrogen peroxide, Fenton reagent, ozone or potassium permanganate.

Fenton (Homogeneous Catalysis (H_2O_2 / Fe^{2+})): The mixture of hydrogen peroxide with catalytic amounts of iron (II) is known as Fenton reagent. This solution has a high oxidative capacity due to the generation of hydroxyl radicals (OH) from the following reaction:



Where the oxidizing agent (H_2O_2) breaks down into hydroxyl radicals and is characterized by being a powerful non-selective oxidant capable of completely mineralizing organic matter of a diverse nature. The cost of the treatment is low, since it is based on a simple operating system and it is used in effluents resistant to biological treatments or toxic effluents. It is a very effective method for discolouration of dyes and pigments, but waste from the dyes and reagents used is generated [22], [23].

Sodium hypochlorite ($NaOCl$): This method is very useful in the treatment of azo dyes, where OCl^- attacks the amino group of the molecule by initiating the breaking of the N=N bond. The use of OCl^- for colour elimination has become rare due to possible production of aromatic amines and other toxic compounds [1].

Ozone (O_3): Ozone is a very unstable agent with a great oxidation potential. Some studies have found an effective path for the decolourization and elimination of COD in the use of ozone in industrial waters. Other works however, consider that this process does not significantly eliminate COD at the same time as colour [24].

Advanced oxidation chemical processes (AOPs): The AOPs have been proposed in recent years as a good solution to the purification of industrial waters. AOPs are characterized by combining more than one oxidative process at the same time. In the same way as oxidative processes, AOPs involve the formation of radical species of high oxidative power essentially the hydroxyl radical (OH). Since radical oxidizing species are poorly stable, they must be generated on site by the use of activators, such as iron catalysts or the application of a source of radiation; The main drawback of AOPs is its high cost by the use of reagents (H_2O_2 , O_3 , TiO_2 , etc.) and its high energy consumption (lamps to generate UV radiation), which adds costs to the process if compared to biological treatments[25].

Some of the most advanced oxidation processes studied in the treatment of contaminated dyes are the following.

Photo-Fenton or Homogeneous Photo Catalysis ($H_2O_2 / Fe^{2+} / UV\text{-vis light}$): Currently, the process where the Fenton reagent is used is considered one of the main AOPs for water treatment as it is an attractive oxidative system that does not require complex

reagents. The combination of the Fenton reagent with UV / visible radiation results in the Photo-Fenton process, responsible for the increase in the oxidation rate of the organic matter as a result of the greater regeneration rate of the Fe^{2+} catalyst, which allows the reaction of Fenton to be continuously carried out, and a greater generation of radicals is obtained. The Photo-Fenton is defined as homogeneous photo catalysis since it is a process in which a photochemical alteration of some species results from the absorption of radiation by another photosensitive species, in this case a catalyst dissolved like the Fe^{2+} . The decolourization rate depends on several factors, such as radiation typology, pH and colour structure [26][27].

Photochemical processes: Photochemical methods for the degradation of pollutants dissolved in water provide energy to chemical compounds in the form of radiation, which is absorbed by the different molecules until excited states reach the necessary time to experience reactions. Radiant energy is absorbed by forming free radicals and giving rise to a series of chain reactions. Ultraviolet radiation constitutes an advanced oxidation process by itself, but generally has a low efficiency in the degradation of organic compounds dissolved if compared to other oxidation advanced processes [28].

Heterogeneous photo catalysis (Semiconductor / UV-vis / H_2O): The concept of heterogeneous photo catalysis is based on the use of a solid semiconductor, such as TiO_2 , which forms a stable suspension under irradiation to stimulate a reaction in the solid/liquid or solid/gas interface [29][30][31].

Ozonation processes (O_3 / UVB, O_3 / H_2O_2 , O_3 / H_2O_2 / UVB): They use ozone as an oxidizer. They are very effective processes capable of reducing the colour in its entirety. Its main drawback, however, is the average lifetime of ozone (about 20 minutes) and sometimes it turns out to be too short in time for total colour elimination [3]. To avoid this, ozone must be used continuously, which considerably increases the cost of these processes [32].

Advanced Oxidation Electrochemical Processes (AOEPs): Wastewater treatment by electrochemical route has been significantly boosted during the past ten to fifteen years thanks to the development of electrochemical technology [33]. AOEPs are based on direct and indirect oxidation, through active electro generated species, of organic matter reaching total (combustion) or partial (conversion) mineralization of organic compounds. These types of treatments can be classified into classical and advanced electrochemical processes. The main classical electrochemical processes are electrodeposition, metal recovery process (membrane processes by concentration gradient, based on the difference of chemical potential between the two sides of an ion exchange membrane), membrane processes by electric gradient (it is an electro dialysis that is promoted in traditional

dialysis, which allows the demineralisation of brackish water), and the elimination and recycling of acids and alkalis. Also phase separation methods, such as electroplating, electro flocculation and electrocoagulation, etc. These processes require little consumption of chemical reagents and generate few sludge. They are efficient methods for the degradation of recalcitrant contaminants such as tints [34][35]. But in relatively high volumes there is a decrease in the elimination of dye and a considerable increase in energy costs.

1.4.1.2 Methods of elimination of the colour component

In these treatments the structure of the colourant remains unchanged. These are methods such as adsorption and membrane processes.

Adsorption in active carbon: The elimination of dye by adsorption in active carbon has been widely studied and used to its effectiveness in most dyes. However, despite the fact that several pilot plants and installations have been developed on an industrial scale using active carbon [36], active carbon adsorption presents some disadvantages such as the high costs associated with the regeneration of active carbon, which is not a selective treatment and that is not effective for all colourants [37].

Membrane processes: These methods are applicable if the effluent contains low concentrations of colour. Systems such as reverse osmosis and ultrafiltration are included. These processes have associated high costs in equipment and in energy consumption; apart from factors such as possible poisoning of membranes and the production of contaminated concentrated sludge that also directly affect the costs of exploitation [1].

Coagulation-flocculation: It consists of adding reagents that cause the agglomeration of colourants in colloidal and later flocculation to be able to separate them from the residual water. An example of this reagent is the cucurbituril, a polymer composed of formaldehyde units, capable of selectively removing dyes forming insoluble complexes between the dye and the polymer by iron sulphate and iron chloride [1][38].

1.5 Biological treatments

Textile wastewater has a very low COD, therefore, because of its organic load, are wastewaters that can be assimilated to urban areas and in some cases they are mixed with urban effluents to treat them in sewage treatment plants. This treatment is of a non-biodegradable nature, both because the dyes have a complex chemical structure and they are accompanied by a high content of compounds as surfactants. In addition, excessive concentrations of toxic metals, extreme pH, the presence of inhibitory substances, and the low biodegradability of the majority of dyes and chemicals used during the dyeing

process, make that conventional biological treatments (for active sludge down and half load) are not always effective. Biological community treatment approaches, as employed by municipal aerobic treatment systems, often display poor efficiency when it comes to organic chemical compound dye decolourisation. There are some exceptions for some dyes targeted by specific biological communities. Furthermore, some dyes, due to their toxicity may even inhibit bacterial activity[39].

Bacterial communities usually extract dyes and other organic contaminants via the process of absorption. This results in recalcitrant pungent toxins in the bacterial sludge. In pilot scale trickling filters operated under aerobic conditions, the support substrate can be constructed out of wood or inexpensive plastic materials. These types of materials can be utilised as bio filters with regards to cleaning wastewater, and more specifically, dye contaminated wastewater. However, several problems exist which must be successfully solved in order to provide a practical treatment procedure for textile effluents. For example, the non-sterile conditions of bioreactor operation present challenges in maintaining bacterial growth and is seen as a key limitation of long-running biodegradation processes. This particular problem can likely be overcome through the use of immobilised reactor systems as these allow for the maturation conditions to be established in an individual manner for each type of bacteria employed[40].

Anaerobic treatment: Anaerobic degradation comprises a first adsorption step in the clay [41], and a second where anaerobic digestion is produced that allows to discolour soluble dyes such as the azo class. This decolourization, however, implies a reduction in the azo binding and it has been shown that reductions in the azo and nitro components generate toxic amines.

Anaerobic treatment followed by aerobics: The use of anaerobic and aerobic combined treatments results in colour elimination (anaerobic phase) and at the same time eliminates problems in the formation of amines (aerobic phase) [42][43]. An example is the SBR (Sequential Batch Reactor) active sludge method, which combines anaerobic and aerobic phases for time cycles in the treatment of colour effluents [44][45][46]. It has been verified that the aromatic amines formed in the anaerobic phase (where colour elimination reached 89%) were reduced in the subsequent aerobic cycle to 92%. This type of treatment has been extended to other families of dyes, such as reactive dyes [47].

1.6 Metallic nanocrystalline and glassy materials

Amorphous materials are a particular form of matter without long range periodicity in the atomic or molecular spatial arrangement, showing only partial short-range order in its structure and, thus, lacking the long-range order present in crystalline materials [48]. The

structure of an amorphous material emerges from the local random atomic packing, lacking the main features of crystalline materials such as atomic planes, crystalline directions, grain boundaries and defects on the structure. Therefore, amorphous materials have the following features [49][50]:

- Isotropy in physical, chemical and mechanical properties, and a continuous change of properties with temperature due to the lack of a first order structural transition.
- Short range order, i.e. disordered arrangement of first and second nearest neighbour atoms but with a certain regularity, such as in the coordination number, atomic spacing, bond angles, bond length, etc.
- Metastable thermodynamic state, which can be driven into the crystalline state by overcoming the energy barrier above the crystallization temperature [51].

According to the above mentioned features, amorphous materials can be roughly divided into various categories, namely, conventional glasses, organic glasses, amorphous polymers, non-crystalline semiconductors and metallic glasses. Metallic glasses, also known as amorphous metals or glassy metals, are solid metallic alloys with a disordered atomic-scale structure [52]. Most of the known metallic alloys have a crystalline solid state, meaning that they have a highly ordered arrangement of atoms. To avoid this crystalline structure, metallic glasses are obtained by fast cooling so as the alloy becomes a highly undercooled liquid; the glass is then a liquid arrested in a given atomic configuration due to extreme increase of the liquid viscosity through cooling, preventing crystallization [53]. By using rapid quenching technique [54], the cooling rate for metallic liquids could reach to 10^5 - 10^6 K/s. which allows obtaining a large number of alloys in the glassy state, in ribbon form. Another completely different route to produce amorphous metals is to induce disorder into the crystalline lattice by applying severe mechanical deformation, usually done in mechanical millers. In both cases, by fast cooling from the liquid or by means of mechanical treatments of the solids, the materials can be obtained in amorphous or nano-crystalline states. These states are metastable forms of the metallic materials which show interesting new properties. This fact has attracted a large scientific attention on metallic glasses both in the field of fundamental understanding of the glassy state and the development of novel engineering materials for industrial applications.

During 1980s, a few techniques for synthesizing metallic glasses and nanocrystalline alloys were developed besides rapid quenching [55], such as hydrogen adsorption [56], mechanical alloying (milling) [57], ion beam mixing [58], and inter diffusion between multi-layers [59]. These techniques are able to obtain powders, or thin wires and sheets,

which usually do not alloy structural application but are very attractive for functional applications as the one exploited in this work. Many different alloy compositions have been obtained in metastable amorphous or nano-crystalline states, including Al-based [60] and Fe-based [61] materials.

1.6.1 Treatment with MPs

The chemical treatments using metallic particles (MPs), either of a single element or alloys, are catching the attention of the scientific world for its potential in different areas of environmental engineering. Its structure, in many cases amorphous or nano-crystalline, determines its chemical properties and corrosion behaviour. In certain applications, as in the case of liquid effluent treatment, this structure can result in certain advantages over conventional metallic materials characterized by a crystalline structure [62].

Different authors have studied the degradation of the molecules of the dyes using MPs formed by different elements and alloys. The most studied is zero-valent iron MPs, since the MPs of this element was shown to have the ability to break the azo links many years ago [62][63][64]. There are different methodologies to obtain MPs. According to different authors, there are methods that are based on a chemical process, such as precipitation methods [65][66], and other based on physical processes, such as gas atomization or mechanical alloying [67]. The latter, usually performed in high-energy metallurgical mills and also known as ball milling, is able to produce metallic powders with inner metastable amorphous or nano-crystalline structure.

1.6.2 Metallic particles to degrade the azo link

The process of reduction of zero-valent metal (ZVM) metallic particles has been extensively studied for environmental remediation. They have been used for the treatment of contaminated waters and chlorinated compounds, nitrates, heavy metals and dyes. The surface activity of ZVM is of crucial importance for the degradation reaction of organic contaminants. ZVM techniques have gathered multi-field attention due to their effectiveness, high efficiency, and eco-friendliness with regards to dye degradation. ZVMs composed of iron, magnesium, zinc, nickel or aluminium are specifically noted for their stability in a wide temperature range in water, high surface area, contaminant degradation efficiency, cheapness and simple mode of operation. They have shown the ability to break down dye molecules into compounds that are easier to mineralise by biological treatment techniques [68]. The surface activity of ZVM is of significant importance with regard to the degradation reaction of organic contaminants, since the degradation reaction involves a redox process in which surface metal atoms lose electrons to cleave the active bonds of organic molecules.

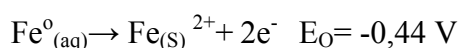
As regards to the reaction mechanism, ZVM particles can provoke the degradation of organic pollutants by chemical reductions but it may also cause simultaneous adsorption or even precipitation. The specific degradation reaction of the contaminant molecules is dependent on the particular interaction between ZVM particles and the contaminated solution which changes as a function of the particles composition and the characteristics of the aqueous solution. Many different mechanisms have been proposed in different systems and, in many cases, they remain still unclear.

Whatever the decolourization mechanism, there will be several factors that will determine the effectiveness:

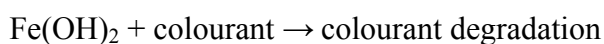
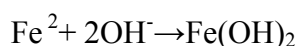
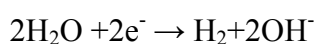
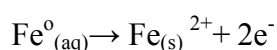
a) First of all, the active surface of the ZVM is important, therefore, the main determinant of the efficiency is the process of preparation of these particles. The more surface and mobility the particle has, the more contact with the dye and, therefore, the more reactivity.

b) Second, good reactivity. A redox reaction is generated in which the surface of the metal loses electrons, so it is oxidized, and breaks the azo bond of the organic molecule of the dye which is reduced [69]. The reaction time usually changes a lot and depends on the reagents or the different mechanisms that can interfere.

In many cases, the degradation of organic molecules with zero valent metals is produced by a series of reactions which will be explained below. For example, the case of the Fe⁰ ZVMs, which have a high reduction potential, allows to reduce the azo bonds efficiently due to the ease of oxidation and transfer of electrons



First the corrosion of the Fe of zero valent is initiated, that is, the ionization of the metal. The electrons derived from the metal are captured by protons generating H₂ and OH⁻, which with the presence of the hydrogenated metal catalyst generates Fe hydroxide. This reacts by breaking the organic molecule that in our case is the colourant. It is also possible that the electrons are directly given to the functional groups of the compounds.



The mechanism of degradation of the azo bond to the surface of the ZVM is shown in Figure 1-6-1. This scheme is a representation of the decolourization of the Orange II dye treated with iron particles. We see the breakage of the double bond and the amines as products of the reaction after all the sub-reactions explained above have occurred.

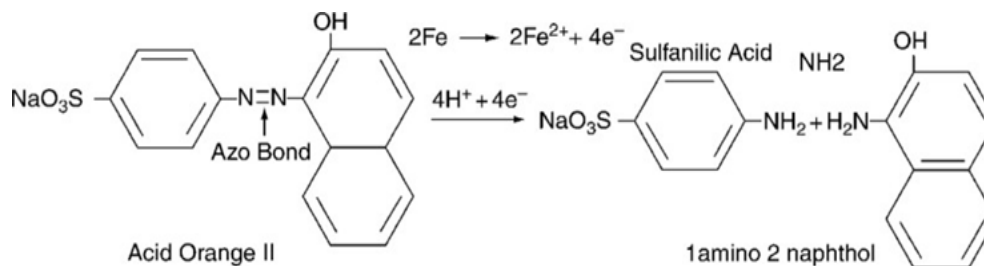


Figure 1-6-1. Diagram of degradation of the azo link of the Acid Orange II dye in a solution using MVZ of Fe and products resulting from the breakage of the link together with the reactions of the elements that intervene[70].

The most commonly used MPs are iron [71] and magnesium [72], but we also found zinc [54], titanium [56] or Mn and Al [73], among others that have high reduction powers to degrade organic compounds.

There are several studies on the decontamination of azo compounds using metallic particles. It should be mentioned that many experiments are carried out using some commercial dyes which are shown to work better. The azo dyes most commonly used in the studies are Reactive Black 5, Orange II - Acid Orange 7 [73], Methyl Orange [74], Orange I [75], although there are studies with multiple different colours such as Methyl Red[76], Remazol Brown[77], Tartrazine[78], Direct Blue71[79], Sudan I[80], Congo Red[81], Methylene Blue[82], Amaranth[83], etc.

Recently it has been discovered that the homogenous single-phase structure of metallic particles in a metastable state radically increases decolourisation water-treatment effectiveness. To be more specific, certain material science production routes - such as mechanical alloying or melt spinning/gas atomization rapid solidification methods - have been used to create metallic metastable particles that deliver a significantly faster response relative to the powders used in the past for decolourisation treatments [84].

Although it seems that there are many studies, tremendous effort is still needed to verify that MPs are efficient for most commercial dyes. It must be shown that it is an efficient method in a generalized way for azo dyes and it is necessary to know all the factors, thoroughly from the search and the validation of the results, before implementing any technology based on this method.

This work's intention is to develop a treatment procedure for the decolourisation of chemically distinct, textile dyed wastewater. Batches of Manganese-Aluminium (Mn-Al)

metallic powder were fabricated by the mechanical ball milling method using respective batches of pure Al and Mn powders. Ball milling is a well-known and ancient technique for grinding and blending materials for a wide variety of applications. The manageable surface shape of Mn particles and Al-based alloys provides a promising surface activation method for novel chemical applications.

2. Objectives

The overall objective of this work is to study the feasibility and efficiency of degrading the azo bond of textile dye molecules in aqueous solutions through metallic particles of manganese and aluminium. To achieve this, several specific objectives were established:

- Design of the production route of MPs and characterization of the MP decolourization capacity as function of the synthesis process. The MPs will be produced by ball milling but using different milling times, thus obtaining different particle sizes as well as different inner structures. The morphology and structure of the synthesized particles will be studied by electronic microscopy and x-ray diffraction.
- Determination of the effects of temperature and pH in order to study the capacity of Mn-Al MPs to break the azo link of the Orange II colour molecule in different conditions. We will use the dye molecule Orange II as a benchmark compound to test the decolourizing efficiency of the Mn-Al particles.
- Determination of the minimum dosage of MPs for complete colour degradation. Tests using different amounts of particles per litter of dyed aqueous solution will be performed.
- Understanding of the underlying mechanisms involved in the decolourization reaction. It is assumed that the decolourization process occurs by the degradation method in which, depending of the author, Aluminium or Manganese are the determining element of the degradation reaction of the azo bond. Therefore, a kinetics study will be carried out to study the activity of Manganese (Mn) and Aluminium (Al) while degrading and this will be verified using Mn-Al particles with different proportions of each element but produced with the same mechanical grinding process. The comparative analysis of which particles work best will be used to determine which is the role of the different elements (Al or Mn) in the reaction. Analyses of the water and the metallic particles of each composition will be done to see how they have interacted with the dye during the decolourization process and compare the decolourization efficiency between the zero-valent iron MPs and the Mn-Al alloy used in this work.
- Since Mn-Al metallic particles work for the Orange II dye, we will test if they are also capable of decolourizing, by the azo bond degradation method, other dyes such as Orange G and Acid Black 58. By means of kinetic studies under different conditions (Temperature, pH, properties and amounts of particles) we will test if

the metallic particles with $Mn_{70}Al_{30}$ composition are able to decolourize and degrade these other colourants. In the case of complete decolourization, particles will be analysed to understand the mechanism.

- Study of the possibility of recovery and reuse of the MPs once used. The reuse of MPs used in a decolourization test is possible, although a decrease in its degradation efficiency is expected. To avoid this reduction, it is assumed that the washing of the particles is useful. Four different treatment paths will be followed in this study. Each alternative will follow the same protocol as regards the degradation test, the method for recovering the particles and the number of cycles performed. Three of the recovery routes will consist of washing with ethanol, acetone or distilled water with pH 3. The fourth way is to reuse particles recovered without washing them. The objective is, following this methodology, to verify which washing is more efficient to maintain the capacity of degradation in the successive cycles; and up to how many cycles can be performed until the particles are inefficient.
- Temperature is an influential factor in the treatment of degradation of azo dyes, so providing thermal energy during this process accelerates the decolourization and, therefore, reduces the reaction time and increases the efficiency. The objective is to characterize with physical parameters the influence of the temperature on the degradation reaction of the colourant studied. For this purpose, tests will be carried out at different temperatures to determine kinetic parameters of interest, such as the characteristic time of reaction and the activation energy.
- Colour present in the textile dye wastewaters can be reduced to a level which is safe to be discharged to fresh water sources. We will examine whether a trickling filter using willow chips is a suitable support medium able to treat the wastewater to meet the environmental regulations standards.

3. Methods and materials

Metallic particles (MP) play a very important role in this treatment methodology, as they are catalysts for the reaction to degrade the colouring molecules present in the textile wastewater. As described in the introduction of this work, there are many types of MPs showing high efficiency for this kind of application, and more are still needed to be investigated. The particles can be of a single type of metals or alloys combining various metallic elements in different proportions. Also, the production methods include different techniques such as rapid cooling, gas atomization or mechanical alloying in metallurgical mills. Both the composition and the method of production are key factors in the decolourization capacity of MPs. In this work we study the decolourization capacity of particles composed of Aluminium and Manganese and produced by mechanical alloying.

Different percentages of molar fraction have been used: Mn (100% Mn), Al (100% Al), $Mn_{50}Al_{50}$ (50 at% Mn and 50 at% Al) and $Mn_{70}Al_{30}$ (70 at% Mn and 30 at% Al). Table 3-1 shows the quantity of each element used in order to produce each batch of the particles:

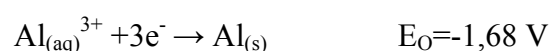
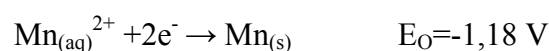
	Mn	Al
$Mn_{50}Al_{50}$	29.0 g	59.00 g
$Mn_{70}Al_{30}$	82.61 g	17.39 g

Table 3-1. Amount of Mn and Al to produce 100 g of $Mn_{70}Al_{30}$ and $Mn_{50}Al_{50}$ MPs.

3.1 Obtaining the alloy

In order to obtain the MPs powder, first of all, the alloy must be obtained with the appropriate proportion of the two metals, making the relevant mixture in certain quantities. The amount of each element needed to produce each composition was calculated taking into account the purity of the material, expressed as an atomic percentage, as indicated by the commercial supplier.

The standard reduction potentials of manganese and aluminium separately in normal conditions, that is to say at a temperature of 25 °C / 298.15 K, a pressure of 1 atm / 100 kPa and in an aqueous solution are:



These high reduction potentials indicate that they can have a good ability for decolourizing. As discussed below, Aluminium has a tendency to oxidize higher than manganese.

Not only does the composition affect a better or worse efficiency to degrade each colour, also the way of production modifies the characteristics of the reaction. The production method includes different factors that are determinants for the final form of the particles, such as the time of consecutive milling and cooling intervals and the rotational velocities of the mills among others.

The production method of the MPs has been the mechanical alloying, which firstly achieves the two original metals to dissolve within each other, forming an Al-Mn alloy. This process consists of a mechanical abrasion treatment. The pure raw elements are introduced into a container with balls of hard material to obtain a powder of particles formed by Al-Mn, with a particle size of the order of micrometres. For this work, MPs have been obtained with three different processing times (20, 30 and 60 hours), also referred as milling times. The difference between the procedures is the total time the machine is working, since it does not do it continuously but at intervals of 10 minutes of milling and 5 minutes leaving the metal resting. The name that identifies the different particles used in this work takes into account only the milling time, it does not include the periods that the metal is resting. An inverse rotating direction was adopted to mill the samples and the speed of the jar upon ball milling was 500 rpm.

The alloy samples were grinded with a mechanical mill Mixer / Mill 8000M, in the Laboratory of the Materials and Thermodynamics Research Group (GRMT), of the Department of Physics of the University of Girona (UdG). In Figure 3-1-1 we can see the mill used to grind the alloy to obtain the Mn-Al powders (a), and the cylindrical container with the metal balls (b). These balls are in charge of breaking and milling the initial materials, reaching a size of the order of micrometres [85].



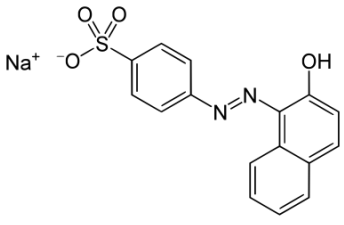
Figure 3-1-1. (a) Mechanical mill Mixer / Mill 8000M. (b) Work cylinder and mill ball (GRMT).

3.2 Dyes

The dyes studied in this work were Orange II, Orange G, Brilliant Green and Acid Black 58. The main characteristic of the first two dyes is the presence of an azo bond in its molecular structure. As explained in the introduction, and will be described in more detail in the results chapter, this link is broken due to the interaction with the MPs, breaking the molecule and eliminating colour. Brilliant Green does not belong to the azo dye family. This compound has been chosen to make a first test of the effectiveness of the decolourization treatment with MPs in other families of dyes.

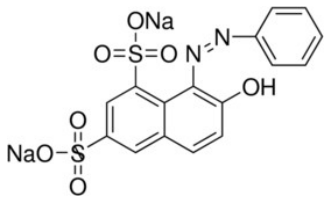
Orange II

Table 3-2-1. Basic data for the identification of the Orange II dye, as well as an image of the molecular structure.

CAS Number:	633-96-5	
Empirical formula (Hill System):	C ₁₆ H ₁₁ N ₂ O ₄ NaS	
Molecular mass (g mol ⁻¹):	350.32	
Beilstein Registry Number:	3898201	
Colour Index Number:	15510	
EC Number:	211-199-0	
Dry weight content:	≥85%	
Absorption (λ _{max}):	485 nm	
Commercial Company:	Sigma Aldrich	
Other Names	<i>Orange II sodium salt, Acid Orange 7, 4-(2-hydroxy-1-naphthylazo)benzenesulfonic acid sodium salt</i>	

Orange G

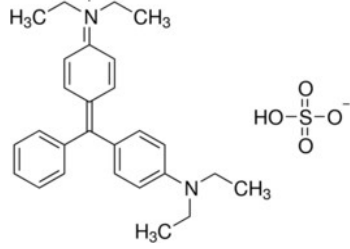
Table 3-2-3. Basic data for the identification of the Orange G dye, as well as an image of the molecular structure.

CAS Number:	1936-15-8	
Empirical formula (Hill System):	C ₁₆ H ₁₀ N ₂ O ₇ Na ₂ S ₂	
Molecular mass (g mol ⁻¹):	452.4	

Beilstein Registry Number:	4120705
Colour Index Number:	16230
EC Number:	217-705-6
Absorption (λ_{\max}) :	474 nm
Commercial Company:	Sigma Aldrich
Other Names	<i>Acid Orange 10, Wool Orange 2G, 7-Hydroxy-8-phenylazo- 1,3-naphthalenedisulfonic acid disodium salt</i>

Brilliant Green

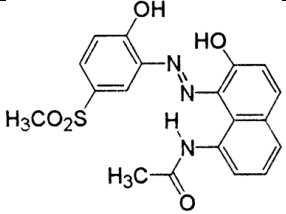
Table 3-2-4. Basic data for the identification of the Brilliant Green colourant, as well as an image of the molecular structure.

CAS Number:	633-03-4	
Empirical formula (Hill System):	C ₂₇ H ₃₄ N ₂ O ₄ S	
Molecular mass (g mol ⁻¹):	482.6	
Beilstein Registry Number:	3901207	
Colour Index Number:	42040	
EC Number:	211-190-1	
Dry weight content:	≥90%	
Absorption (λ_{\max}) :	628 nm	
Commercial Company:	Sigma Aldrich	
Other Names	<i>Brilliant Green, Basic Green 1, Ethyl Green, Malachite Green G, Diamond Green</i>	

Acid Black 58

Table 3-2-5. Basic data for the identification of the Acid Black 58 colourant, as well as an image of the molecular structure.

CAS Number:	12218-94-9	
-------------	------------	--

Empirical formula (Hill System):	C ₁₉ H ₁₇ N ₃ O ₅ S	
Molecular mass (g mol ⁻¹):	399,42	
Beilstein Registry Number:	3901207	
Colour Index Number:	12230	
Absorption (λ _{max}):	689 nm	
Commercial Company:	Sigma Aldrich	
Other Names	<i>Neutral Grey BL, Acid Grey BLN, Acid Grey GL, Irgalan Grey BL, ...</i>	

3.3 Decolourization treatment

The decolourization treatment consists in using MP as catalysts for the reaction. Firstly, a solution of the colourant is prepared with a determined concentration in water. In the case of the study of the degradation of the Orange II dye, this concentration has remained constant in most trials. Subsequently, a certain amount of MP is added to the solution. This dosage of particles has changed throughout the trials, in order to optimize the relationship between the concentration of colourant and the dosage of MP powder most suitable to study the kinetics of the reaction, i.e. determining its kinetic parameters and, at the same time, study extreme values of the colourant concentration vs MP dosage ratio. Once the dyed aqueous solution sample and the MPs are put in contact, the test begins. The sample should be kept in continuous agitation in order to keep the particles in suspension and promote, as much as possible, a homogenous reaction in the whole medium. With this aim, the degradation tests were carried out in glasses of precipitation using a magnetic stirrer with constant agitation (400-500 r.p.m.).

3.3.1 Preparation of the solutions

To prepare the solutions, a volume of 1 litre of distilled water was measured with a volumetric flask, and a quantity of colourant powder, of the order of milligrams (mg), measured with a high precision scale (Semi-micro Discovery 8), was dissolved. Once the mother solution was prepared, a test tube of a volume of 100 millilitres (mL) was extracted in order to perform each decolourizing test. In the trials made at different pH, the necessary amount of hydrochloric acid (1 molar), or sodium hydroxide (2 molar), was added to reach the desired pH values.

For the study of the kinetics, the Orange II and Orange G dyes were used, with colouring solutions at a concentration of 40 mg per litre (mg/L) of distilled water. For the study of toxicity before and after the treatment, measured in the three colourants, the concentrations of the dyes were chosen as 150 mg/L. Acid Black 58 solutions were prepared also with 150 mg/L.

3.3.2 Colour analysis

During the decolourizing tests, a sample of the dyed solution was taken prior to the start of the test and, afterwards, at specific time intervals once the test started. The extracted samples were used to monitor the change in the dye concentration as function of reaction time. The samples extracted from the coloured solutions, that contain MPs in suspension, must be filtered in order to not interfere with the reading of the spectrophotometer. The amount of solution extracted in each one of the samples was 5 mL, the minimum volume necessary to fill the cuvette of the spectrophotometer. The MPs were separated with filters with a light pass of 1.2 micrometres (Titan 3™ Thermo Fisher Scientific), since the size of the MPs is superior and they are therefore retained in the filter. During the decolourizing experiments, absorbance was measured at regular time intervals, every 5min in most of the cases. The duration of the experiments was variable depending on the conditions, in most cases they lasted until the visible colour was vanished and the water became transparent or until the decolourization reaction stabilized. Figure 3-3-1 shows an image of the filter used. Several tests were done in different temperature (25°C, 35°C and 45°C) and pH conditions (4, 7, 10). To modify the temperature, the magnetic stirrer heating plate was used while the solution was in agitation.



Figure 3-3-1. Filter Titan 3 of 1.2 µm.

To analyse the colour of the sample before, during and after treatment, a UV-2600 Shimadzu UV-vis spectrophotometer was used. The test parameters were configured to monitor absorbance (Abs) with a 1 nm wavelength pass, in the area of the spectrum of visible and ultraviolet light, wavelengths (λ) between 200 and 800 nm, producing an absorbance-vs-wavelength spectrum of 601 points.

Absorbance can be defined as the amount of light absorbed by the solution and will be proportional to the concentration of the molecule that absorbs the light, in this case the dye molecules, according to the Beer-Lambert law. In the configuration used, the spectrophotometer measured the transmittance (T), which relates the amount of light, or transmitted intensity (I_t) that reaches the photosensitive cell, and the light emitted, or incident intensity, which illuminates the sample (I_0). Absorbance is determined from transmittance by means of the equation (3-1)[86] and is a magnitude proportional to the concentration of the molecule that contains the chromophore group responsible for the absorption of light. The absorbance results from the spectrophotometer were obtained by the UV-probe software program. Before starting each test, a target was made with distilled water (baseline) to have a point of reference for the rest of the measurements.

$$T = I_t / I_0 \quad (3-1)$$

$$\text{Abs} = -\log(T) \quad (3-2)$$

As mentioned above, a filter was used when sampling during the decolourization test. One of the concerns here was to assess if the filter could produce a decolourization effect by itself due to adsorption of the dye molecules. In order to check that the results were not affected by the filtering method an absorbance analysis of a non-decolourized solution sample was performed with and without filtering. Figure 3-3-2 shows that the effect of the filter is barely observed in the spectrum. Figure 3-3-2 also shows the difference between a decolourized sample with and without the filter, where the effect of the MPs in suspension is clearly seen in the spectrum.

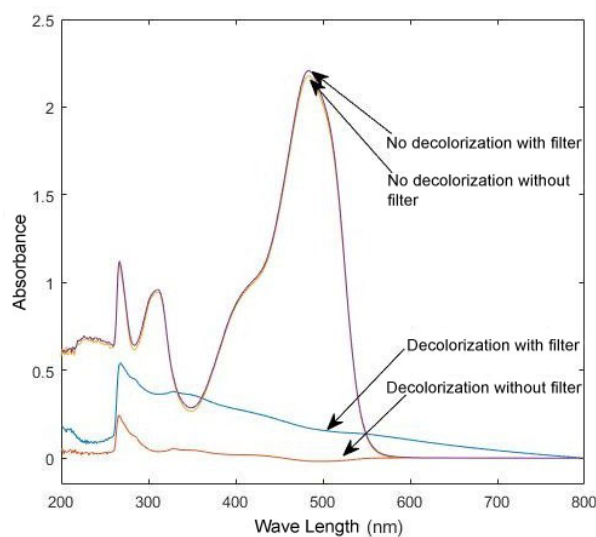


Figure3-3-2. Absorbance analysis of non-decolourized solutions before adding MPs with and without passing through the filter and comparison of decolourized solutions after adding MPs with and without filtering.

In the case of the decolourized sample, that is, only the distilled water solution with Orange II, it can be seen that the use of the filter does not produce significant changes in the measurement of absorbance. This discards that the filter adsorbs dye molecules and therefore may affect the results. On the other hand, in the decolourized sample, there is a great difference that justifies the need to use a filter. This difference is due to the presence of MP suspension in the aqueous solution [87][88].

The separation of the MPs from the dyed solution by filtering, instead of other methods like centrifugation used in many other works of MP-mediated decolourization reactions, has the advantage of being an almost ‘instantaneous’ method, as the filtering is performed at the time of sample extraction. This avoids some artefact effects on the determination of the reaction kinetics that could be caused by the delay between the extraction, the MP separation and the colour analysis. The effect can be important in the case of very fast reactions as the ones usually reported in this kind of works [89][90][91].

In the particular case of the decolourization experiments of Acid Black 58 as an additional experiment to verify and understand the decolourizing process, a Medifriger BL centrifuge was used in the laboratories of Baix Llobregat Campus of the UPC. The program used was 10 min, 3000 r.p.m. at 20 °C. The reason of the use of centrifugation in this case is that this colourant presented a high degree of adsorption on the surface of the particles, and also in the filter, and the centrifugation was used to assess this aspect as will be discussed in the results section.

In order to relate the absorbance measured with the dye concentration, calibration curves were obtained from solutions prepared with different dye concentrations. The calibration curve of Orange II dye is shown in Figure 3-3-3. The absorbance value used is the one measured at the peak of the absorbance of Orange II at 485 nm [92].

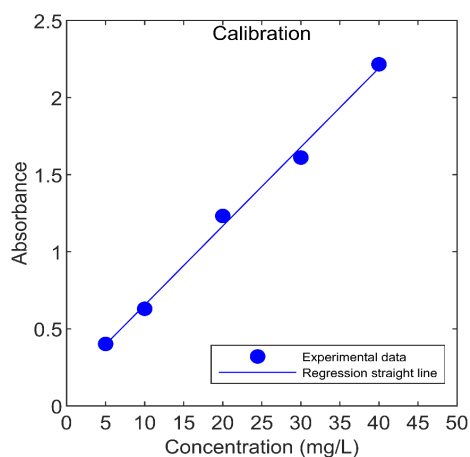


Figure 3-3-3. Calibration straight ($R^2 = 0.9826$; $y = 0.0562x$) to the maximum absorption of the molecule of Orange II.

The curve of the figure allows to transform the results of absorbance into concentration (mg /L) of active dye molecules. The calibration curves of Acid Black 58 and Orange G were obtained in the same way by measuring different dilutions diluted in different ratios with distilled water; Orange G: 1/5, 1/10, 1/20 and 1/30 and for Acid Black 58: 1/10, 1/75, 1/100, 1/125 and 1/150. Obtaining the calibration curves shown in Figure 3-3-4.

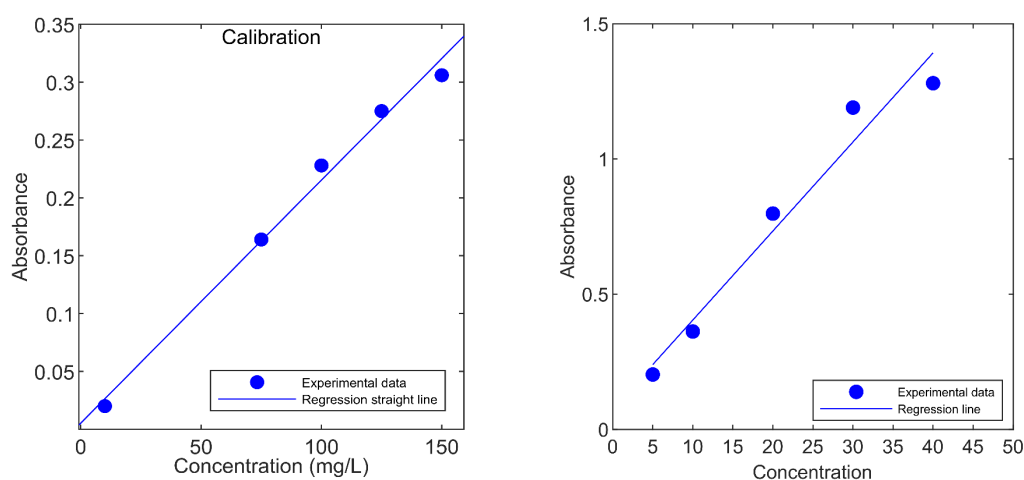


Figure 3-3-4: Acid Black 58 calibration line ($R^2 = 0.99$, $y = 0.0021x$) between concentration and the absorbance at the maximum peak. Orange G calibration line ($R^2 = 0.99$, $y = 0.039x$) between concentration and the absorbance at the maximum peak [93].

In all the colour fading tests a minimum of three replicas were made. The temperature at which they were made was noted. The initial pH was measured but its evolution during the treatments were not monitored. To serve as a visual example, in Figure 3-3-5 we can see a sample of distilled water solution with dissolved Orange II (left) and a sample of the same water after the decolourization process was finished, with a total degradation of the dye.

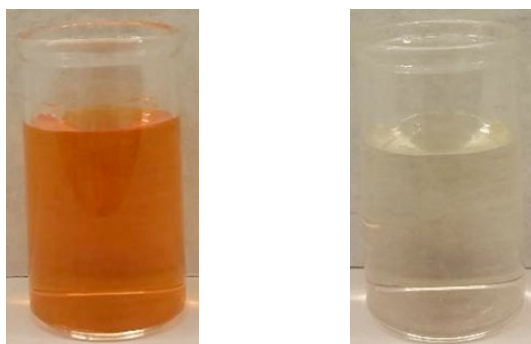


Figure3-3-5. Sample of the solution with Orange II dye before the decolourization treatment (left) and after (right). The treatment was with MP Mn₇₀Al₃₀ with a dosage of 50mg of particles / 100mL of solution.

3.4 Kinetics

The study of the degradation kinetics of the Orange II, Orange G and Acid Black 58 dyes have consisted in the analysis and processing of the data obtained from the spectrophotometer with Excel and MATLAB software.

In addition to obtaining the spectrum graphs, some basic kinetic parameters were defined to characterize the reaction kinetics, such as the characteristic time of the reaction (τ) and the activation energy of the reaction. The calculations of activation energy are explained below. To determine the τ of a reaction, an adjustment was made where the quadratic error between the experimental values and the theoretical kinetic model was minimized. Kinetics of a first order reaction were always considered, corresponding to the equation (3-3)[94]

$$C(t) = C_{sat} + (C(t_0) - C_{sat}) e^{-t/\tau} \quad (3-3)$$

taking as the initial concentration $C(t_0)$ the value of the initial solution. The saturation concentration value C_{sat} takes zero value whenever the decolourization process is completed. In cases where the process stops, before complete decolourization, the concentration of saturation takes the value of the concentration of the sample at the moment when the degradation of the dye stopped.

Once the theoretical value of concentration was determined at each time interval, and the quadratic error between the theoretical and experimental values calculated, the Excel software, in particular Solver function, was used to determine the value of τ that minimizes the difference between the model and the experiment. This value of τ changes depending on the test conditions, such as temperature, pH or the amount of MP used. Once the value of τ was determined at different temperatures (25, 30, 35, 40, 50 °C), the activation energy E_a of the reaction was determined according to the Arrhenius equation (3-4) as the product between the slope of the straight line resulting from the graph $\ln(\tau)$ vs $1/T$ and the ideal gas constant ($R = 8,314 \text{ KJ / mol}$). The value of the activation energy of the reaction is therefore obtained in units of J / mol.

$$\ln(\tau) = \ln(\tau_0) + E_a/RT \quad (3-4)$$

The activation energy determines the sensitivity of the reaction to the change of temperature. Along with this parameter, a pre-exponential factor in time units, which depends on the degree of contact between MP and colourant molecules, can be also determined.

3.5 Toxicity

The analysis of the toxicity of the samples was done at the Universitat Autònoma de Barcelona, in the Department of Chemical Engineering, with a Microtox System from Microbis Corporation. The test is based on the use of the *Photobacterium phosphoreum* microorganism, which exhibits bioluminescence. The objective of this analysis is to evaluate the toxicity of the colourant before being treated, as well as that of the products generated as a result of treatment with MP.

The reagents used in the toxicity analysis were:

- Lyophilized *Photobacterium phosphoreum*, is stored at -20°C and is re-suspended at the time of the trial (Microtox Acutue Reagent Ref. AZF686010A)
- Reconstitutive solution (Microtox Diluent Ref. AZF686004)
- MOOS osmotic solution (NaCl 22% by weight)
- Dilute solution (NaCl 2wt%)

The toxicity value that is obtained from the analysis, the EC50, corresponds to the concentration of the sample analysed that causes the decrease of luminosity by 50%, thus quantifying the amount of sample analysed that causes the death of 50% of the population of *Photobacterium phosphoreum*, under certain conditions of time and temperature. The higher the value of this parameter the less toxic is the sample. Measurements for the test were done with 5-minute trial times, at a temperature of 15 °C and pH 7. Toxicity units are expressed in TU. The relation between EC50 and TU is given in equation (3-5). From this trial, it can be determined whether the aqueous solution increased or reduced the toxicity after the treatment, and therefore if the bleaching method would be really useful for application in real water treatments.

$$TU(\%) = 100 / EC_{50} \quad (3-5)$$

3.6 Chemical analysis of the decolourized water

High-resolution liquid chromatography (HPLC) was performed at University of Girona (UdG). We analysed qualitatively and quantitatively the Orange II dye in the coloured solutions and the intermediate components generated during the decolourization. These techniques were used to analyse and determine the distribution of the molecules of the substance according to its mass and analyse with

great precision the composition of the different chemical elements. The HPLC-MS study was carried out with a Beckman Gold chromatography equipment. We injected first of all 50 μL as blank, 20 μL for Orange II coloured solution and 50 μL of degraded samples, using a Zorbax Eclipse Plus C18 column, Narrow Bore (2.1x150mm) 5-Micron at 30°C. A dissolution of ammonium acetate and methanol 90:10 (v/v) was used as a mobile phase. The selected pressure was 400 bars. The flow rate was 0.5 mL/min with a stop time of 30 min. Chromatography was obtained at 485 nm wavelength for the dye (maximum colour wavelength) and 250 nm for degraded samples, where we believe that we could find the compounds originated from the degradation according to the bibliography [63].



Figure 3-6-1. High resolution liquid chromatograph (HPLC).



Figure 3-6-2. Mass spectrometer (MS).

Flame Atomic Absorption Spectrometry (A-2000, Hitachi, at Universitat de Girona) was carried out as a chemical analysis technique to analyse the content of metals (Mn and Al) that existed in the water once decolourized. This technique allowed us to assess the amount of metal particles dissolved in the aqueous medium during decolourization. Only some selected samples were analysed with this technique. The samples analysed were decolourized water by $\text{Mn}_{70}\text{Al}_{30}$ particles (60h) and $\text{Mn}_{50}\text{Al}_{50}$ (60h) at pH 4 and $\text{Mn}_{70}\text{Al}_{30}$ (60h) at pH 7. The calibration lines are shown below:

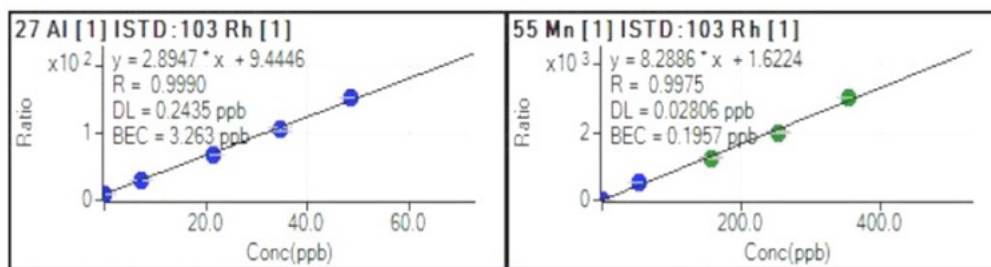


Figure 3-6-3. Calibration of Al and Mn for atomic absorption.

3.7 Analysis of the Mn-Al particles

Scanned electronic microscopy (SEM) was used with compositional analysis using X-ray dispersive energy (EDX) in a Hitachi TM3030Plus Desktop SEM and Phenom

XL equipment at the Research Center in Multiscale Science and Engineering (UPC) to analyse MP samples before and after the treatment. This allowed us to check the morphology of the particles as well as the changes produced during the decolourizing reactions.

The SEM technique is based on an accelerated electron beam applied on an area of the sample. As a result of this interaction, a topographic image of the surface of the samples is obtained and thus its morphology can be studied. In addition, EDX is able to give a very large range of information from the sample surface, such as the proportion of Mn and Al present in the particles. To proceed to the analysis, the particles of the degraded solution were separated and allowed to dry at room temperature for a few days. Once in the SEM lab, the particles were conditioned and disposed on the sample holder discs. The conditions of the SEM study were in secondary mode of electrons, at a voltage of 10 kV for the zoom x175 and 15 kV for the other magnifications. The compositional analysis was also done at 15 kV.

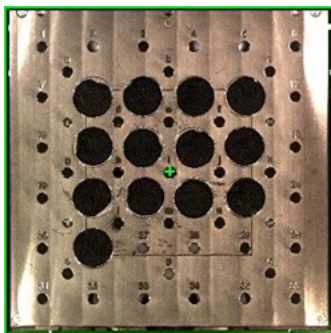


Figure 3-7-1. Samples of MP attached on carbon stickers, prepared for the SEM analysis.

The milled powder was also analysed by X-ray diffraction (XRD) on a Bruker D8 Advance equipment at the Research Center in Multiscale Science and Engineering using Cu-K α radiation to check out the structure of the milled powders.

Specific surface measurements were performed by means of the Brunauer-Emmett-Teller (BET) model in a Micrometrics ASAP 2020 apparatus using nitrogen as adsorbate and helium as non-adsorbing gas for the dead volume calibration. The specific surface is a very important factor in the analysis of the kinetics of this process, since the more surface they have the more points of reaction will be available to interact with the dye. In order to investigate this, measurements were made of the specific surface area of the particles of Mn, Al, Mn₅₀Al₅₀ and Mn₇₀Al₃₀ powders through BET analysis. The specific surface measurements were made in the Department of Materials Science and Metallurgy of the UPC.

Figure 3-7-2 shows a graphical abstract of the colourant degradation experiments including the different characterization steps of the water solutions and the particles.

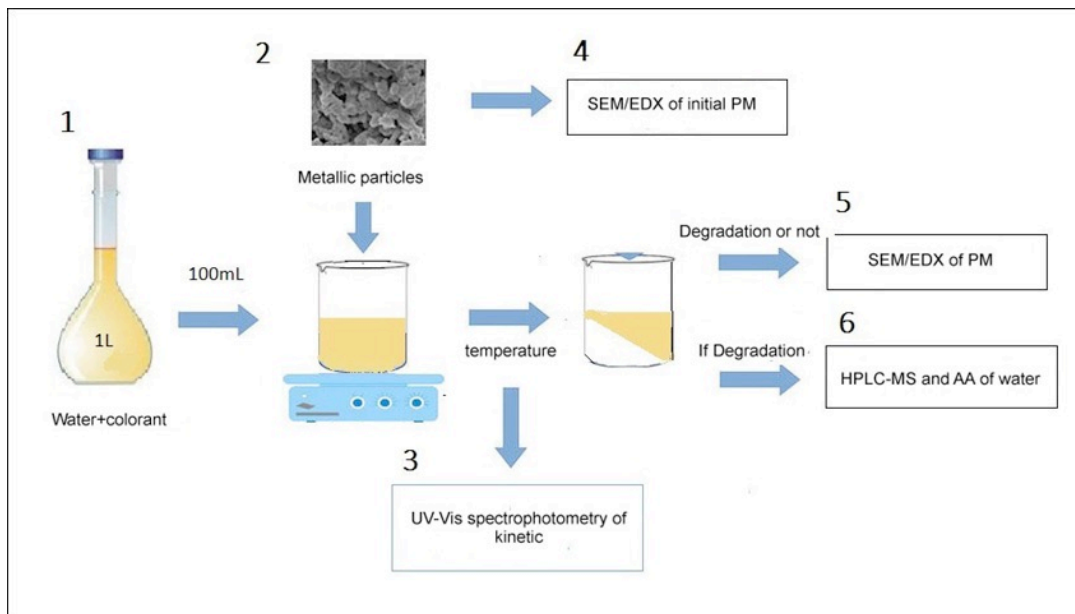


Figure 3-7-2. Summary of the basic steps of the decolourizing experiments and the subsequent analyses.

3.8 Analysis of particle reusability

The objective of this point is to study the efficiency of degradation of the dyes by MPs recovered from previous decolourizing cycles and washed following different methodologies. This study was restricted to colourant Orange II and $Mn_{70}Al_{30}$ particles since, as will be seen in the results section, they show the greatest efficiency in the decolourization process.

As will be detailed below, different types of washing methods were assessed. For each type of washing 4 cycles of decolourizing-recovery-decolourizing were carried out, including the first cycle that was carried out with the as-produced MPs. For each cycle and type of wash, a minimum of three replicas were done. In addition, the 4 decolourization cycles were also performed with recovered but not washed particles.

In order to obtain enough amounts of recovered particles we performed decolourizing experiments with larger amounts of MPs. We used dosages of 0.2g of MPs / mL of coloured solution with different volumes of total solution. The degradation tests were carried out in glasses of precipitation, at room temperature (25 ± 2 ° C) and using a magnetic stirrer with constant agitation (400-500 r.p.m.) similarly to all the other decolourizing tests. To carry out the essays, the same methodology as the decolourizing experiments detailed above was followed, with the difference that instead of discarding the used MPs these were recovered.

3.8.1 Recovery of particles

After each decolourization assay, the solution with MPs inside was allowed to precipitate for 24-48 hours. In order to ensure that the time difference that was left to precipitate did not significantly influenced the subsequent efficiency, we did bleaching trials with MPs that were being precipitated both during 24 and 48 hours. The obtained results were almost identical.

Subsequently, the supernatant was removed with a pipette and a pi-pump. The remaining liquid content was extracted by evaporation by placing the glass on a heating plate. The last step was to measure the amount of particles recovered with the precision scale in order to carry a control.

3.8.2 Particle washing

Three different reagents were used to wash the particles: ethanol, acetone and distilled water with pH = 3 (adjusted with a properly calibrated pH meter by means of hydrochloric acid HCl). Washings were done once the MPs had been recovered after each decolourization cycle.

To wash with ethanol, 0.2 mL of 96% ethanol was used for every 1 mg of MPs recovered. It was left in contact for 4 hours and then removed the supernatant with pipette and pi-pump; the rest of present liquid was removed by evaporation on a heating plate.

The washing with 99.5% acetone and distilled water with pH 3 were carried out with agitation, both following the same methodology: 0.4 mL of the corresponding reagent was added for each 1 mg of MP recovered. They were maintained at constant stirring (300 r.p.m.) with the magnetic stirrer for 2 hours. Then in still conditions for precipitation during 1 hour. The particles were dried in the same way as in the washing with ethanol, by evaporation.

The morphology and composition of the reused MPs were analysed by SEM. The MP characterized by SEM were only those obtained after the first and third degradation-washing cycle (Figure 3-8-1).



Figure 3-8-1. MP analysed with the SEM: not washed (1-3 cycles), ethanol (cycles 1-3), acetone (cycles 1-3), pH3 (cycles 1-3).

It is necessary to specify that the MPs were analysed by SEM once the washing was done; not after recovering them. This choice was made to relate the morphology and composition after being recovered (including the washing step) with its degradation efficiency in the next cycle.

3.9 Biological method

Below, shown in Figure 3-9-1, can be found a schematic diagram depicting the pilot scale trickling filter that was employed in our study.

The trickling filter was comprised of a number of components. First and foremost was a Plexiglas tube with an internal diameter of 20 cm and a total height of 120 cm. Willow chips and plastic were used to construct the supporting material for bacterial growth. A fixed flow distributor was installed at top of the filter to ensure the wastewater was fed to the filter's free surface at a constant flow rate. The wastewater was stirred in a storage tank prior to being fed into the reactor. Air was supplied to the system via an air pump connected to the bottom of the filter. Effluent from the filter's drainage system was collected by a 6L settling tank. The effluent from this tank was drawn to the sewage whereas the supernatant could be fed via a recirculation stream to the top of the filter by use of a recirculation pump.

Effluent release from this tank was managed via a valve and depended on the mode of filter operation; either continuous or SBR (Sequential batch reactor). When the filter was operated in SBR mode the system would employ the typical fill, react, settle, and draw phase sequence. A *settle* phase was included in the timed schedule in order to allow the settlement of escaping solids (if any) in the filter's effluent inside the settling tank. The operation cycle was 1 day, which was composed of a filling phase that lasted 0.5 h, followed by an aerated reaction phase of 23 h, a settling phase of 0.5 h, and finally a

drawing phase that was near-instantaneous. The drawing phase was effected through the manual opening of an outlet valve. An air pump provided the necessary oxygen supply to the flasks. The pH of the treated wastewater was maintained to values between 7-8 inclusive using H_2SO_4 and $NaOH$ solutions. Note that the wastewater was enriched with appropriate amounts of N and P in order to aid microorganism growth.

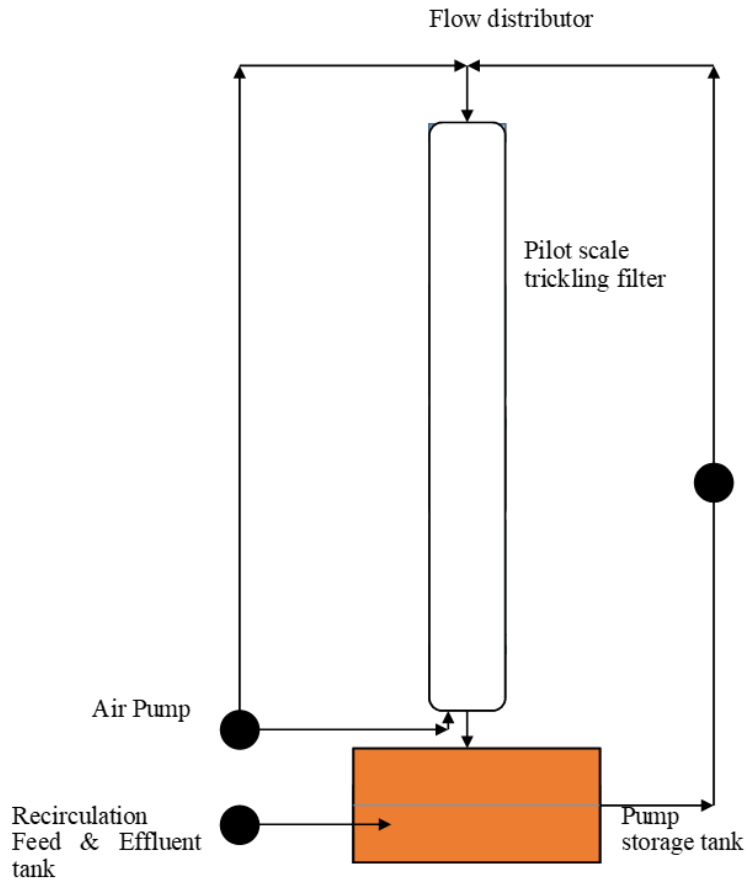


Figure 3-9-1. Schematic diagram depicting the pilot scale trickling filter.

4. Results and discussion

In this work, the efficiency of Mn-Al metallic particles for decolourizing dyed aqueous solutions has been assessed in different ways. In this section we will present and discuss the results obtained for different types of particles, dyes, water conditions like pH and temperature, as well as the analyses in order to characterize the particles and the water after the degradation process. The efficiency of Mn-Al particles on other dyes and the ability of being reused have been also assessed. In this section we will present the results of each of these studies, each sub-section includes the respective analysis and discussion of the results.

4.1 Decolourization tests of Orange II by Mn₇₀Al₃₀-30h particles

The degradation of the Orange II azo-dye was studied controlling different parameters that affect the reaction, including the temperature, the MP dosage and the pH. In this section all the results correspond to MP particles of Mn₇₀Al₃₀ obtained by milling during 30h.

To better understand the degradation of the Orange II dye molecule, in Figure 4.1-1 the spectrum of a coloured aqueous solution is presented at a concentration of 40 mg L⁻¹, where it can be seen that the molecule absorbs the wavelengths of the dye well below 550 nm, resulting in orange colour. The maximum absorption in the visible part of the spectrum corresponds to 485 nm, this wide absorption peak is due to the azo bond (N=N) of the molecule [50]. The peaks at 310 and 230 nm are caused by the aromatic rings of naphthalene (310nm) and benzene (230nm) respectively [95], which are linked to auxochromes (-OH, -SO₃, etc.). The peak in which the study will focus is that of 485 nm, since the decrease in the absorbance of this one indicates the breaking of the molecule.

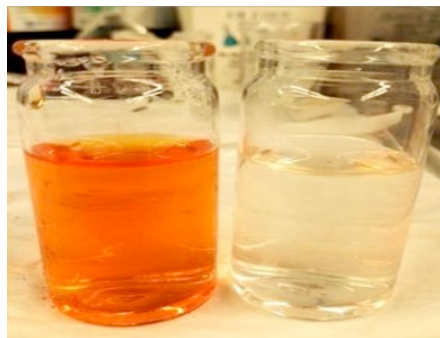
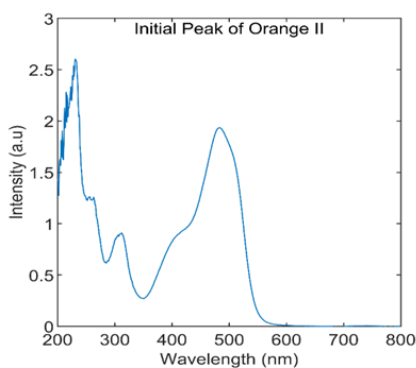


Figure 4.1-1. (Left) Orange II colourant absorbance spectrum at a concentration of 40 mg L⁻¹. (Right) Sample of Orange II coloured solution compared to a decolourized solution.

4.1.1 Effect of temperature

Temperature is an important factor to consider when it comes to studying the kinetics of a reaction. As can be seen in Figure 4-1-2, peaks located at 485 nm and 311 nm wavelength, which according to [95] correspond to the azo bond and the benzene ring of the Orange II dye molecule, decrease as the treatment develops, but they do it at a different rate depending on the temperature at which the treatment is realized.

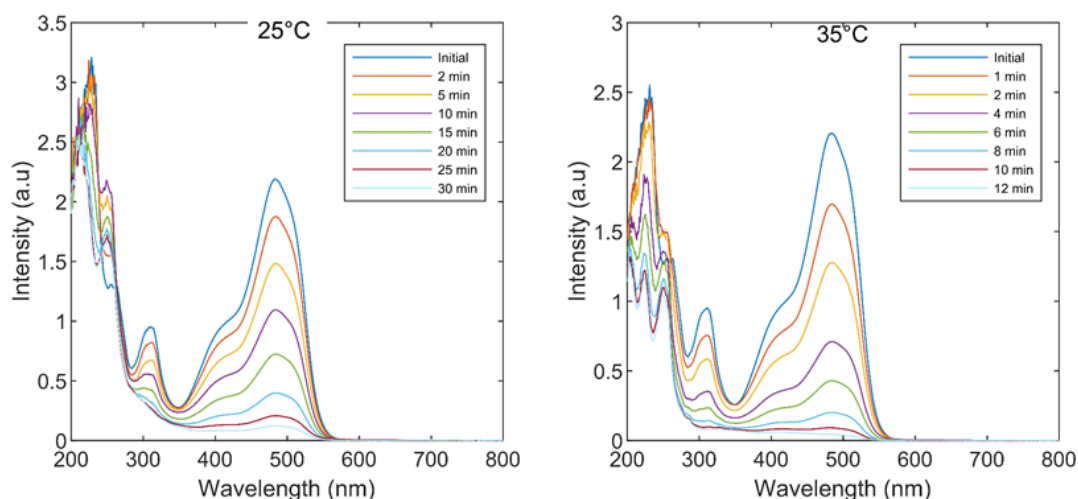


Figure 4-1-2. Absorbance change of the Orange II dyed solution with 100 mg / 100 mL of MP (Mn70Al30-30h) at 25°C and 35°C.

As expected in a reaction following first order kinetics, the change in temperature produces an exponential effect to the reaction rate. Once the absorbance data were obtained, and in order to analyse the results, a mathematical fitting was made as detailed in the Methods and materials section. In this way, the ability of first order kinetics to describe the degradation reaction generated by the Mn-Al particles can be assessed. Subsequently, based on the results obtained at different temperatures, activation energy was also calculated.

Figure 4-1-3 shows the consequences of the temperature on the occurrence of the chemical process studied, where the reduction of the reaction time can be clearly seen as the temperature increases.

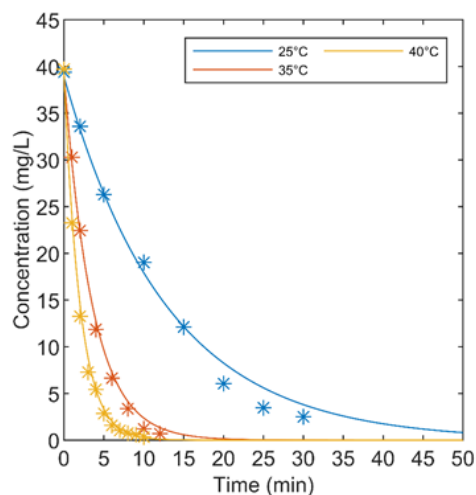
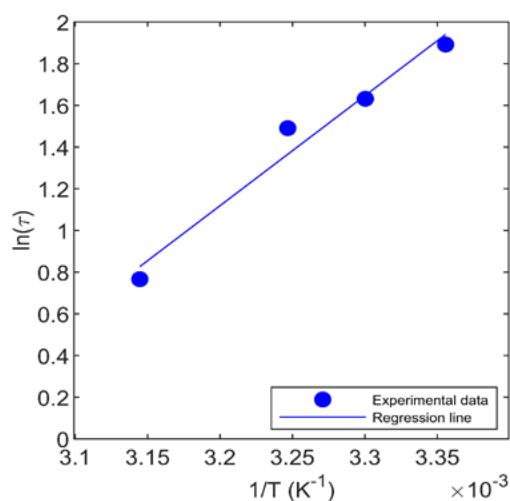


Figure 4-1-3. Kinetics of the reaction at different temperatures (MP 30h; pH 7).

With the experimental data collected in the different tests, we have been able to represent the equation (3-4), in order to calculate the value of the E_a according to its slope. Figure 4-1-4 shows the representation of the above-mentioned equation, along with the experimental data used by that graph. The activation energy, of the degradation reaction of the Orange II molecule, with MPs of $Mn_{70}Al_{30}$ as a catalyst is 43.9 kJ mol^{-1} . Obtaining this activation energy allows to characterize the effect of the temperature on the rate of reaction, which is an important property and, at the same time, allows us to determine the optimal conditions of temperature during the treatment of decolourization. In other works, they determine the value of the activation energy of the degradation reaction of azo dyes with iron MP, obtaining similar values between 27.9 kJ mol^{-1} and 114 kJ mol^{-1} [49][54].



Temperature (K)	T(min)
298	6.6
303	5.1
308	4.4
318	2.1

Figure 4-1-4. Arrhenius Equation ($R^2 = 0.9685$; $f(x) = 5276.3x - 15.765$).

4.1.2 Effect of the particle dosage

The amount of particles used to treat dyes has an effect on the decolourization process, especially in the duration of the treatment. The process of decolourization with different amounts of MP ($\text{Mn}_{70}\text{Al}_{30}$ -30h), all at the same temperature of $25\text{ }^{\circ}\text{C}$, is seen in Figure 4-1-5. It is seen how the rate at which the decolourization of the studied sample is produced is directly proportional to the amount of MPs. It is worth noting what shows the graph regarding the treatment with a dosage of $30\text{ mg} / 100\text{ mL}$, since the process is not fulfilled, and it stops after one hour of treatment. This indicates the lower limit of dosage that can be used in order to obtain a complete decolourization of Orange II solutions. Precisely, the tests performed with dosages of 30 mg and 10 mg of MP ($\text{Mn}_{70}\text{Al}_{30}$ -30h) showed that the reaction was not completed, reaching final dye concentrations of 15.57 and 27.71 mg L^{-1} respectively.

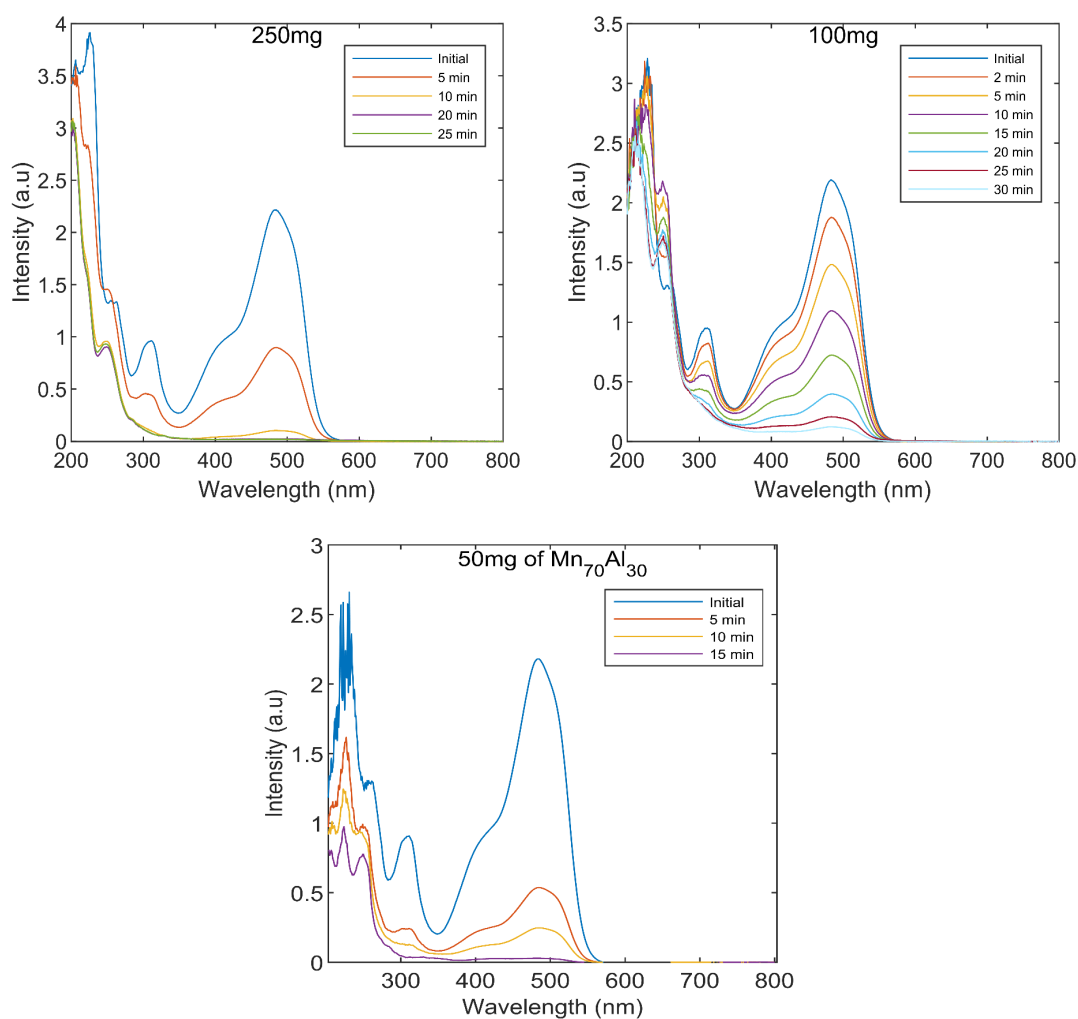


Figure 4-1-5. Absorbance changes of the Orange II dyed solutions after applying different dosages of MP ($\text{Mn}_{70}\text{Al}_{30}$ -30h) at $25\text{ }^{\circ}\text{C}$.

The MPs used have been those obtained by milling during 30 h, since they allow a greater control of the decolourization process with not very fast or very slow kinetics. As shown in Figure 4-1-6, as the concentration of MP decreases, the reaction is slower. A minimum dosage of 50 mg / 100 mL is needed to complete the decolourization reaction in less than one hour.

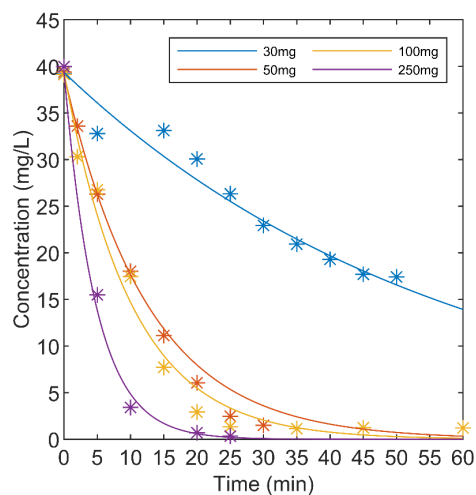


Figure 4-1-6 : Kinetics of the reaction with a different amount of MPs (Temperature 25 °C; pH 7).

As can be seen in the figure the decolourization using 30 mg MP / 100 mL solution does not arrive clearly to saturate, but the characteristic time significantly increases comparatively to the behaviour observed for dosages between 250 and 50 mg. This suggests that we are approaching the minimum dosage limit in order to achieve complete decolourization. To clearly establish the minimum dosage of MPs, it would be necessary to carry out longer-duration decolourization tests.

4.1.3 Effect of pH

The acidity of a dissolution may have an effect on a chemical reaction, and textile industrial waters tend to have variations in their pH. For this reason, the degradation of the Orange II colouring molecule at different pH (4, 7 and 10) were studied to determine if there are significant differences in the rate of degradation. In Figure 4-1-7 we can see the results of the three trials at a different pH, where no significant difference in the reaction is observed. In the next chapter, a more detailed analysis of the data will be made to conclude which effects produce the variations of this parameter.

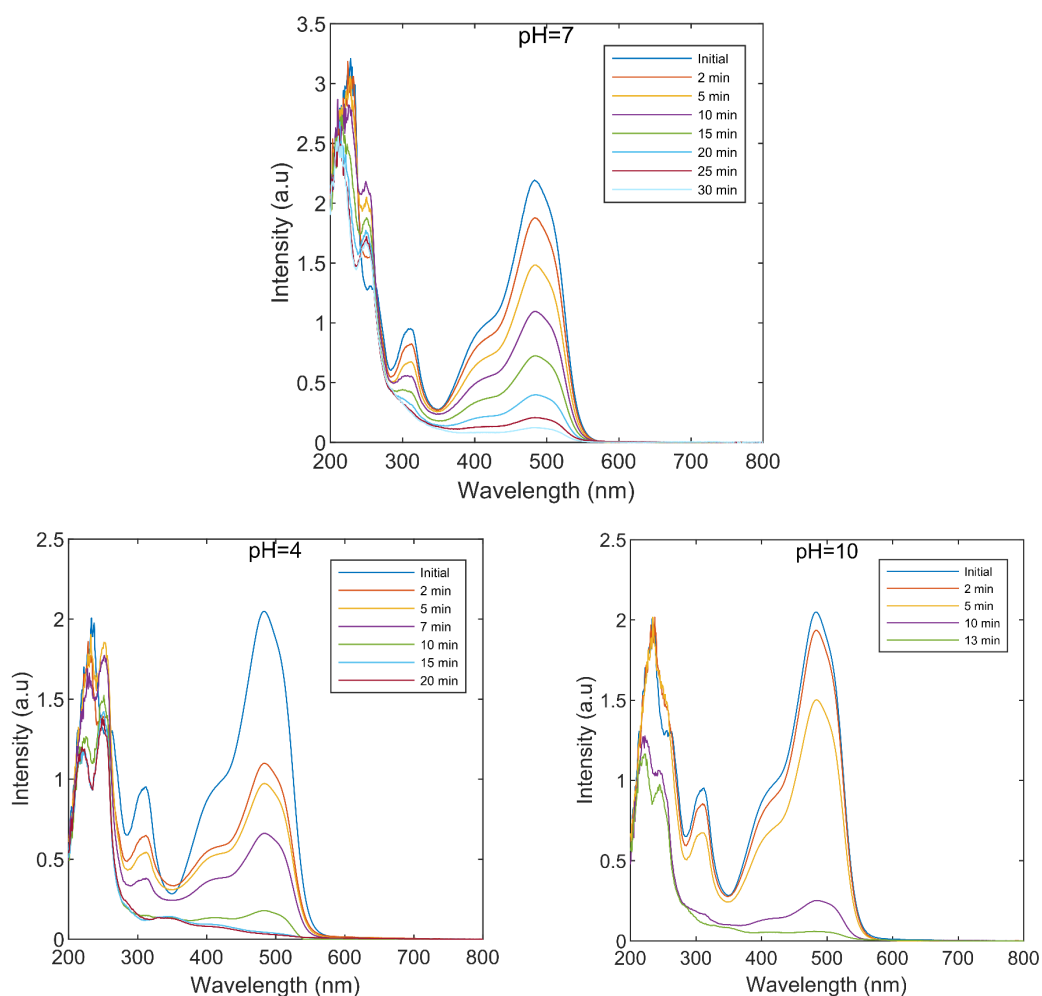


Figure 4-1-7. Absorbance changes of Orange II dyed solutions after applying MP powders at different pH conditions (pH 4, 7 and 10).

As we observe in Figure 4-1-8, the reaction at pH 4 is the fastest of all, but the difference with the others is very small. Therefore, the reaction rate is higher as the medium is more acidic, although the effect of this parameter is not significant. This low influence of the pH is an unexpected and interesting result, since in the majority of the studies in which the decolourization of Azo dyes is studied using metallic particles of other materials such as Fe or Zn, the decrease in pH usually results in a significant increase of the reaction rates. Studies similar to those carried out in this work but using other dyes will allow to determine if the low sensitivity to the pH is a general characteristic of the Mn-Al particles [94][96].

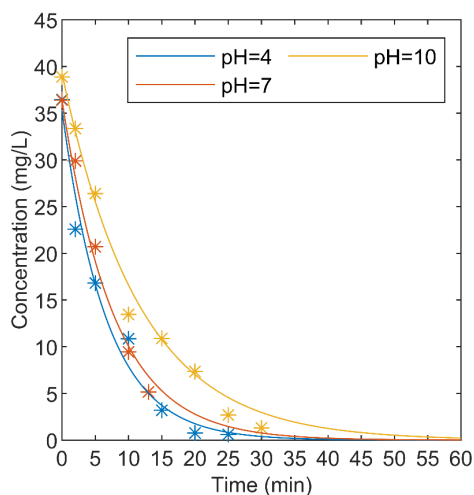


Figure 4-1-8: Kinetics of the reaction with different pH (Temperature 25°C; MP 30h).

4.2 Decolourization tests of Orange II by different types of Mn-Al particles

4.2.1 Effect of the milling time

The effect of milling time during the production of the MP powder was studied using three types of particles produced with different milling times (20 h, 30 h and 60 h). The evolution of the different absorption spectra and the duration of the test was significantly affected. As shown in Figure 4-2-1, MPs milled for 60 hours completely degraded the coloured solution in 15 minutes, while the MPs produced by 20 hours of milling lasted 70 minutes to degrade only three-fourths of the Orange II molecules [97][98].

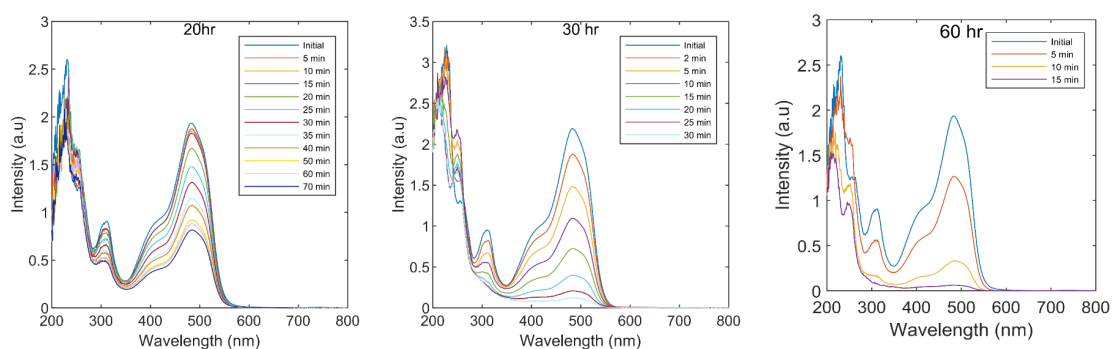


Figure 4-2-1. Absorbance change of the Orange II dyed solution after applying 100 mg / 100 mL of MP particles produced by different milling times: 20 h, 30h, 60h Pat 25 °C.

As mentioned above, the MPs used in this work have been developed with different grinding times, producing differences in their size and internal structure. Figure 4-2-2 shows the microscope images of the different types of MPs obtained by changing the milling time.

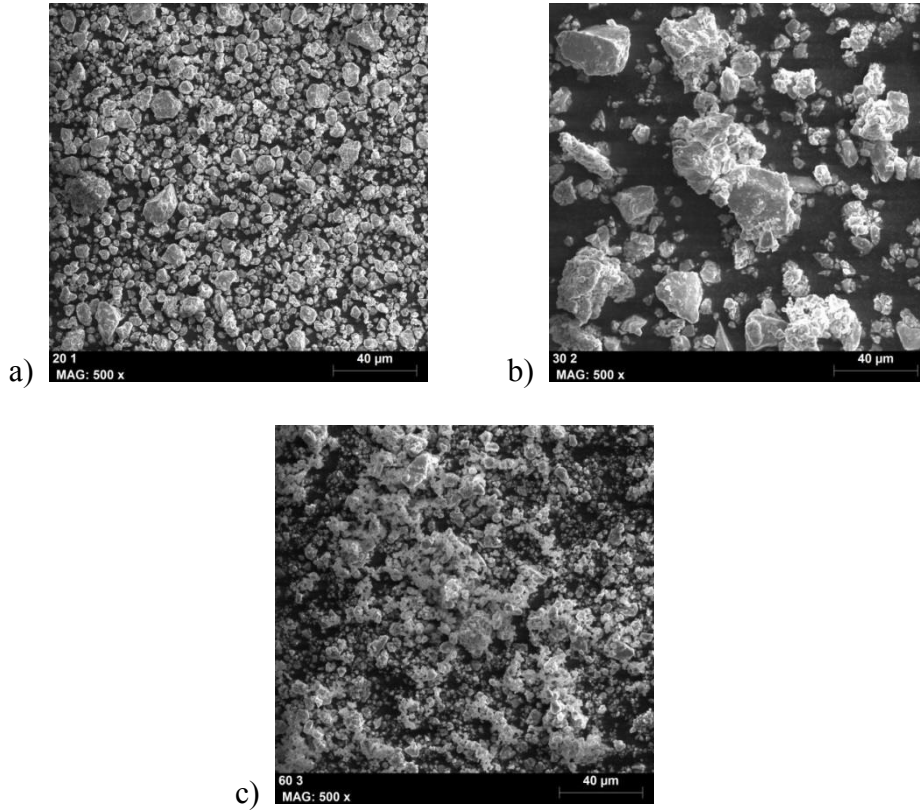


Figure 4-2-2. SEM images of different $Mn_{70}Al_{30}$ MPs produced by milling (a) 20 hours (b) 30 hours (c) 60 hours.

The images in the figure correspond only to a small area of the sample, allowing only a qualitative description. As can be appreciated, the size of the particles is very scattered with a size less than $20\ \mu m$ for most of them. Figure 4-2-2 (b) shows larger particles and aggregates. These large particles do not appear only in the images of the samples milled during 30h, but they are also observed for other times depending on the area of the sample analysed. It is necessary to emphasize the difference between the milled sample at 60h and the others. For this sample, the obtained powder has a finer particle size and the surface of the particles has significantly more roughness.

Figure 4-2-3 shows the XRD patterns obtained from the powders. Together with the SEM-EDX results detailed below, the diffraction patterns reveal that the particles are composed of two crystalline phases, a solid solution of α -Mn(Al) with some regions of pure fcc Al phase. The broad peaks observed in all cases indicate that the size of the inner crystallites composing the particles is smaller than $100\ nm$. The broader peaks observed

for the samples produced by 60h of milling, in comparison with 30h and 20h powders, indicate a higher level of induced strain and smaller size of the crystallites forming the particles.

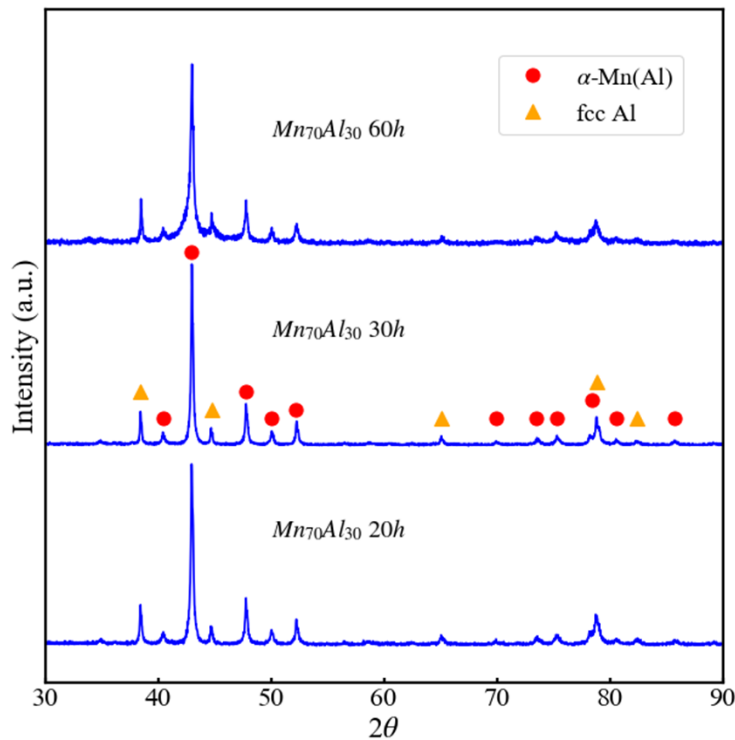


Figure 4-2-3. X-ray diffraction patterns obtained for the samples produced with different milling times.

As already mentioned above, three different types of particles have been studied according to the grinding time that was used for its elaboration. As shown in Figure 4-2-4, the different particles do not catalyse in the same way the degradation reaction of the Orange II dye. It can be seen very clearly as the reaction using $Mn_{70}Al_{30}$ -20h is much slower compared to the particles obtained with 30 and 60 hours. This fact is due to that in addition of the increase the roughness of the particles surface with milling time, the particles obtained are, on average, smaller, and therefore, with the same amount of MP powder there is more specific surface to catalyse the reaction [99]. In addition, as shown by the XRD results in the previous figure, the 60h particles are not only smaller but they contain higher level of strain and smaller crystallites, both things decreasing the stability of the alloy and possibly contributing also to the significant increase in reactivity observed for the $Mn_{70}Al_{30}$ -60h particles.

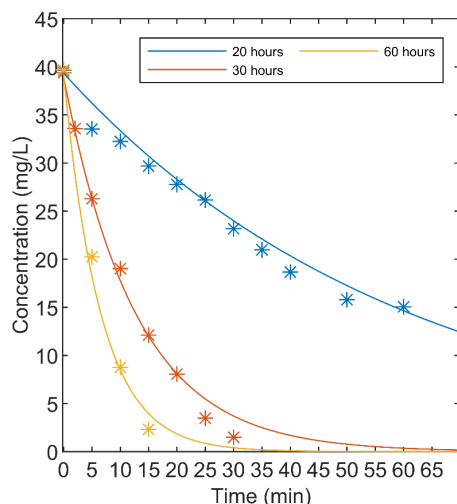


Figure 4-2-4. Kinetics of the reaction with different $Mn_{70}Al_{30}$ MPs produced with different milling times (Temperature 25 ° C, pH 7).

4.2.2 Effect of the particle composition

Following the experimental design explained in the Methods and materials section, the absorbance spectra of the Orange II solutions was monitored while being decolourized by four types of MPs compositions: Al, $Mn_{50}Al_{50}$, $Mn_{70}Al_{30}$ and Mn produced by 30h of ball milling. Figure 4-2-5, Figure 4-2-6, Figure 4-2-7 and Figure 4-2-8 are representative examples of the spectra obtained during the trials.

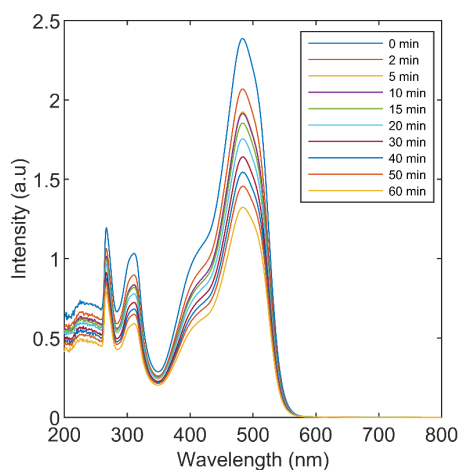


Figure 4-2-5. Degradation of the Orange II dye with MP $Mn_{50}Al_{50}$ 30h.

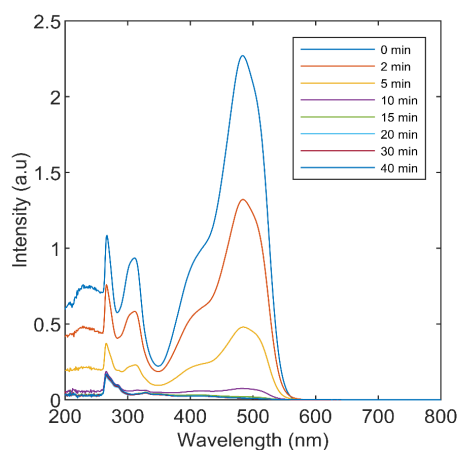


Figure 4-2-6. Degradation of the Orange II dye with MP $Mn_{70}Al_{30}$ 30h.

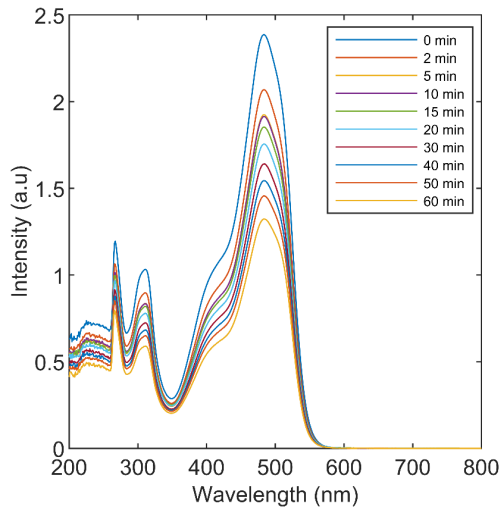


Figure 4-2-7. Degradation of Orange II dye with Mn 30h.

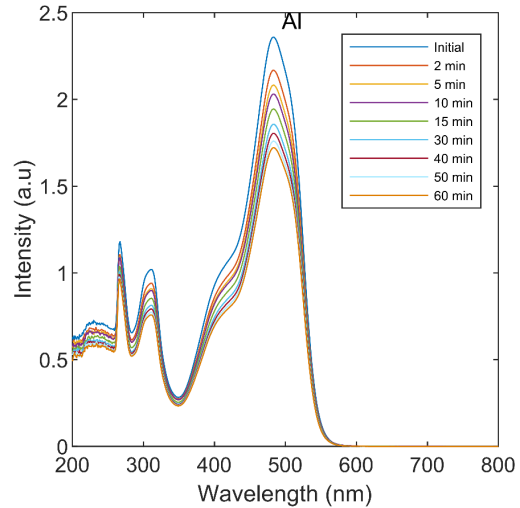


Figure 4-2-8. Degradation of Orange II dye with Al 30h.

From these data the adjustment to a first order reaction was made to build Figure 4-2-9, where the experimental points with the corresponding error and the adjusted kinetics can be seen following Equation 3-3 for the decolourization reactions. As mentioned above, the experimental points correspond to the average of at least three trials. It can be observed that the most efficient MP composition to decolourize water with Orange II azo dye is $Mn_{70}Al_{30}$; With this composition, 100% decolourization is achieved after around 20 minutes of reaction. On the other hand, none of the other MPs achieves a total degradation of the dye. The manganese MP are the next to show more efficiency, although only 45% of decolourization is achieved after 60 minutes. Aluminium particles are those that show a lower efficiency; of 28% after one hour [99][100].

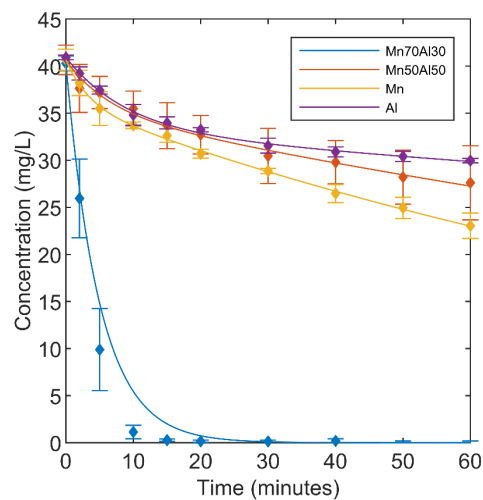


Figure 4-2-9. Experimentally obtained decolourization kinetics (* average and error) and the corresponding adjustments using the Equation 3-3 (solid lines). The dosage was 50mg MP / 100mL solution.

The minimum colourant concentration reached by the $Mn_{70}Al_{30}$ particles is not an average between what is achieved with only pure manganese and pure aluminium, it is clear that by mixing manganese 70% and Al 30% the change is very radical. Thus, the formation of the two-phase particles by mechanical alloying produces a new material with a much higher colourant degradation capacity [101][102].

Figure 4-2-10 shows the inverse of τ , the characteristic reaction time, and the concentration after 1h, as function of the percentage of manganese. A very low saturation concentration and a short reaction time are the desired characteristics, since we want the reaction to be fast and achieve a final concentration of low or zero colour. The MPs that show the best of these characteristics are the $Mn_{70}Al_{30}$.

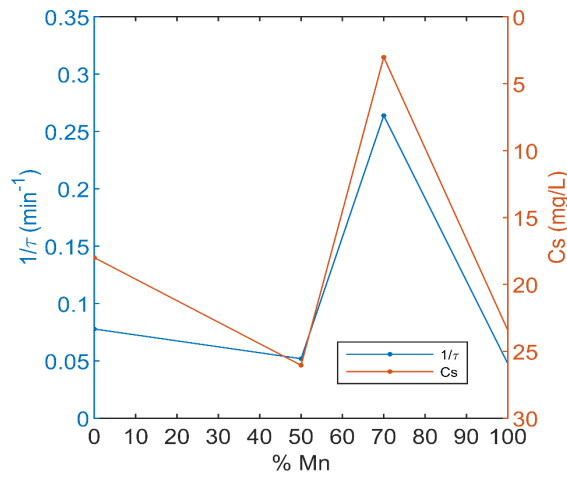


Figure 4-2-10. Saturation concentration (C_s) and $1/\tau$ (inverse of characteristic reaction time) as function of the composition of the metallic particles.

The final concentration at the end of the tests decreases as manganese content increases in the MP, reaching a minimum at 70% atomic concentration and decreasing for higher concentrations after reaching this point [103]. Regarding the reaction rate, $Mn_{50}Al_{50}$ and Mn are those that obtain a lower value, 0.052 and 0.048 s^{-1} respectively. Of course, more compositions should be produced and tested in order to determine the material with the optimum concentration.

4.2.2.1 Morphology and surface analyses of the particles

In Figure 4-2-11, Figure 4-2-12, Figure 4-2-13 and Figure 4-2-14, SEM images are shown to study the morphology of the surface of the MPs of the various compositions. For each composition of MP three images were made.

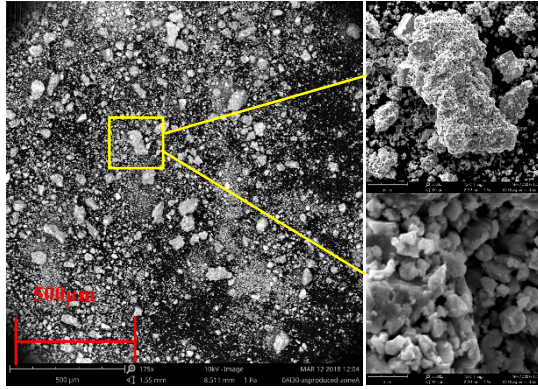


Figure 4-2-11. SEM of the $Mn_{70}Al_{30}$ particles at three different magnifications: x175, x2000 and x20000.

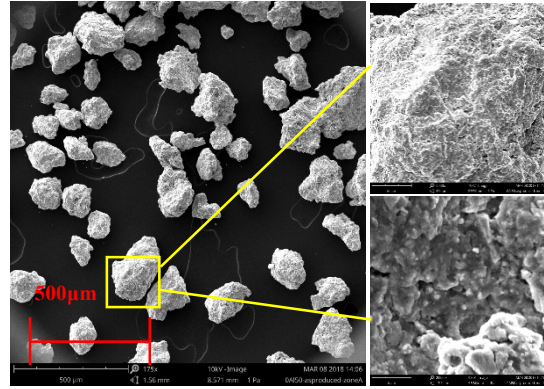


Figure 4-2-12. SEM of the $Mn_{50}Al_{50}$ particles at three different magnifications: x175, x2000 and x20000.

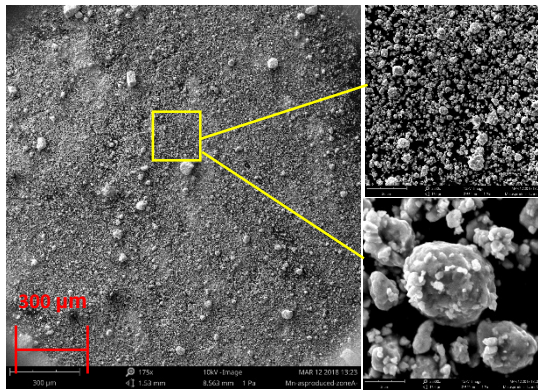


Figure 4-2-13. SEM of the Mn particles at three different magnifications: x175, x2000 and x20000.

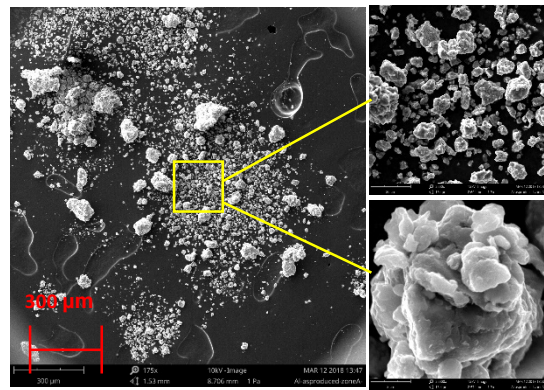


Figure 4-2-14. SEM of the Al particles at three different magnifications: x175, x2000 and x20000.

Regarding the uniformity of MPs within the same composition, it can be seen that the $Mn_{50}Al_{50}$ are those that show a greater degree of uniformity; the size of the particles is quite similar. The other three types of MP show lesser degree of size uniformity. The manganese MP are the smallest and the particles of $Mn_{70}Al_{30}$ and Al are quite similar among them. Regarding the surface, it can be observed that all of them have a rough surface. But they could be classified, qualitatively, according to their roughness as follows: $Mn_{70}Al_{30} > Mn_{50}Al_{50} > Al > Mn$.

On the other hand, the efficiency of degradation can be related to the composition of the MPs; with the presence of manganese, aluminium and oxygen on the surface. It is interesting to see if these elements are distributed homogeneously. With this aim, the compositions of the particles were analysed by means of dispersed X-ray spectroscopy in the same electronic microscope. The results are shown in the figures: Figure 4-2-15, Figure 4-2-17, Figure 4-2-18 and Figure 4-2-19.

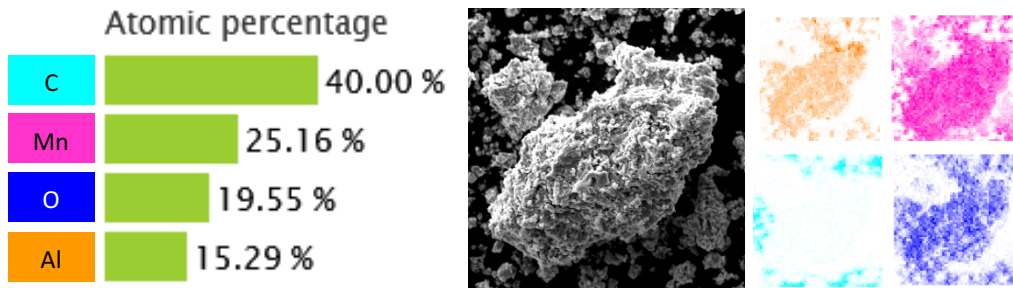


Figure 4-2-15. Compositional analysis of MP $Mn_{70}Al_{30}$. a) Atomic percentage of the elements present in the sample. b) Image of a particle of 244 μm . c) Aluminium (orange), manganese (magenta), carbon (cyan) and oxygen (blue) on the surface of the particle of the image b.

In Figure 4-2-15 it is shown the analysis of the $Mn_{70}Al_{30}$ particles. The element with greater presence is the carbon; but this is due to the carbon adhesive used to fix the sample. Also it can be observed that there is oxygen (blue) on the surface distributed in a homogenous way; the particle is at least partially oxidized. Manganese (magenta) and aluminium (orange) are also homogeneously distributed.

Bearing in mind only manganese and aluminium, its percentage is 62.2% and 37.8%, respectively, close to the nominal percentage, 70% (Mn) and 30% (Al). It should be noted that this is only the analysis of one single particle. The compositional analysis, average and error, of five different points within the sample is shown in Figure 4-2-16.

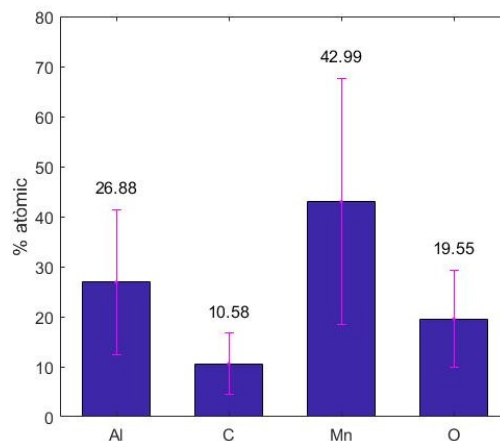


Figure 4-2-16. Mean and error of the atomic percentage of C, Al, Mn and O of five points of the sample $Mn_{70}Al_{30}$.

Taking into account the errors, this result is very close to what was obtained with the compositional map and the one that was the objective when producing the particles.

In Figure 4-2-17 we can see the compositional analysis of one particle of the $Mn_{50}Al_{50}$ powder. Carbon is again very present for the reasons already explained. Manganese (magenta) and aluminium (orange) are homogeneously distributed, and oxygen on the surface is again present.

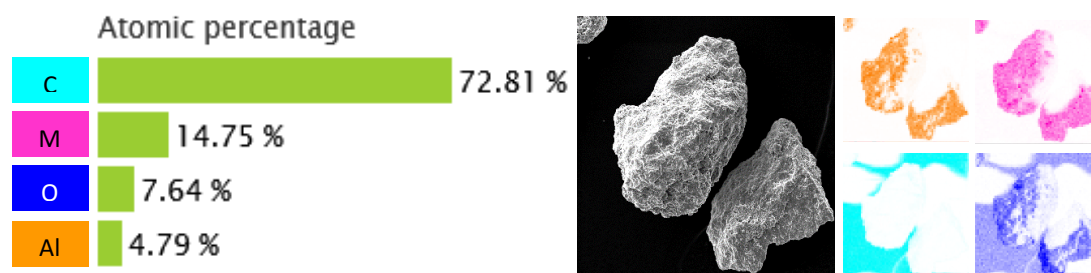


Figure 4-2-17. Compositional analysis of MP $Mn_{50}Al_{50}$. a) Atomic percentage of the elements present in the sample. b) Image of a particle of 395 μm . c) Aluminium (orange), manganese (magenta), carbon (cyan) and oxygen (blue) on the surface of the particle of the image b.

Regarding the relationship between manganese and aluminium, the percentage between them is 75.5% and 24.5%, respectively. Several points have also been analysed on the particle. This composition is far from the nominal composition. After the analysis of several particles, this is found to be consequence of a grate inhomogeneity of particle compositions, with particles with high content of Al and others with high contents of Mn.

In Figure 4-2-18, we can see the homogeneous distribution of manganese (magenta) on a particle of the pure Mn powder. We can also see a large amount of oxygen (oxygen), 29.45%, which indicates that the surface is oxidized. In this case, carbon (cyan) is not only around the particle but also on the surface. Although the production route is the same as the one used for obtaining the Mn-Al samples, the presence of C on the surface suggests that Mn alone is more prone to adsorb or interact with compounds present in room ambient conditions than when is combined with Al. This could be one of the reasons that reduces the decolourization power of Mn compared to Mn-Al powders.

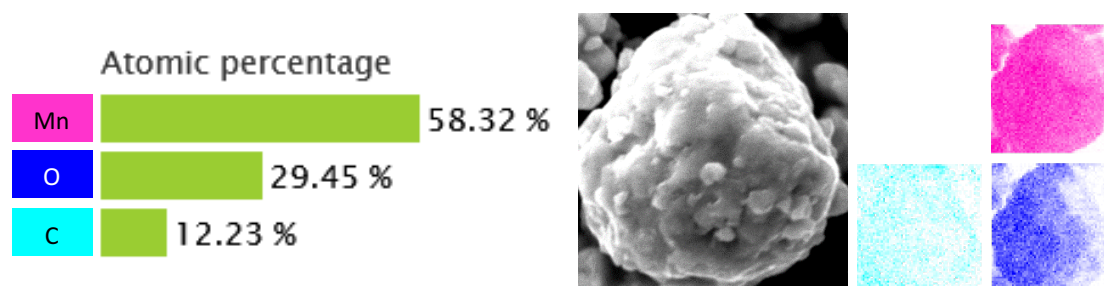


Figure 4-2-18. Compositional analysis of MP Mn. a) Atomic percentage of the elements present in the sample. b) Image of a particle of 13.4 μm . c) Manganese (magenta), oxygen (blue) and carbon (cyan) on the surface of the particle of the image b.

In the case of aluminium MP (Figure 4-2-18), carbon (cyan) occupies a large number of the atomic percentage, but is mostly around the particle, therefore, corresponds only to the signal from the carbon sticker. Oxygen is also present in abundance, constituting 14.1% of the atomic percentage. With regard to aluminium, it accounts for 31.8%. This element does not seem to be distributed homogeneously to the surface of the particles, indicating that there are zones of particles more oxidized than others. The presence of manganese (magenta) by 4.2% is also worth mentioning. Since these particles are made

of aluminium, manganese must not be present. Its presence can be due to contamination when it comes to making particles or at the time of preparing samples for the SEM.

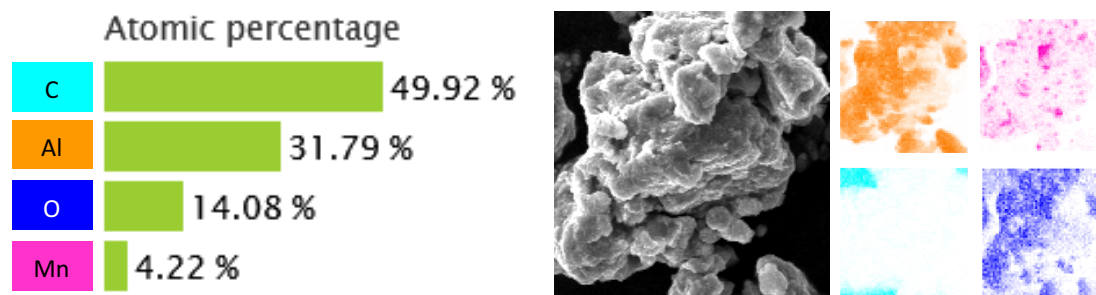


Figure 4-2-19. Compositional analysis of MP Al. a) Atomic percentage of the elements present in the sample. b) Image of a 168 µm particle. c) Aluminium (orange), manganese (magenta), carbon (cyan) and oxygen (blue) on the surface of the particle of the image b.

From the analysis of the surface composition of the particles of the 4 compositions we can highlight a main result. Although both $Mn_{70}Al_{30}$ and $Mn_{50}Al_{50}$ particles have been produced using the same mechanical alloy protocol, the first ones have a homogeneous composition of the two elements quite close to the nominal composition. While the latter present heterogeneous compositions between one particle and another, with particles mostly composed of aluminium and others with a higher concentration of manganese.

As already mentioned, important parameters for analysing the colouring degradation reaction by MP are the morphology and size of the particles. The morphology and particle size determine the specific surface, which indicates the amount of area available to interact with the colourant. The results of the Brunauer, Emmett and Teller (BET) analysis for the particles $Mn_{70}Al_{30}$, Al and Mn can be seen in Table 4-1.

MP	Surface Area (m ² /g)
Al	1.1106
$Mn_{70}Al_{30}$	0.5653
Mn	0.9285

Table 4-1. Specific surface area of the particles of $Mn_{70}Al_{30}$, Al and Mn ball milled during 30h. Result of the BET analysis.

It can be observed that particles that show a greater specific surface area per gram of material are those of aluminium, while those with the lowest surface area are those of $Mn_{70}Al_{30}$. This coincides with what had been observed previously, that the MP $Mn_{70}Al_{30}$ had a larger size and, therefore, a smaller specific area. To relate the influence of this parameter with the MP degradation capacity, Figure 4-2-20 was plotted, where the characteristic reaction time and the saturation concentration have been normalized by the specific surface area [104].

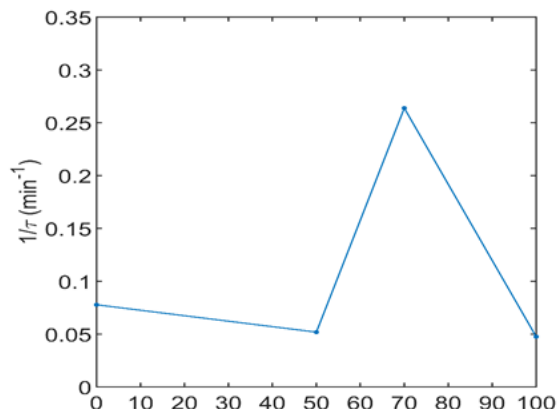


Figure 4-2-20. Normalized reaction time as function of the percentage of manganese MP.

In this graph, we try to visualize the differences between the intrinsic reaction activity of Mn-Al compared to pure Mn and Al by plotting the normalized reaction time $\tau_a = a\tau$, i.e. the reaction times normalized by the specific surface of the powders. It can be observed that MP $\text{Mn}_{70}\text{Al}_{30}$ have a normalized reaction time even more differentiated than the direct reaction time shown in Figure 4-2-20. Those that showed a longer reaction time continue to be aluminium particles, although the sample had a larger area to interact.

The combined results of the microscopy, chemical composition and specific surface analysis indicate that the mechanical alloy process in the case of the $\text{Mn}_{70}\text{Al}_{30}$ composition generates a material with an intrinsic colour degradation capacity much higher than that of the Mn and Al elements separately. This reaction capacity is not due to a larger specific surface, but to a different mechanism where the reactivity of aluminium and manganese are mutually enhanced by being homogeneously distributed within the particles. The fact that for the particles of $\text{Mn}_{70}\text{Al}_{30}$ the shorter reaction time is obtained, despite having the smallest specific surface, it is a positive factor, since it indicates that the same material manufactured in particles of smaller size would react in even a more efficient way. This could be achieved in a simple way, for example, increasing the grinding time during the mechanical alloy process as we already assessed in the previous section by producing $\text{Mn}_{70}\text{Al}_{30}$ by 60 h of ball milling.

Summarizing, we assessed the degradation efficiency of the Orange II dye using four different alloys of manganese and aluminium metallic particles: Al (100% Al), $\text{Mn}_{50}\text{Al}_{50}$ (50% Mn and 50% Al), $\text{Mn}_{70}\text{Al}_{30}$ (70% Mn and 30% Al) and Mn (100% Mn). Although all four compositions are likely to degrade this colour, the most efficient ones are those of $\text{Mn}_{70}\text{Al}_{30}$. These have achieved a greater percentage of degradation (100%) with a lower reaction time [105].

4.2.2.2 Assessment of $Mn_{70}Al_{30}$ and $Mn_{50}Al_{50}$ decolourizing efficiency at different pH conditions

In the previous study, the efficiency of $Mn_{70}Al_{30}$ particles was found very high, compared to other compositions in the same Mn-Al system. We will check now if this is also valid when changing the pH conditions of the reaction. Although aluminium is the element that has the most reducing power, apparently, if there is manganese, the reaction goes faster. The Aluminium is very prone to be protected by an oxide layer which does not let it act against dye. This phenomenon, called passivation, helps the particles that have less aluminium to act better since the process of passivation of the surface of the particles is less efficient [106]. This could be an explanation of why particles with more aluminium are less efficient.

As found in other studies such as ref. [107] for Methyl orange or refs. [74][101] for Orange II, there is a lot of bibliography where, in a generalized manner, it is mentioned that the decolourization reaction usually proceeds faster in acidic conditions than when the solution is alkaline. In Figures 4-2-21 and 4-2-22, it is shown that the degradation process is faster when there is less aluminium content. In Figure 4-2-22 the reaction at pH 4 occurs very quickly, being complete with approx. 25min. And when the pH is 10 the reaction is slower. Instead, in Figure 4-2-21, it is seen that for pH 4 and 10 the colour does not utterly disappear in 60 min.

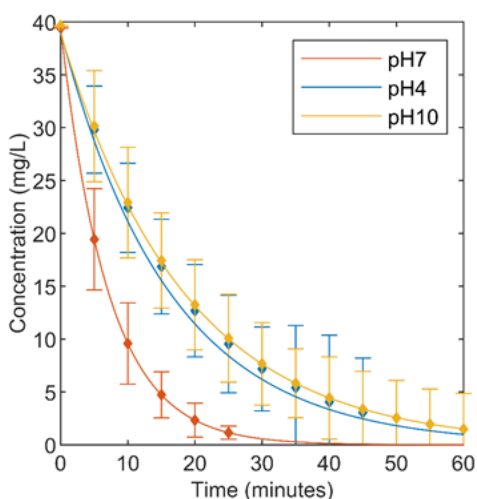


Figure 4-2-21. (Left) Kinetics of the reactions at pH 4, 7 and 10 using 50 mg of $Mn_{50}Al_{50}$ to decolourization of 100 mL of solution.

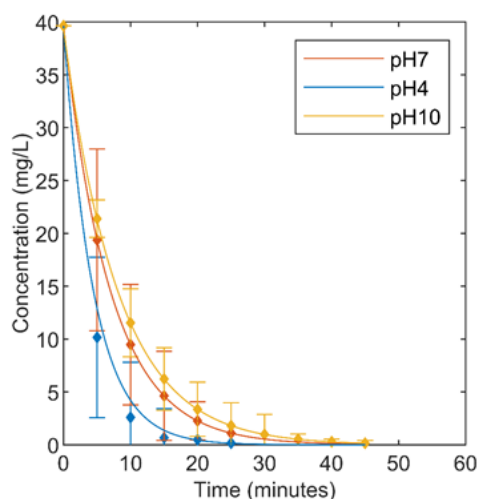


Figure 4-2-22. (Right) Kinetics of the reactions at pH 4, 7 and 10 using 50 mg of $Mn_{70}Al_{30}$ to decolourization of 100 mL of solution.

Ref. [108] reported the effect of pH on the degradation reaction with MPs of Fe in different dyes, among which there was Orange II. They showed that in low pH the reaction was faster due to the fact that using HCl to acidify the solution can break the

layer of oxide formed on the surface of the particles and generate more active surface. In the case of $Mn_{50}Al_{50}$ particles, when establishing the solution at pH 4, after 10 minutes of initiation of the treatment, the pH was increased and restored to the initial pH (6.8). On the other hand, preliminary tests with a more acidic conditions (pH 3) were performed and the decolourization happened very quickly and the pH did not return to the initial pH. The fact that pH 4 does not trigger a faster reaction can be given by the effect of passivation that, at pH 3, ceases to be so effective.

4.2.3 Comparison with Iron particles

In addition to studying the effect of Mn-Al MPs, a comparison with pure Fe particles was also performed. As explained in the introduction, the effectiveness of decolourization of MP of this element has been extensively studied and it is therefore a kind of benchmark to assess the effectivity of other materials. To do this we used a dosage of 100 mg of Fe MPs / 100 ml of solution, and the results were very different than with Mn-Al alloy. During the first three hours of experiment, there was only a 30% decrease in dye concentration. At this point, it was shown that iron MPs were not as efficient as those of Mn-Al. According to the bibliography consulted, the Orange II dye can be degraded by MPs of Fe, but it is necessary to apply higher amounts of particles [109][63] per volume of solution.

4.3 Analysis of the decolourized water solutions

4.3.1 Chemical analysis of the decolourized water solutions

To understand the mechanism of the decolourization reaction, we performed high-resolution liquid chromatography (HPLC) and Mass Spectrometry (MS) that allowed us to analyse the Orange II dyed solution and the products generated by the decolourization reaction. To analyse the results presented in Figure 4-3-1, we determined first the blank (a). Then we observed the maximum peak of the absorbance of the Colourant Orange II (b), which appeared at 483 nm according to the literature [63][110]. This peak appeared approximately at 10 minutes and is called peak "1". At this time, it was found a molecular weight of 326.8 g / mol, when we looked for the negative loads (c), and 329.1 g / mol when we looked for it in positive loads (d).

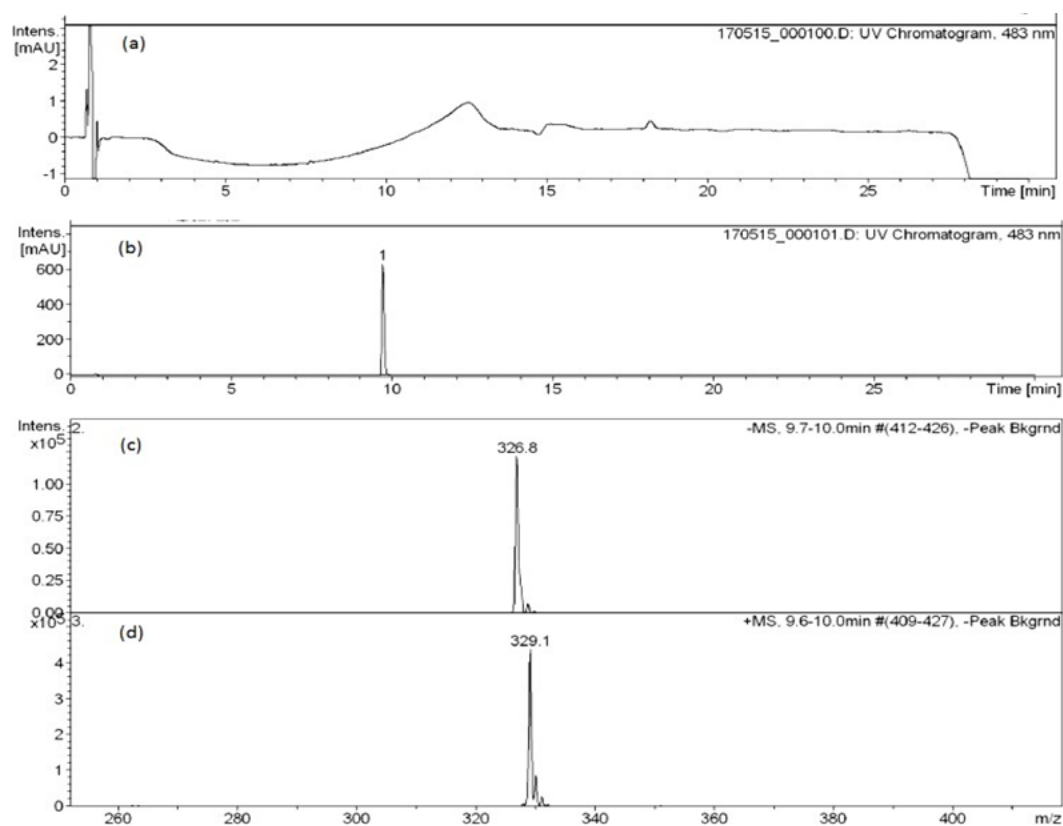


Figure 4-3-1. Ellipse profile of the HPLC (a) the target, which is distilled water. (b) the Orange II and the mass spectra of the peak "1" of the min. 9.8- 10 for (c) $\lambda = 483$ nm anion (d) $\lambda = 483$ nm cation.

These molecular weights correspond to the colourant molecule because the Orange II molecule $C_{16}H_{11}N_2SO_4Na$, that has a weight of 350.32 g / mol, loses sodium (-23 g / mol) when it is in aqueous medium and therefore it stays with a molecular weight of 327.32 g / mol. This molecular weight corresponds to the given values taking into account that these are observed with negative (326.8 g / mol) and positive (329.1 g / mol) loads.

According to ref. [63] and as shown in Figure 4-3-2, the breaking of the dye molecule occurs in two phases. In the first stage, there is a partial breaking of the azo bond but the molecule is still maintained together, as can be deduced from peaks 5 and 6 (at 8.1-8.4 min.) where we found molecular weights of 314, 8 (-) and 317.1 (+) g / mol. In the second stage the total breakage of the link occurs, and, therefore we found the presence of two amines. One amine appears at pic 3, with a weight of 195 g / mol that is coherent with the weight of 192 g / mol (+) determined by MS and highlighted in Figure 4-3-3. The second amine, with an expected molecular weight of 159 g / mol, was found in peak 12 (at 10.2-10.6 min.) with a molecular weight of 156.8 g / mol (-). The decomposition of the colourant molecule in the two amines is coherent with the fact that the characteristic wavelength of the absorbance moved from 483 nm, due to the azo bond, to 191 and 228 nm expected for the two amines.

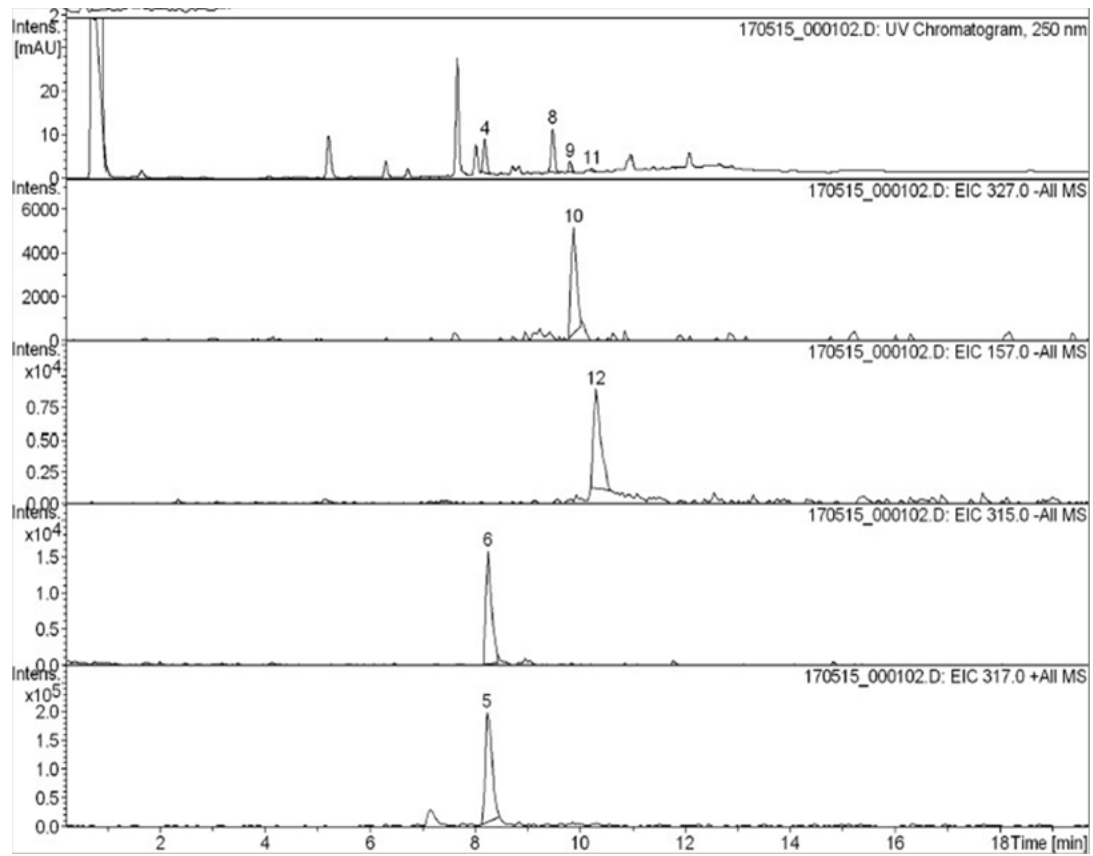


Figure 4-3-2. HPLC eluate profile of the solution with Orange II decolorized with the Mn-Al particles at 25 °C and at a 250 nm wavelength.

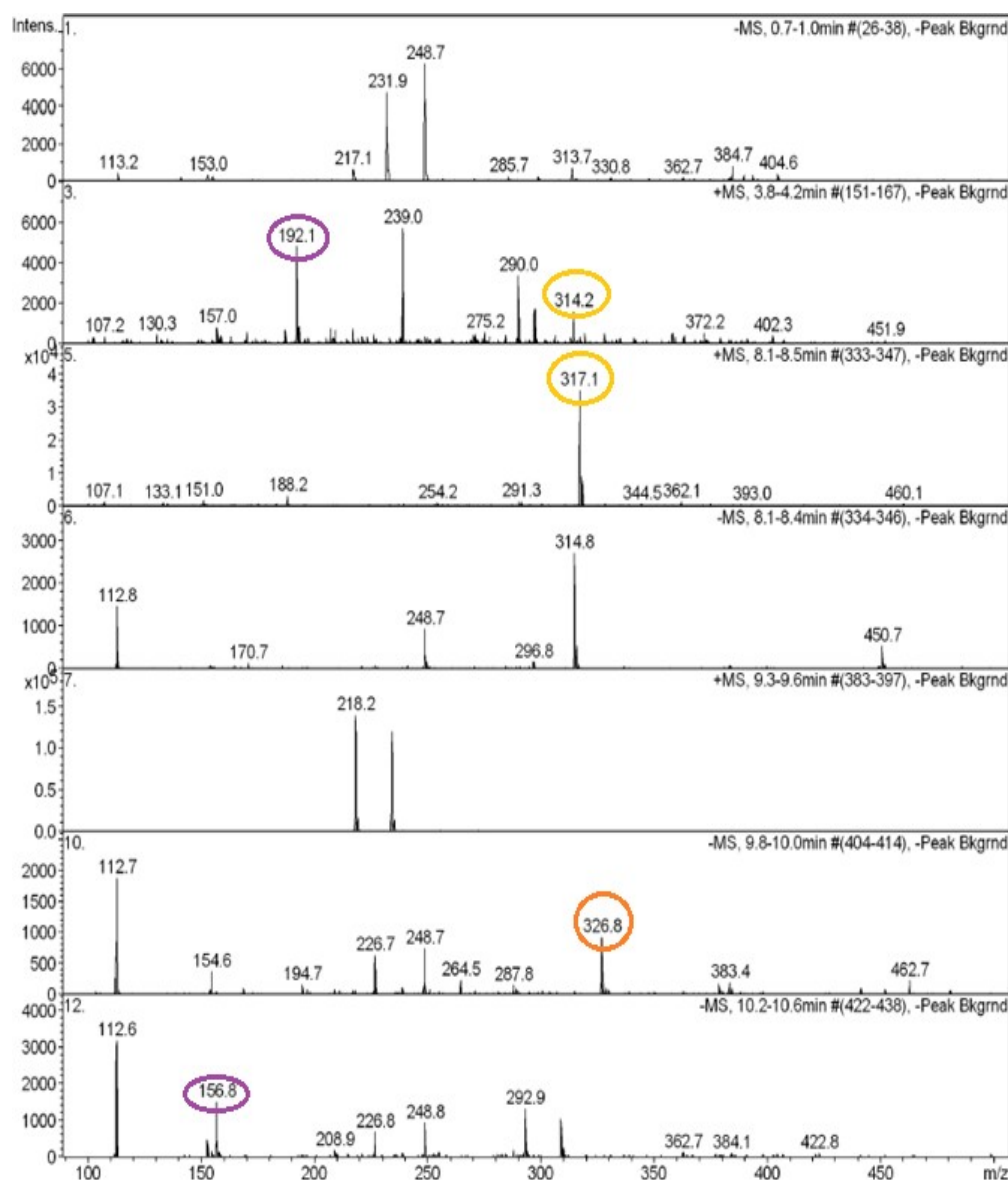


Figure 4-3-3. The mass spectra of the peaks 1, 3, 5, 6, 7, 10 and 12 (enumeration in the upper left part of each box).

Chromatography of the decolourized water solutions obtained from other tests, where dyed water was decolourized in different conditions such as pH 4 or using particles with different Mn-Al compositions, were also performed. They showed similar results indicating the mechanism of the decolourization reaction did not change.

From the HPLC results, we can deduce that the process of degradation by the Mn-Al particles is based on the same breakage procedure of the azo bond that occurs with Fe particles, which has been studied in various articles [108][111]. As outlined in Figure 4-3-4, we found a transition product and final degradation products that are believed to be aromatic amines identified by their molecular weight. A small concentration of the colourant was also found in the final water, even in the cases where a complete decolourization occurred, due to a possible reversible reaction.

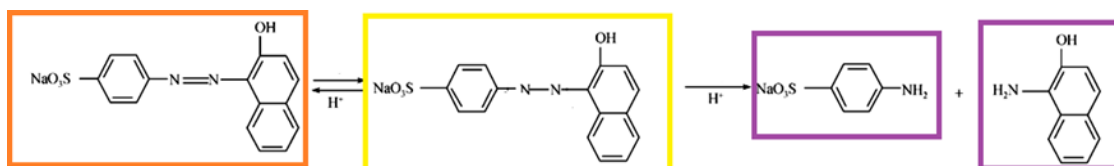


Figure 4-3-4. Scheme of the degradation of azo bonds using metallic particles of Mn-Al.

To deepen in the characterization of the decolourized water, flame atomic absorption spectrometry was used to evaluate the content of metals (Mn and Al) that are dissolved in water as a result of the decolourization process. These results helped us to understand the interaction with the colourant.

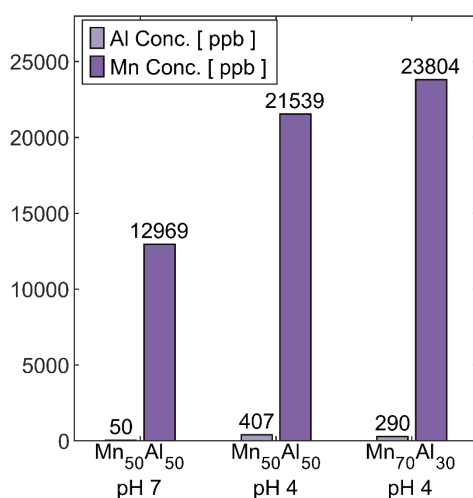


Figure 4-3-5. Amount of Mn or Al in ppb that are dispersed in the water that was decolourized by Mn₅₀Al₅₀, at pH 4 and pH 7 and Mn₇₀Al₃₀ at pH 4.

As we observe in Figure 4-3-5, in all cases there is more Mn than Al ions in the water. In the case where there is an acid medium, there is more detachment of Mn and Al than when they are in a more basic environment. In all cases, there is more Mn dissolved in water than Al, considering that the initial proportions of these were 1: 1 in the case of Mn₅₀Al₅₀ particles. We also see that by varying the proportions of the elements in the particles there was not much difference in behaviour.

From these results we deduce that the process of corrosion of the particles implies a certain amount of dissolution of Mn in the water. The analysis of the reaction products does not tell us which element, manganese or aluminium, is the most reactive one. On the one hand, the greater efficiency in the particles with more proportion of Mn would indicate that this element is the one that contributes more to the reaction. On the other hand, its role could be indirect. As seen in Figure 4-3-5, Mn dissolves more easily in the water and this process could generate a new surface free of oxides (not passivated) and, therefore, allow Al to continue acting as a reducing element.

The dissolution of certain amounts of Mn is probably one of the factors that permits to explain the great efficiency of these particles but can suppose a problem for its application if the concentration of Mn ions becomes too high in the treated water. It would be necessary to assess the amount of Mn released in water after a real wastewater decolourization process and verify that it does not exceed the limit to be considered harmful.

4.3.2 Toxicity of the decolourized water solutions

The results of the toxicity test can be seen in Table 4-2. We present here the toxicity results obtained for different types of colourants in addition to Orange II. Some results regarding the application of Mn-Al particles to aqueous solutions of these other colourants will be presented below. As shown, all treated dyed solutions reduced their toxicity after the application of Mn-Al MPs. Later on, however, we will discuss whether this reduction in toxicity is enough to consider the treated dyed waters as not toxic for the environment.

Colourant	Initial toxicity (TU)	Final toxicity (TU)
Orange II	100	20
Orange G	5,6	4
Brilliant Green	81	33,3

Table 4-2. Table results of toxicity analysis (TU = toxicity units). Comparison between the initial dyed solutions before the application of the Mn-Al particles and the final decolourized solutions.

The toxicity value was measured as specified in the Methods and materials section, based on the loss of luminous intensity emitted by a bioluminescent bacterium (*Photobacterium phosphoreum*). The toxicity value is given as $TU=100 / EC50$, where EC50 corresponds to the effective concentration of the sample analysed that causes a 50% decrease in luminosity under certain conditions of time and temperature. The higher the value of EC50, the lower the value of TU and the less toxic the sample. In general terms, if the TU value is greater than 25% (in *Photobacterium phosphoreum*) the medium is considered as toxic. Because the water used is colourful in the case of the initial solutions before the treatment, a colour correction protocol is applied, which takes into account this parameter when measuring the toxicity.

Previously we commented that in all the analysed samples the toxicity decreased after the treatment with Mn-Al MPs. In table 4-3, we can see the comparison of the toxicity values obtained after the Mn-Al MPs treatment and the ones after a biological treatment, with the microorganism *Trametes versicolour*, which was studied by Dr. Núria Casas in the framework of her doctoral thesis [10][112][113]. Both treated dyes (Orange G and

Brilliant Green) present a lower toxicity after being treated with MP ($Mn_{70}Al_{30}$) than after the biological approach.

Colourant	Final toxicity (TU)	
	<i>T. versicolour</i>	MP
Orange II	-	20
Orange G	4,7	4
Brilliant Green	75,9	33,3

Table 4-3. Comparison of biological treatment with *T. versicolour* and treatment with Mn-Al MPs.

In spite of the reduction of toxicity, the effluents of these treatments can be considered toxic by the environmental norms. According to EPA 2004 (Environmental Protection Agency USA), a sample is considered toxic when the TU exceeds the value of 10. In either of the two treatments, only the effluent coming from the Orange G dye would be considered non-toxic after treatment. In Catalonia, Decree 130/2003 of 13 May, 2003, that approves the regulation of public sanitation services, defines the limit of toxicity at which an effluent can be treated in a sewage treatment plant in 25 Equitox. These units of toxicity are equivalent to a unit of TU. Therefore, the maximum value accepted by the administration to consider a non-toxic effluent, and therefore that it can enter the cycle of a wastewater treatment plant (WWTP) is 25 TU.

4.4 Analysis of the metallic particles after decolourization of Orange II solutions

During the degradation treatment, the particles undergo a corrosion process due to the reaction with the dye and the water. The analysis with the SEM allows us to observe at the microscopic level the change in morphology on the surface of the MPs.

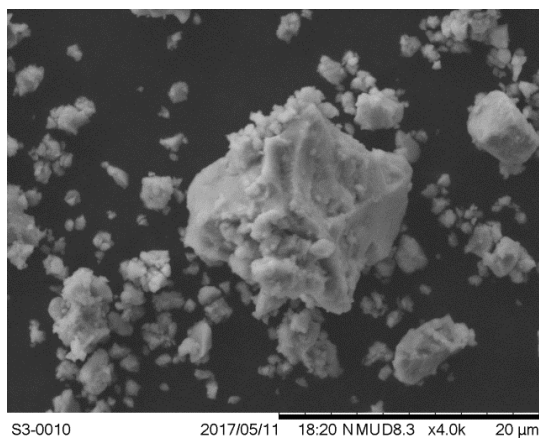


Figure 4-4-1. Morphology of the surface of the initial MP.

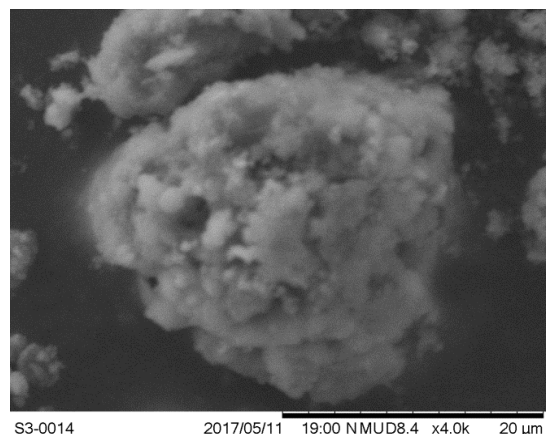


Figure 4-4-2. Particle surface morphology after the degradation of Orange II.

The initial particles, as seen in Figure 4-4-1, are of different sizes, they form aggregations but they are easily discernible. On the other hand, the particles shown in Figure 4-4-2, which are the result of the degradation treatment of the Orange II dye, have a layer around the surface that does not permit to determine the details of the particles topography. This layer may be formed by corrosion products generated on the particles surface due to immersion in an aqueous medium as well as adsorption of both dye molecules and the products of the dye degradation. From the washing of the used particles we saw that in this diffuse layer there was a small quantity of adsorbed dye, as demonstrated by the slight orange colour of the washing solution (Figure 4-4-3).



Figure 4-4-3. Image of the liquid used for the washing of particles (Water and ethanol) after drying them when they had already done the treatment of decolourization of Orange II.

This shows that there is not only a decolourization due to degradation of the azo bond but also a phenomenon of adsorption of the colourant to the metallic particles that contributes to a faster decolourization. This fact is also mentioned in [114] where Orange II is absorbed in compounds such as iron-benzenetricarboxylate (Fe(BTC)).

By means of SEM-EDX, we compared the compositions in the particles before and after being used in decolourizing treatments. In this case we will show the results obtained by the particles milled during 60h, but similar conclusions could be obtained for other milling times. The initial conditions of the particles of $Mn_{50}Al_{50}$ -60h are shown in Figure 4-4-4. As discussed above they present variable sizes and therefore have a distribution of size with high dispersion.

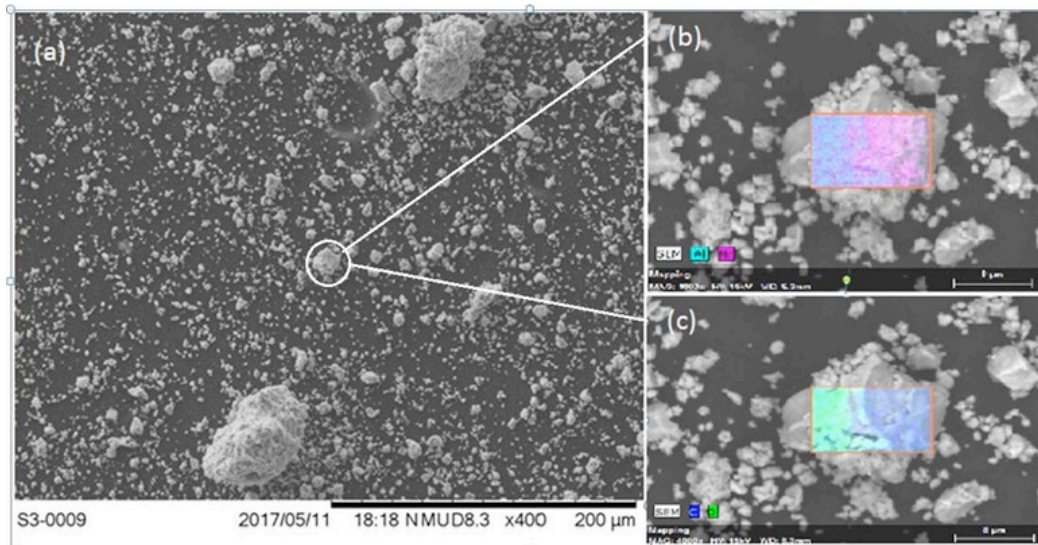


Figure 4-4-4. Morphology of the $Mn_{50}Al_{50}$ -60h particles. (a) Sample of powder showing the dispersion in particle size in an SEM (SE) image. (b) Combination of SEM and EDX where the distribution of Mn (pink) and Al (blue) is represented on the surface of one of the particles. (c) Presence of C (green) and O (blue) on the surface of one of the particles.

As already discussed, the distribution of the Mn and Al is not homogeneous in the particles, as shown in image (b) of the figure above. In the image (c) it is shown how the occurrence of oxygen (green) is higher on the part that there is more aluminium (pink). The distribution of the elements within the particles is not homogeneous, indicating that they are not formed by a single intermetallic phase as already deduced from the XRD results in Figure 4-2-3.

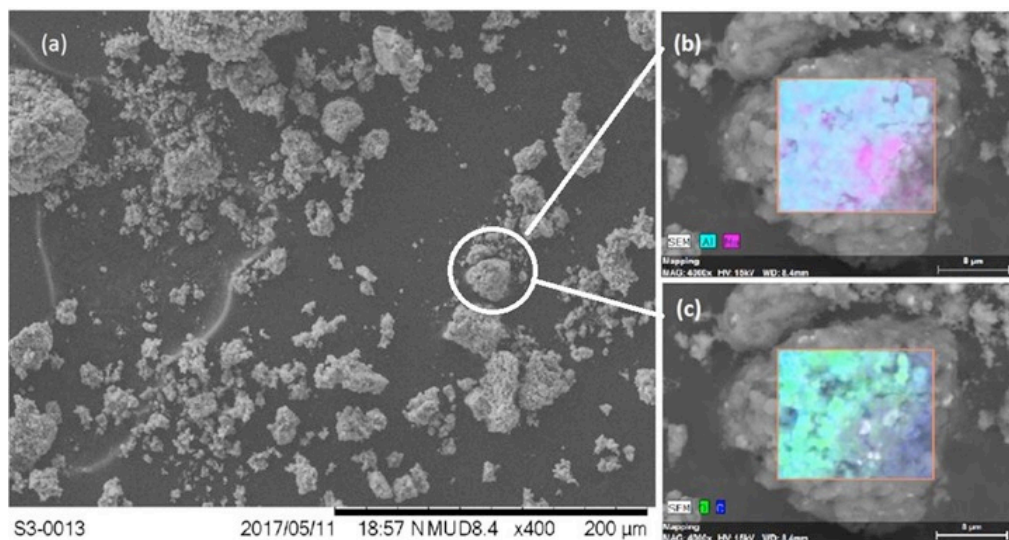


Figure 4-4-5. Morphology of the $Mn_{50}Al_{50}$ -60h particles resulting from the degradation of Orange II at 25°C. (a) Sample of powder showing the dispersion in particle size in an SEM (SE) image. (b) Combination of SEM and EDX where the distribution of Mn (pink) and Al (blue) is represented on the surface of one of the particles. (c) Presence of C (green) and O (blue) on the surface of one of the particles.

Figure 4-4-5 (a) shows the final conditions of the particles of $Mn_{50}Al_{50}$ -60h once they were used in a decolourization process at 25°C. Figure 4-4-5 (b) shows how the Mn (pink) and Al (blue) are distributed inhomogeneously. In different zones of on particle. As for the O (green) its concentration was found still more higher on the Al-rich regions while the concentration of C (blue) was distributed more homogeneously over the particles.

Regarding the composition, Figure 4-4-6 shows that there was almost a 1: 1 ratio of Mn and Al considering the error margin of precision of the EDX used. Compared to the initial concentrations, the used particles showed a large amount of C and O due to the decolourization process and the reaction of particles in the aqueous medium. They also showed two new elements, sulphur coming from the dye molecule and a small contamination of silicon.

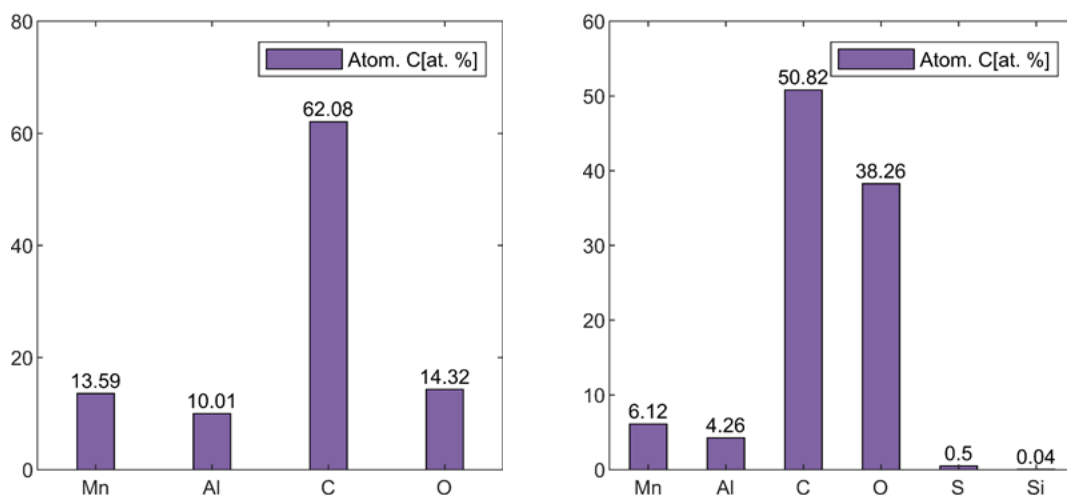


Figure 4-4-6. Chemical compositions of $Mn_{50}Al_{50}$ -60h powder obtained by EDX. Left: Initial composition of the as-produced particles. Right: Composition of particles used in a decolourization treatment of Orange II.

The analysis performed to study the change on the $Mn_{70}Al_{30}$ -60h particles produced similar results than in the case of the $Mn_{50}Al_{50}$ powder. Figure 4-4-7 and Figure 4-4-8 shows how in this case the Mn distribution was more homogeneous than that of aluminium, this is because the Mn content was higher and therefore this element was more widespread. As in the other cases oxygen was found to be more present on the sites with aluminium content. After the decolourization process at 25°C, the final conditions of the $Mn_{70}Al_{30}$ -60h particles showed a rugged layer on the surface due to the corrosion suffered during the process of decolourization and adsorption of molecules of colourant and colourant degradation products.

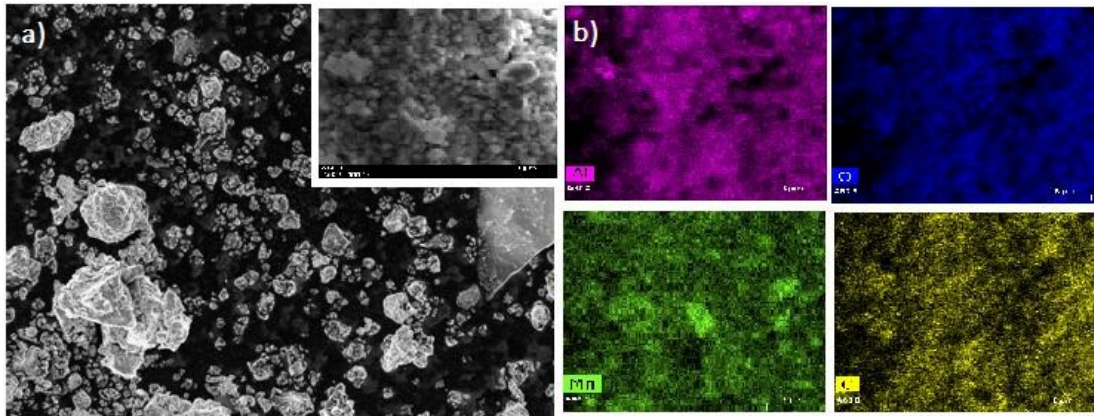


Figure 4-4-7. Morphology of the $Mn_{70}Al_{30}$ -60h particles. (a) Sample of powder showing the dispersion in particle size in an SEM (SE) image. (b) Presence of Al (pink), Mn (green), O (blue) and C (yellow) on the surface of one of the particles.

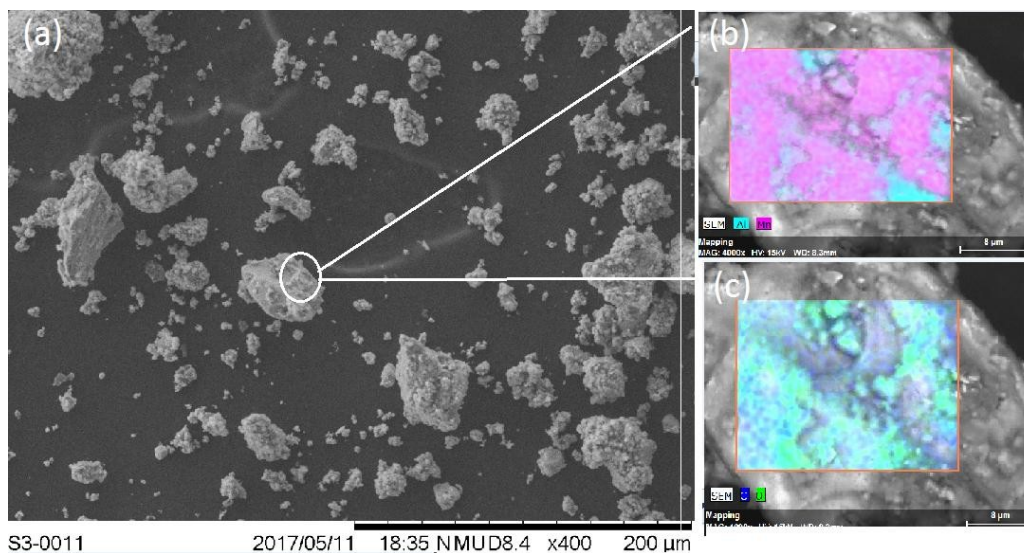


Figure 4-4-8. Morphology of the $Mn_{70}Al_{30}$ -60h particles resulting from the degradation of Orange II at 25°C. (a) Sample of powder showing the dispersion in particle size in an SEM (SE) image. (b) Combination of SEM and EDX where the distribution of Mn (pink) and Al (blue) is represented on the surface of one of the particles. (c) Presence of C (green) and O (blue) on the surface of one of the particles.

The content of chemical species is shown in Figure 4-4-9. The decrease of both Mn and Al after being used in the decolourization process is similar, and it is due to the increase of C and O detected on the surface. Compared with the initial conditions, the amount of carbon and oxygen increased considerably and the particles contained a small concentration of sulphur coming from the dye.

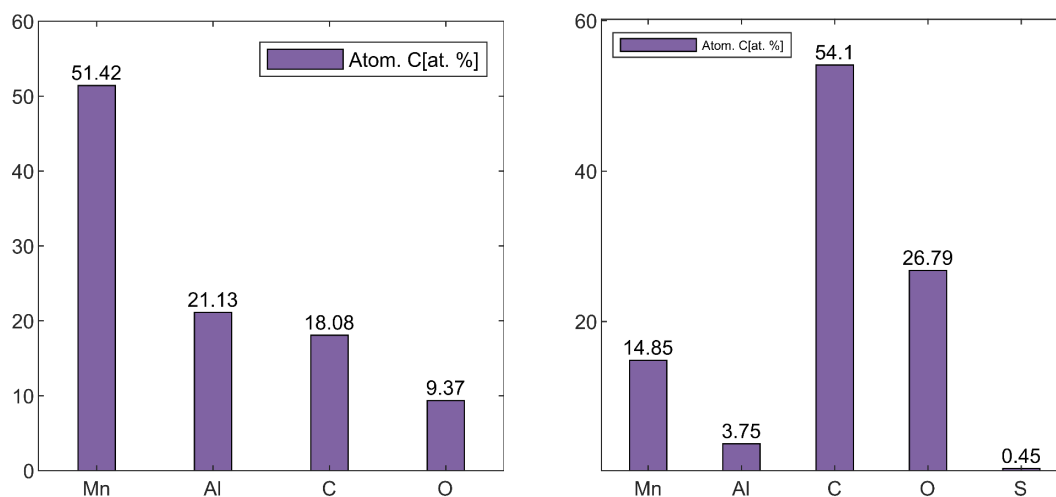


Figure 4-4-9. Chemical compositions of Mn50Al50-60h powder obtained by EDX. Left: Initial composition of the as-produced particles. Right: Composition of particles used in a decolourization treatment of Orange II.

4.5 Efficiency of Mn-Al particles on the degradation of other dye molecules

Although this study has focused mainly on the use of the Mn-Al MPs for the degradation of the Orange II dye, we assessed also how these particles could be efficient to catalyse the degradation of other azo dyes, such as Orange G and Acid Black 58. In this section we will analyse in some detail the degradation of Acid Black and Orange G by Mn₇₀Al₃₀ metallic particles.

4.5.1 Degradation tests of Acid Black 58 dye

Below, it is shown in Figure 4-5-1 the absorbance curve of a solution with the colourant Acid Black 58. Figure 4-5-1 shows how the maximal peak of absorbance is at 689 nm inside the visible range, which is the peak corresponding to the azo link (N = N). We found very little information about the Acid Black 58 dye. As relevant information [86], for decolourization, we only found that this dye can form metallic complexes. There are no decolourization studies of this dye and therefore we did not know if the zero-valent metal method would work.

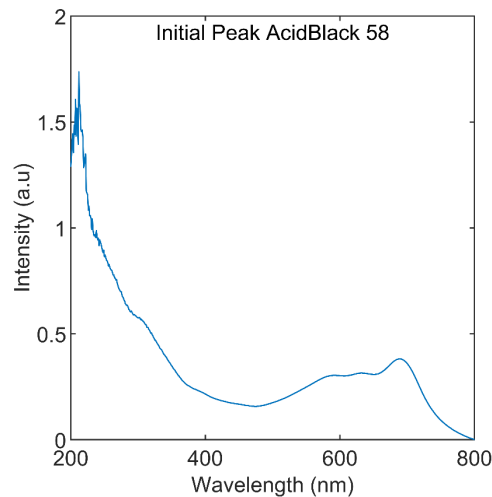


Figure 4-5-1. Absorbance spectrum of a solution with 150 mg / L of Acid Black 58 colourant.

As shown in Figures 4-5-2 and 4-5-3, Acid Black 58 solutions are prone to fade with the application of Mn-Al MPs, the water becoming transparent once the particles were applied and, after stopping the agitation, they precipitated on the bottom of the glass. However, as it will be shown in this section, it does not happen in the most common form of degradation, with the break of the azo bond.



Figure 4-5-2. (Left). Coloured water with 150mg / L of Black Acid 58.



Figure 4-5-3. (Right). Coloured water with 150mg / L of Black Acid 58 once treated with MPs of $Mn_{70}Al_{30}$.

For the degradation treatments, MP of $Mn_{70}Al_{30}$ and $Mn_{50}Al_{50}$ were used, which we knew worked for other dyes. The Figures below show the results obtained for Acid Black 58 applying Mn-Al particles at different temperature and pH conditions as well as different dosages and particles produced by different milling times.

Effect of temperature

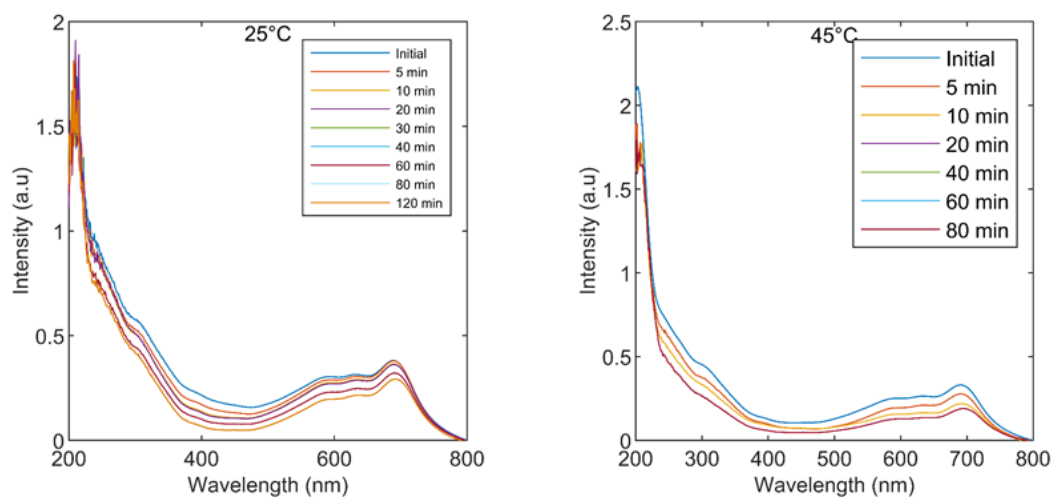


Figure 4-5-4. Degradation of Acid Black 58 by particles $Mn_{70}Al_{30}$ at 25 °C and 45 °C.

Dosage of particles

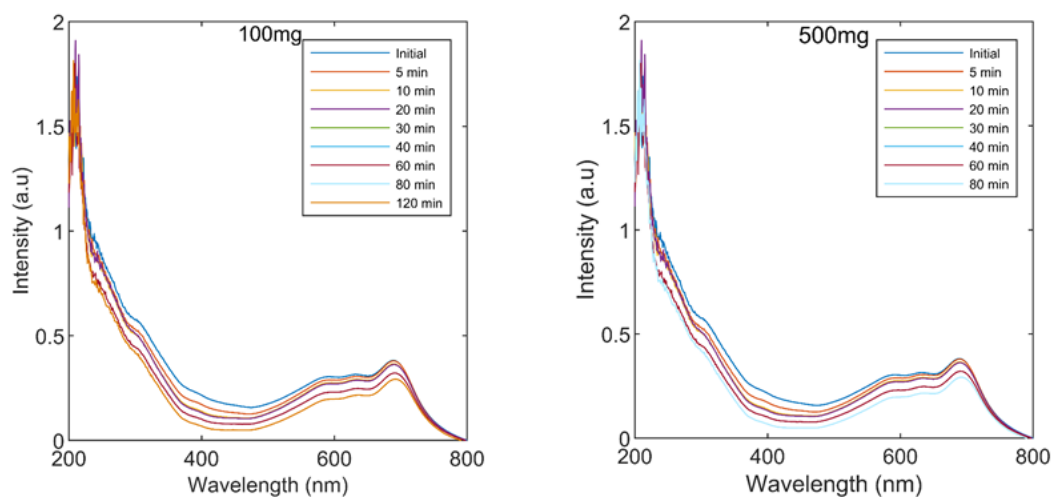
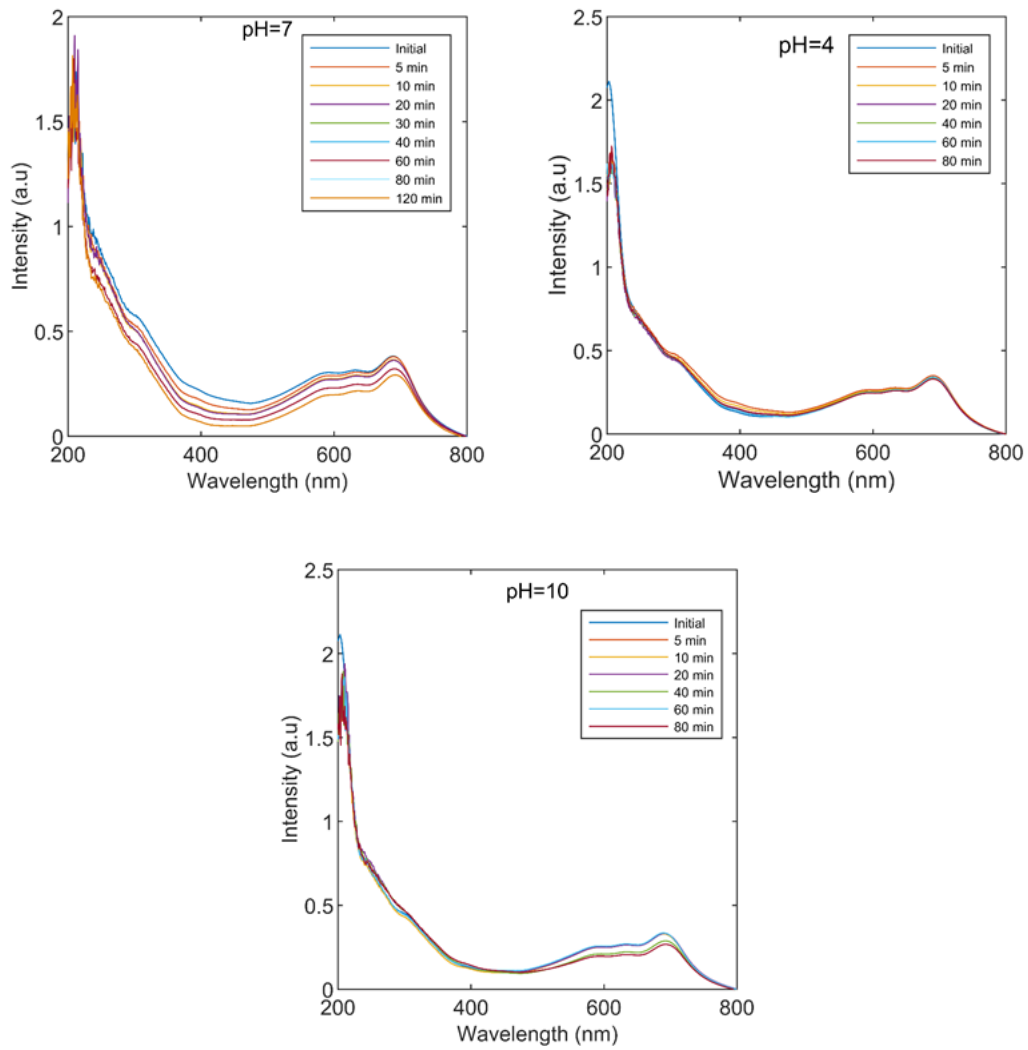


Figure 4-5-5. Acid black 58 degradation applying 100 mg and 500 mg of $Mn_{70}Al_{30}$ particles.

Effect of pHFigure 4-5-6. Degradation of Acid black 58 at initial pH 4, 7 and 10 with $Mn_{70}Al_{30}$ particles.

Hours of mechanical milling

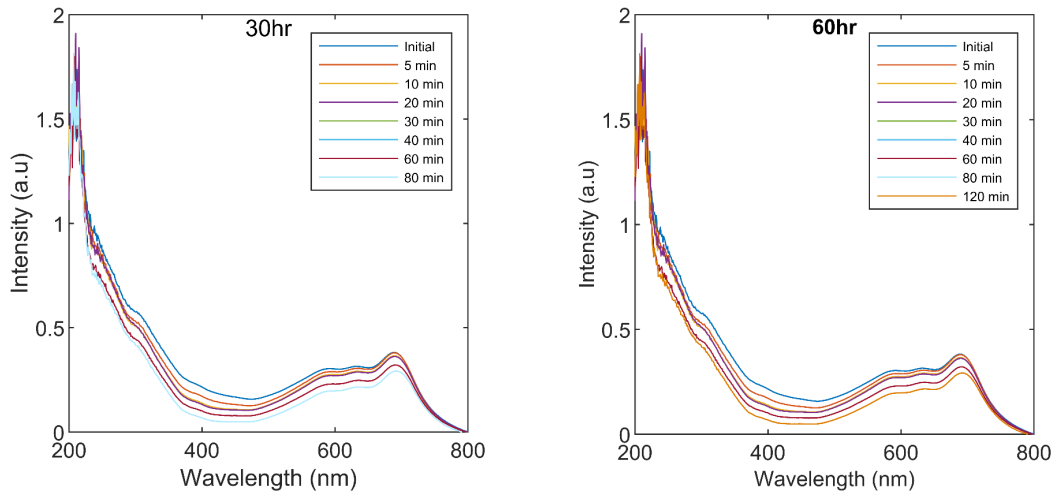


Figure 4-5-7. Degradation of the solution with Acid black 58 by MP ($Mn_{70}Al_{30}$) produced with mechanical grinding time of 30h and 60h.

Figures 4-5-4 to 4-5-7 compare the degradation kinetics of Acid Black 58 in different conditions such as at different temperatures, dosage of particles, pH and mechanical milling. Kinetics remained very slow in all cases and there were no changes in the colour intensity of the solution. Even in the case of very long treatments (Figure 4-5-8) the decolourization process showed little efficiency while the particles were maintained in constant agitation.

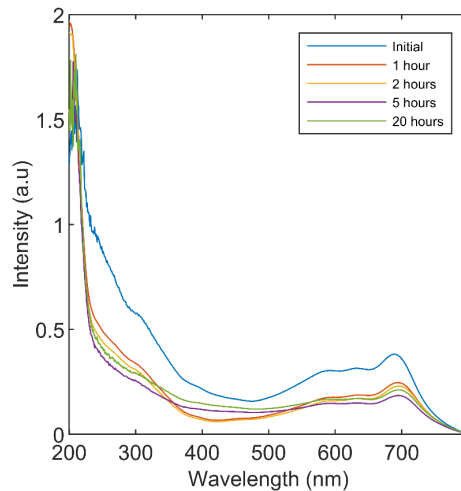


Figure 4-5-8. Decolourization of the solution with Acid black 58 by $Mn_{70}Al_{30}$ particles.

However, the decolourization was evident after stopping the agitator and the solutions were left to rest after the treatment. These results are shown below in figure 4-5-9.

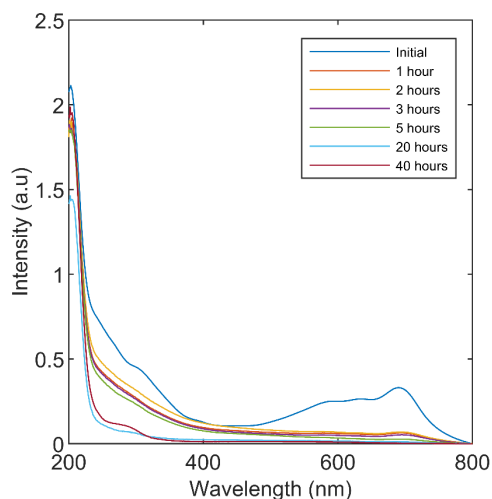
Post-treatment resting hours

Figure 4-5-9. Decolourization of the solution with Acid black 58 by 2h treatment with particles of $Mn_{70}Al_{30}$ and after different post-treatment resting hours.

During the treatment with metallic particles there was no visible decolourization of the Acid Black 58 solution, but there was a clear decolourization when leaving the particles to rest. After applied for about 2 hours, they leave a completely decolourized water once they precipitate. Having little weight, the precipitation is not instantaneous and therefore it takes about some hours of resting to obtain a 100% decolourization. A plausible explanation is that the particles adsorb the colourant molecules and therefore we only see the decolourization once these have precipitated. We also checked if the water would be decolourized by centrifugation (separating solid particles from the liquid) after a 2h treatment. The result was positive as can be seen in the following figure.



Figure 4-5-10. Complete decolourization after a centrifugation process for 10min of an Acid Black 58 solution treated during 2h with Mn-Al MPs.

A study of the particles was performed in order to understand the MP-colourant interaction. The analysis with the SEM allowed us to observe at the microscopic level the change of the morphology on the surface of the particles $Mn_{70}Al_{30}$ -60h used to degrade Black Acid 58.

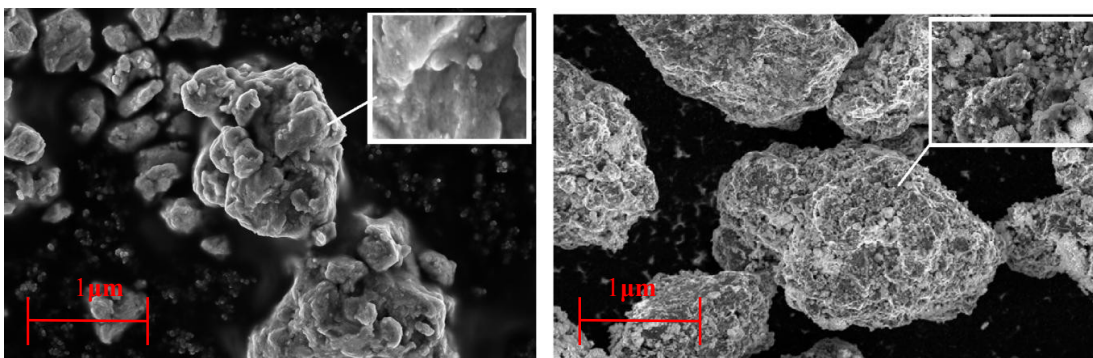


Figure 4-5-11. Morphology of the surface of the as produced MPs (left). Morphology of the surface of the MPs after the degradation of Acid Black 58 (right). Images taken by SEM-SE.

Comparing the two images, the initial particles and those after treatment, the latter showed a layer around them, a greater surface roughness due to the interaction with the colourant. This roughness is due to the corrosion caused during the treatment and the dye molecules adsorption to the surface, which was verified by performing a washing of the used particles after recovering them from the decolourized solution and being dried. After washing the particles with water and ethanol the solution was intensely stained with the colour of Acid Black 58 as shown in Fig. 4-5-12.



Figure 4-5-12. Image of the the washing solution (water and ethanol) after washing the dried particles used in Black Acid 58 decolourizing treatments.

From the SEM-EDX analysis we found sulphur and silicon appearing again as well as other elements such as K, Mg, Ca, Na and Cl typical of the tap water used in this case. Carbon and oxygen were found more abundant due to the treatment.

The study of de decolourization of Acid Black 58 leded as to the following conclusions. The treatment with Mn-Al particles was effective as a mean of decolourization, but the decolourization mechanism found for these dye is different than for Orange II. While in Orange II the main mechanism was the breaking of the N=N bond and the transformation of the dye molecule into molecules with absorption of light out of the visible range, in the case of Acid Black 58 the main mechanism is the adsorption of the molecule to the particles surface. Although a quantitative study has not been performed, the washing

experiments suggest that most part of the dye molecules are not split but remain active as colourants.

4.5.2 Degradation of the Orange G dye

In this section we will study the degradation kinetics of the Orange G dye in an aqueous solution using metallic particles of $Mn_{70}Al_{30}$. Firstly, we present the absorbance curve of a solution with Orange G. Figure 4-5-13 shows how the maximal peak of absorbance is at 478 nm inside the visible range, which is the corresponding peak due to the azo link (N=N). The other two peaks correspond to the chromogenic groups: Naphthalene (310 nm) and benzene (230 nm), which are linked to auxocroms (-OH, -SO₃, etc.) [115].

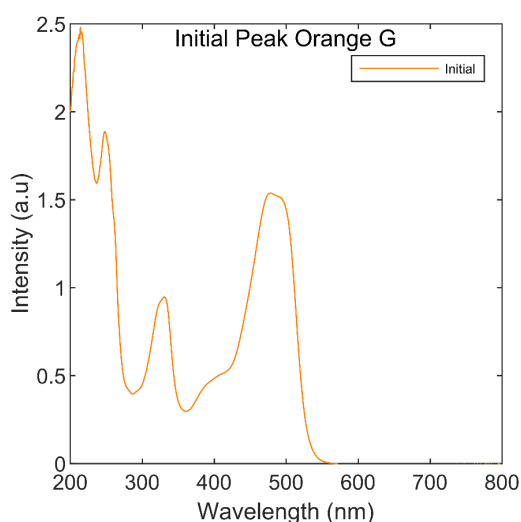


Figure 4-5-13. Absorption spectrum of a solution with 40 mg / L of orange G colourant.

According to ref. [106], Orange G colourant can be degraded by using nanoparticles of Iron and Nickel. They showed how the process was accelerated in acid conditions or the number of metallic particles. The products of degradation were toxic aromatic amines: aniline and naphthol which should be treated later.

The first result of this section is that we verified that it was possible to use the metallic particles of $Mn_{70}Al_{30}$ to degrade this colourant. However, as a result of various trials and experiments in different conditions, we saw that the Mn-Al particles did not achieve a complete decolourization and that they are not as efficient as they were for the case of Orange II. The following figures show the results of the decolourization tests for different temperature, pH and types of particles.

Temperature

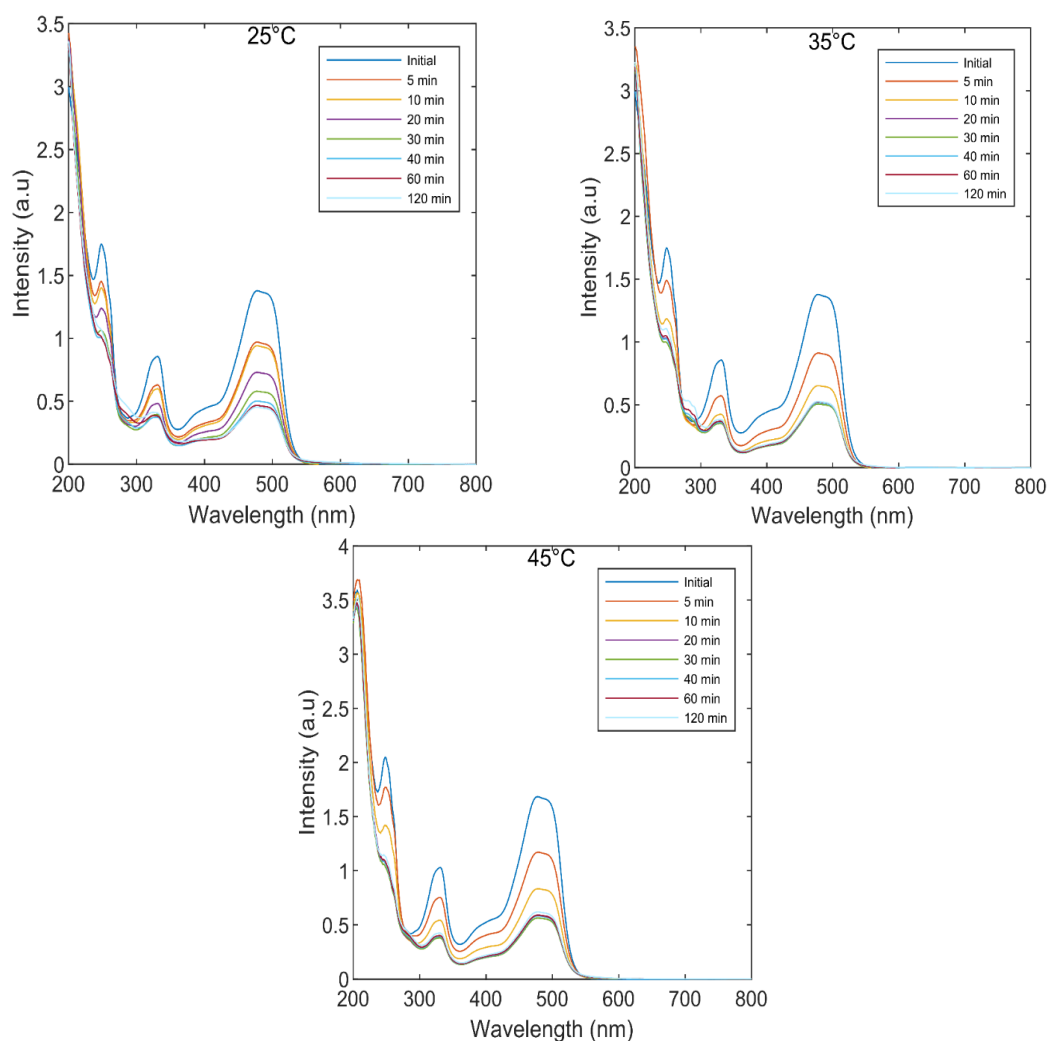


Figure 4-5-14. Decolourization of the Orange G solution by 100 mg / 100 mL of $Mn_{70}Al_{30}$ at 25 °C, 35 °C and 45 °C.

With a temperature increase, the efficiency of degradation is higher. At 60 min the solution decolourized at 45 °C showed double degradation than the solution treated at 25 °C. The effect of temperature has an important influence in this case, at ambient temperature the reaction stops at one point and it is not possible to completely decolourize [116].

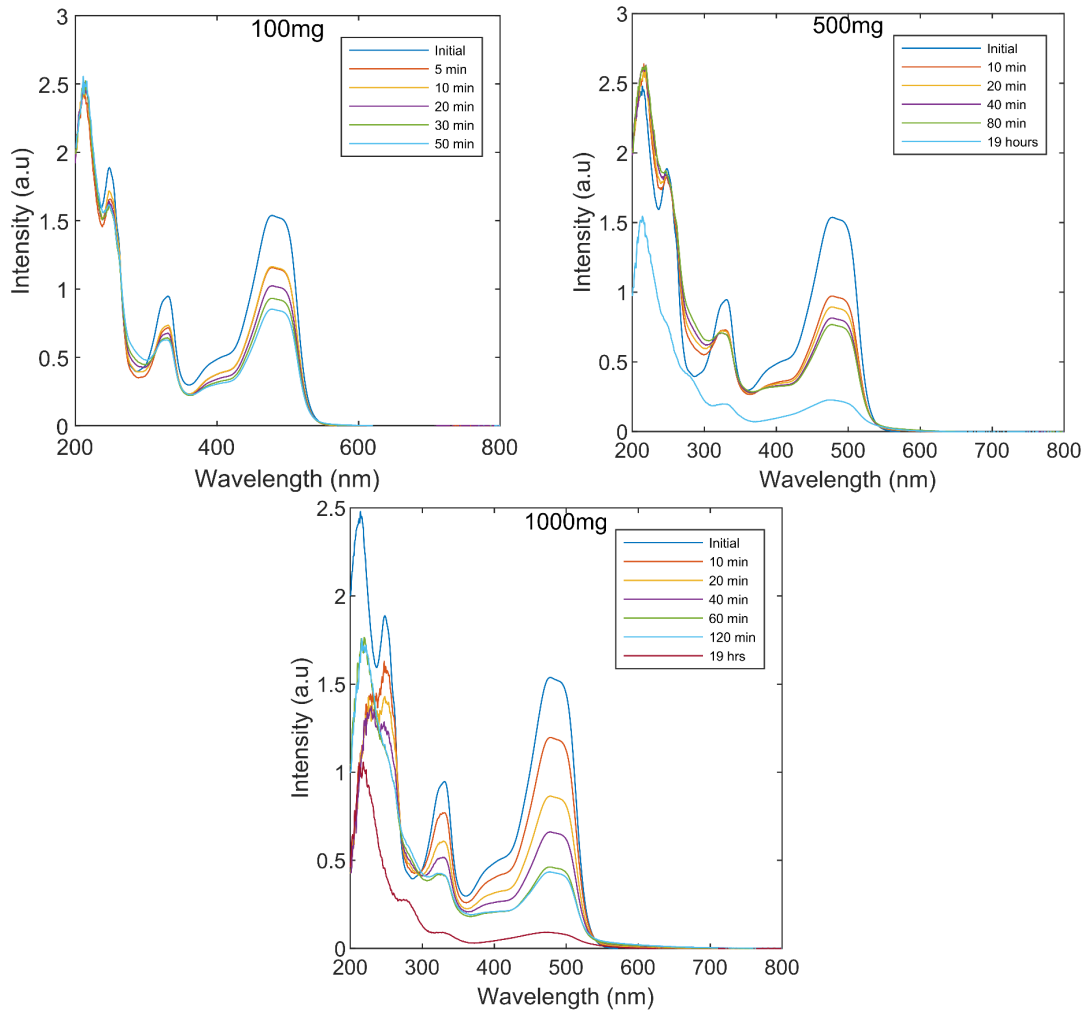
Dosage of particles

Figure 4-5-15. Decolourization of the Orange G solutions by 100 mg, 500 mg and 1000 mg dosages of $Mn_{70}Al_{30}$ particles.

The increase in metallic particles slightly increases the efficiency of degradation. Increasing the amount of MP causes more significant drops in colour intensities. For 100 mg and 500 mg the intensity is approximately 0.8 and 0.6 after 40 min respectively and it is below 0.5 when applying 1000 mg.

Effect of pH

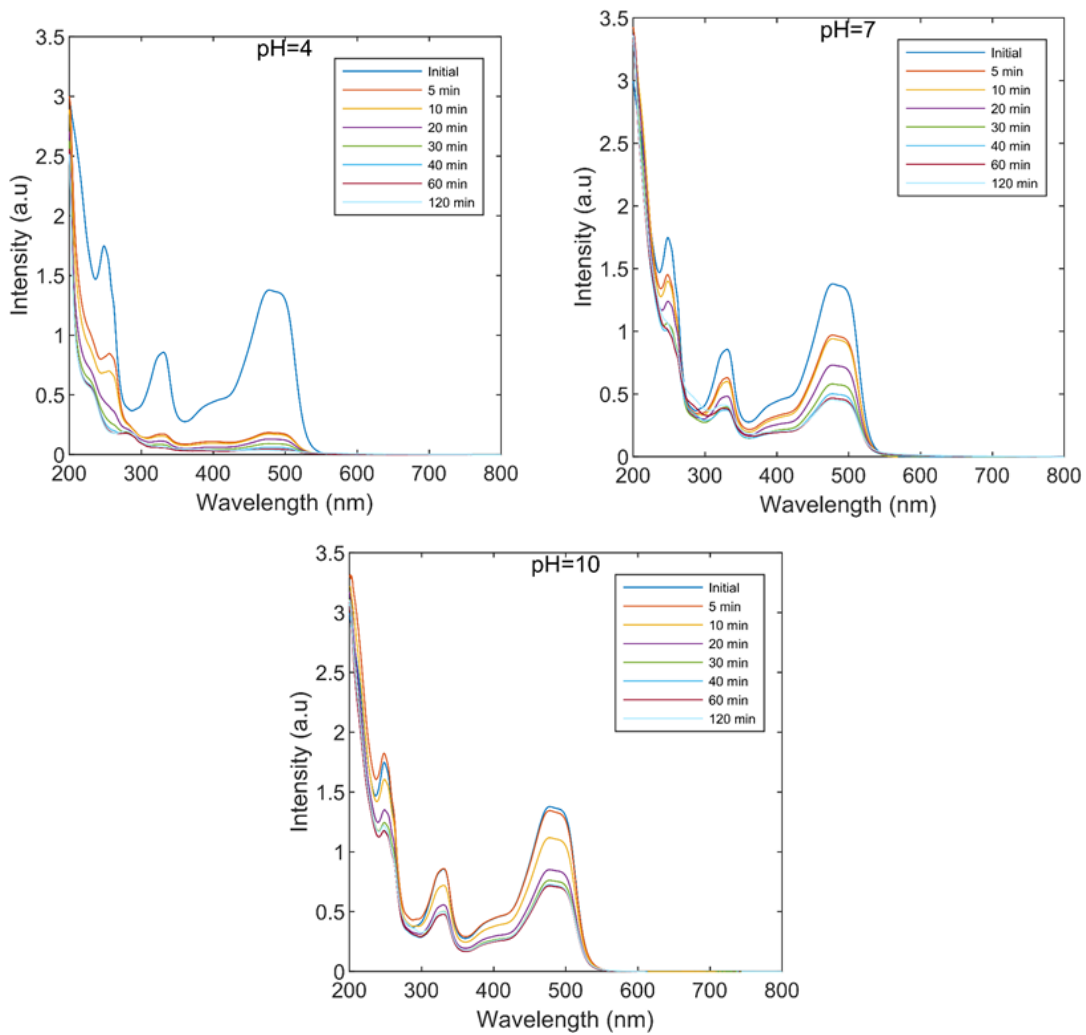


Figure 4-5-16. Decolourization of the Orange G solutions by $Mn_{70}Al_{30}$ particles at different pH conditions.

If the pH is modified, either if it is acidified or alkalinized, the reaction was produced more quickly. In the case of pH 4 the reaction was the fastest and there was almost complete decolorization. In the three pH conditions there was a slowdown of the reaction and after 60 min the reaction stopped. The degradation efficiency of the Mn-Al particles in the case of Orange G therefore very sensitive of the pH conditions, and the particles become efficient in acidic media [106][116].

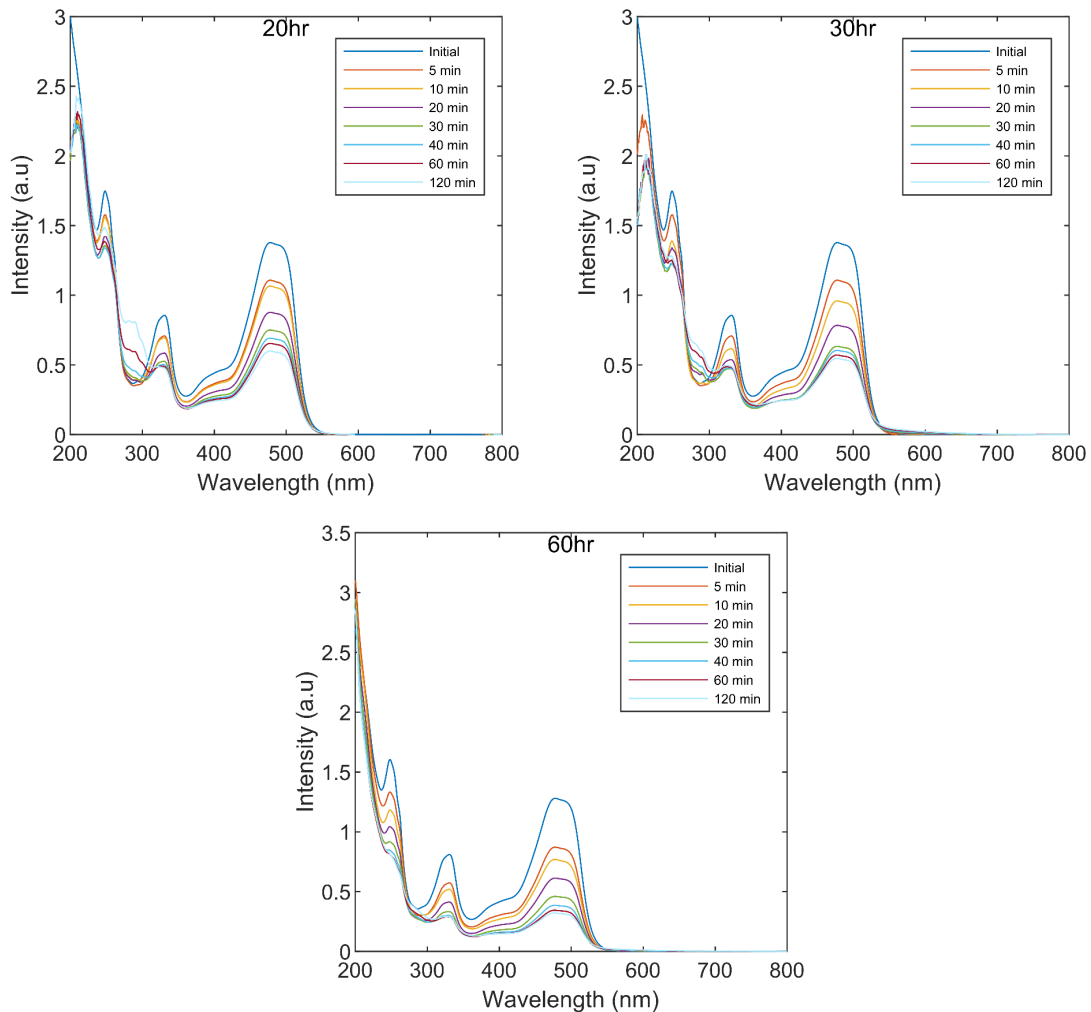
Milling time

Figure 4-5-17. Decolourization of the Orange G solutions by particles $Mn_{70}Al_{30}$ particles produced by mechanical different milling times.

As we can see in the figure, in the case where the metal powder was produced by milling during more time, and therefore there is more contact surface with the dye molecules, we found that more colourant degradation. In any case, however, there was not a complete decolourization during the tests with standard durations. Only after 20 hours of treatment the decolourization became almost complete, the process showing very slow kinetics [117].

4.6 Study of the reusability of the Mn-Al particles

Following the experimental design explained in Materials and Methods section, the MPs of $Mn_{70}Al_{30}$ were recovered and washed in four different ways after being used for decolourization of Orange II solutions. The results will be presented, separately, according to the method of washing.

4.6.1 Decolourization tests of Orange II with reused particles

Firstly, in Figure 4-6-1, the degradation kinetics of four cycles of decolourization-recuperation-decolourization are presented. In this case the MPs were reused without any washing treatment. One can see how from the first to the second cycle there is a radical change in kinetics; After the second cycle the reduction is more attenuated but the efficiency of the particles continues to diminish as more decolourization-recuperation cycles are performed. In the fourth cycle, the efficiency of degradation reached almost zero.

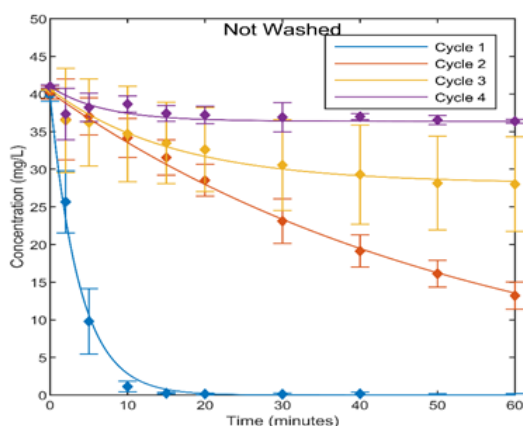


Figure 4-6-1. Kinetics of decolourization obtained experimentally (average and error) and the corresponding adjustments using the model of Equation 3-3 with MPs not washed and reused during four cycles.

On the other hand, in Figures 4-6-2, 4-6-3 and 4-6-4, the degradation kinetics can be seen following the other three methods of washing (with 96% ethanol, 99.5% acetone and with distilled water with pH = 3). Following all three methods, a clear reduction in efficiency can be observed with respect to the first cycle, which had been done with the as-produced particles.

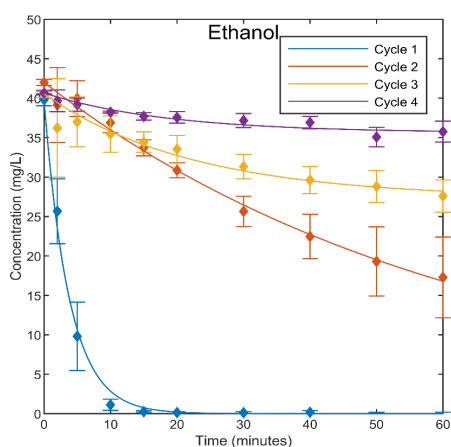


Figure 4-6-2. Kinetics of degradation of Orange II using Mn-Al MPs washed with ethanol and used during four cycles.

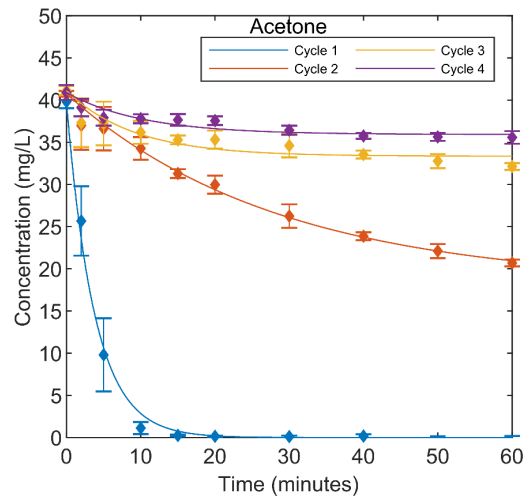


Figure 4-6-3. Kinetics of degradation of Orange II using Mn-Al MPs washed with acetone and used during four cycles.

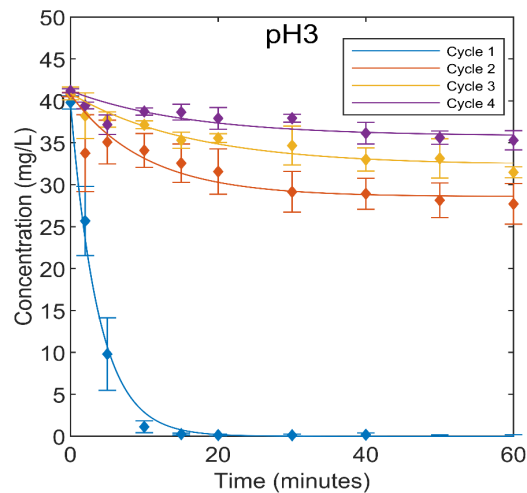


Figure 4-6-4. Kinetics of degradation of Orange II using Mn-Al MPs washed with distilled water with pH 3, and used during four cycles.

Figure 4-6-5 shows the percentage of final decolourization (at 60 minutes of test) for each of the four cycles according to the washing method. All the lines are decreasing and all reach a similar percentage of decolourization in the fourth cycle, 12.5% on average.

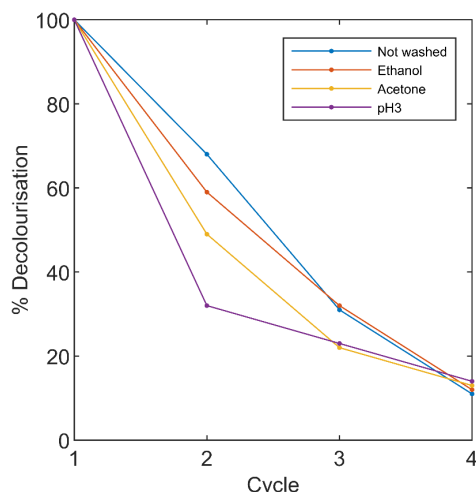


Figure 4-6-5. Colour degradation percentage after 60 minutes of treatment using particles recuperated and washed by different methods.

It is also possible to observe that in the second cycle, the order of efficiency of degradation of the colourant is: not washed > ethanol > acetone > pH 3. However, in the third cycle the order changes: ethanol > not washed > pH 3 > acetone. In any case, however, the difference in decolourization between the particles washed with ethanol and those not washed, and between acetone and distilled water with pH 3 is minimal.

4.6.2 Analysis of the reused Mn-Al particles

Here we present a surface study based on the results of electronic microscopy for MPs recovered after the first and third decolourization-washing cycles. These images will be compared to those of $Mn_{70}Al_{30}$ obtained in the previous sections and discussed along with the results obtained for the degradation kinetics. To proceed with the analysis, it will be done in three parts, analysing: the size of the particles, the shape of their surface and their composition.

The figures below show images of MPs after the first decolourization cycle (and washed if applicable) and after the third cycle (and washed if applicable). The size is an important factor as it will influence the available surface to interact with the dye. In the case of recovered but not washed particles, it can be observed that the particle size remained more or less constant (Figure 4-6-6 and Figure 4-6-7).

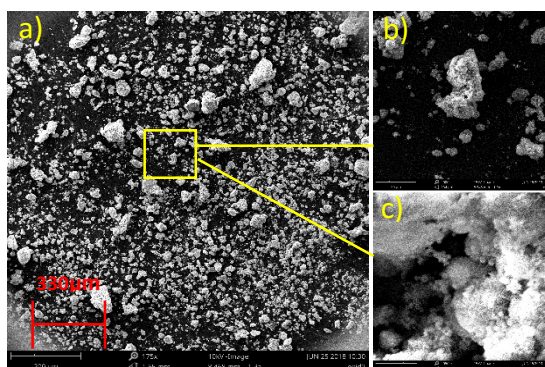


Figure 4-6-6. Morphology of MP $Mn_{70}Al_{30}$ recovered after the first decolourization cycle, at three magnifications: x175 (a), x2000 (b) and x20000 (c).

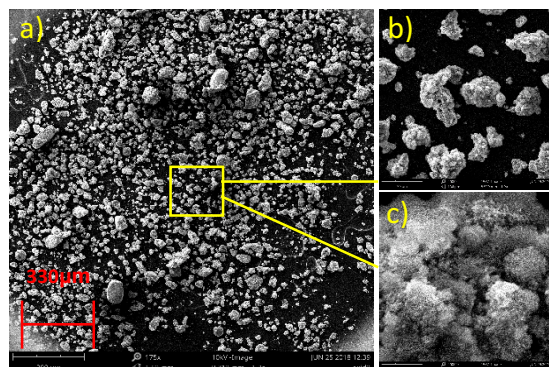


Figure 4-6-7. Morphology of MP $Mn_{70}Al_{30}$ recovered after the third decolourization cycle, at three magnifications: x175 (a), x2000 (b) and x20000 (c).

In the case of ethanol-washed particles (Figure 4-6-8 and Figure 4-6-9), MP after the third cycle show a much more homogeneous size than after the first cycle. In this case the particles seemed to have a larger size.

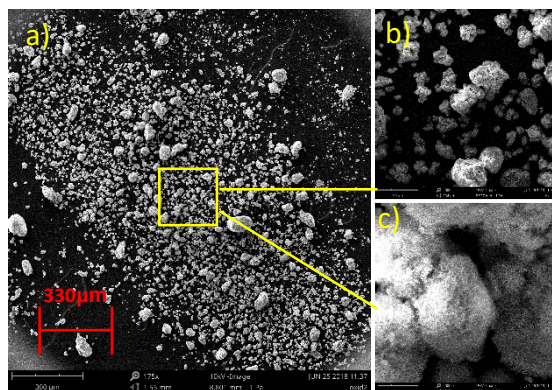


Figure 4-6-8. Morphology of MP $Mn_{70}Al_{30}$ recovered after the first decolourization cycle and washed with ethanol, at three magnifications: x175 (a), x2000 (b) and x20000 (c).

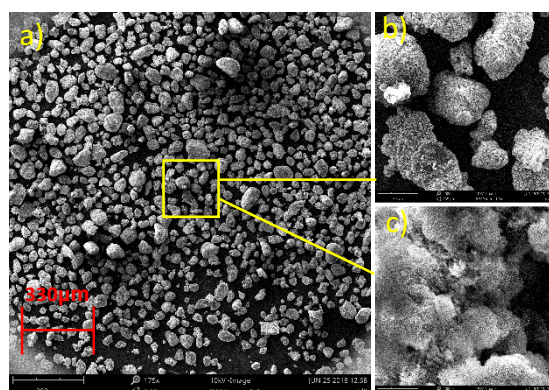


Figure 4-6-9. Morphology of MP $Mn_{70}Al_{30}$ recovered after the third cycle of decolourization and washed with ethanol, at three magnifications: x175 (a), x2000 (b) and x20000 (c).

Regarding the particles washed with distilled water with pH 3 (Figure 4-6-10 and Figure 4-6-11) and washed with acetone (Figure 4-6-12 and Figure 4-6-13), after the third cycle, they presented the same size and homogeneity as the ones washed with ethanol. They also seemed to be bigger than in the first cycle.

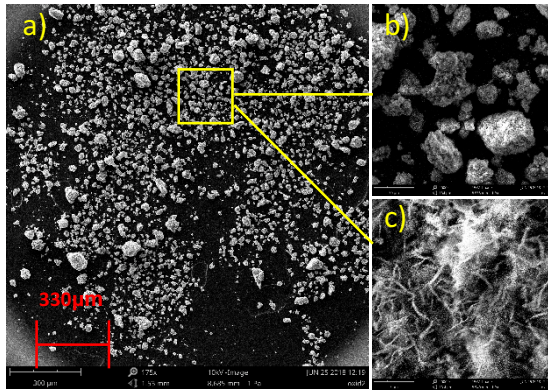


Figure 4-6-10. Morphology of MP $Mn_{70}Al_{30}$ recovered after the first decolourization cycle and washed with distilled water with pH3, at three focus magnifications: x175 (a), x2000 (b) and x20000 (c).

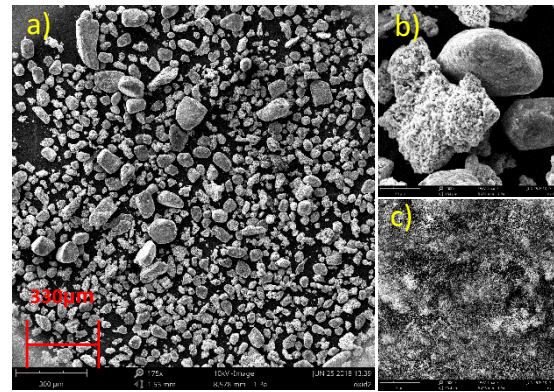


Figure 4-6-11. Morphology of MP $Mn_{70}Al_{30}$ recovered after the third decolourization cycle and washed with distilled water with pH3, at three magnifications: x175 (a), x2000 (b) and x20000 (c).

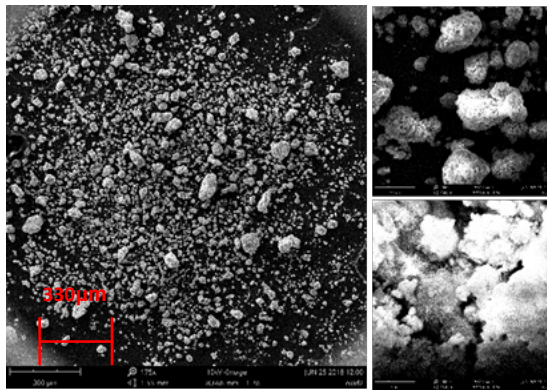


Figure 4-6-12. Morphology of MP $Mn_{70}Al_{30}$ recovered after the first decolourization cycle and washed with acetone, at three magnifications: x175 (a), x2000 (b) and x20000 (c).

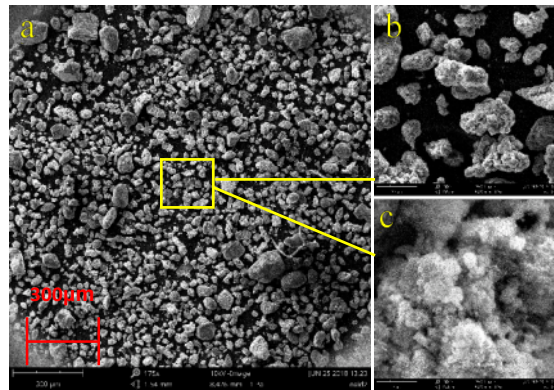


Figure 4-6-13. Morphology of MP $Mn_{70}Al_{30}$ recovered after the third cycle of decolourization and washed with acetone, at three magnifications: x175 (a), x2000 (b) and x20000 (c).

Washings with acetone and water with pH 3 had been carried out with stirring for two hours. A consequence could have been a greater physical degradation and decrease in size. But from this analysis it can be determined that this did not happen. It should be noted that among the particles washed with water at pH 3, a very large heterogeneity of the surface morphology was observed after the third cycle which was not observed after the first cycle (Figure 4-6-14).

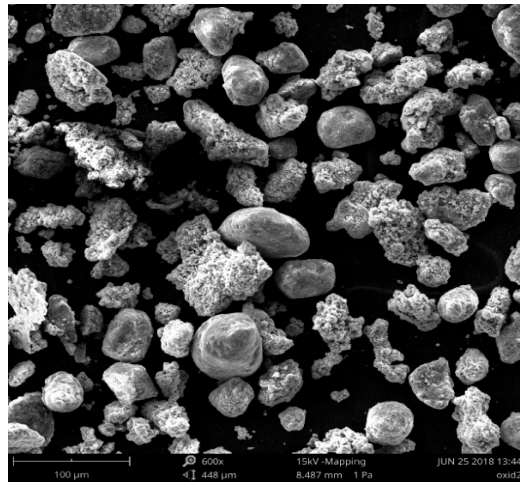


Figure 4-6-14. MPs after the third cycle and washed with distilled water with pH 3.

In order to study the morphology of the surface of the samples, the images of the different decolourization-washing cycles obtained at the highest magnification will be compared. Evident changes can be observed on the surface of the MPs once recuperated after the first decolourization cycle (Figure 4-6-15), after washing with ethanol (Figure 4-6-16) and after washing with acetone (Figure 4-6-17). There is a kind of ‘hairy’ layer that covers the particles and that is more grown after the third cycle. There is also a decrease in the roughness of the surface due to the coating of the surface by these precipitates. Although part of aluminium and manganese were expected to dissolve ionically in water [90][118], the size of the particles was not sensibly affected by this dissolution.

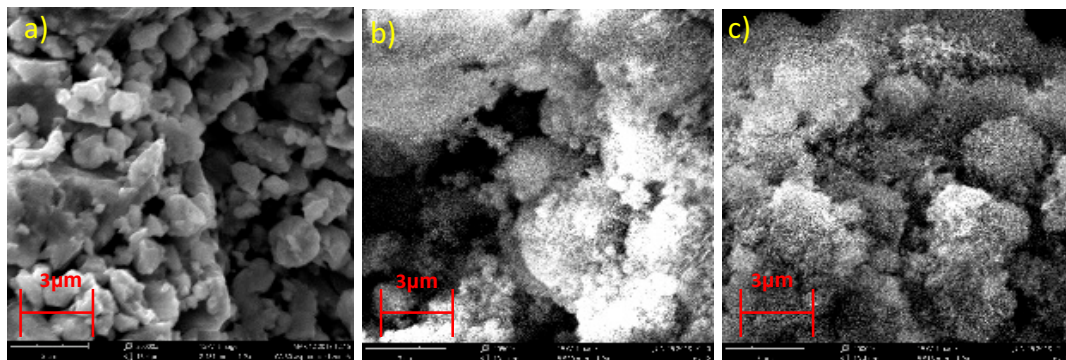


Figure 4-6-15. Morphology of the $Mn_{70}Al_{30}$ particles before using them (a), after the first decolourization cycle (b) and after the third cycle (c).

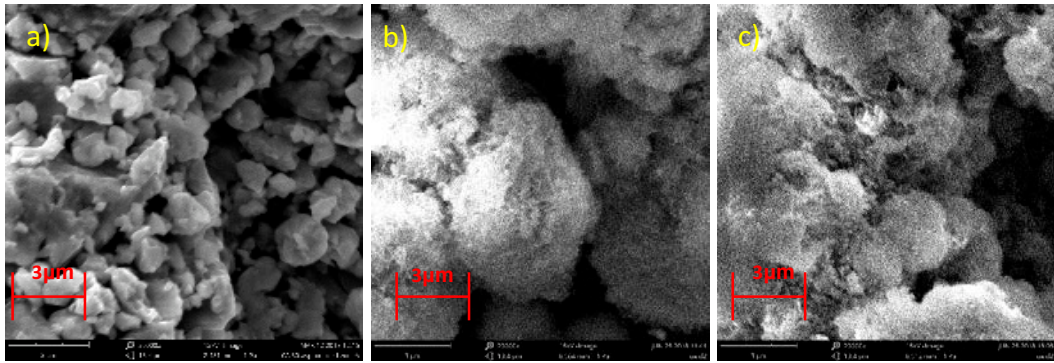


Figure 4-6-16. Morphology of the $Mn_{70}Al_{30}$ particles before using them (a), after the first cycle of decolorization and washing with ethanol (b) and after the third cycle and the same washing (c).

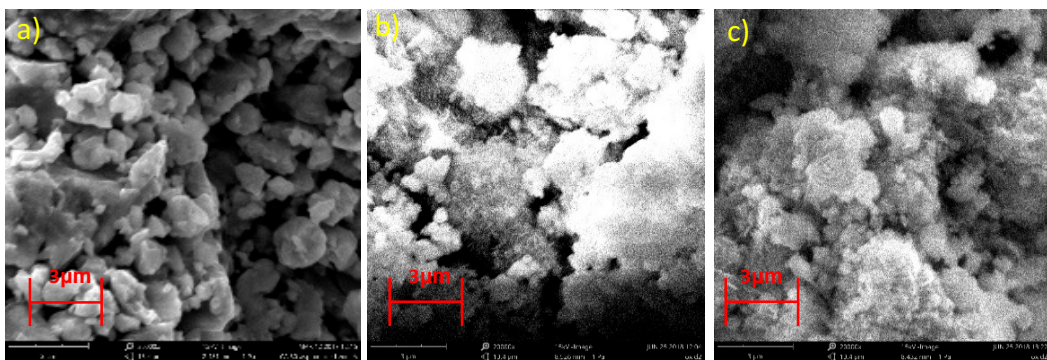


Figure 4-6-17. Morphology of the $Mn_{70}Al_{30}$ particles before using them (a), after the first cycle of decolorization and washing with acetone (b) and after the third cycle and the same washing (c)

In the case of the particles washed with distilled water with pH 3 the morphology of the surface was different (Figure 4-6-18). The roughness of the surface was also decreased, but instead, it seems covered with a layer of filaments or precipitates of lenticular or needle shape; more pronounced after the first wash than the third.

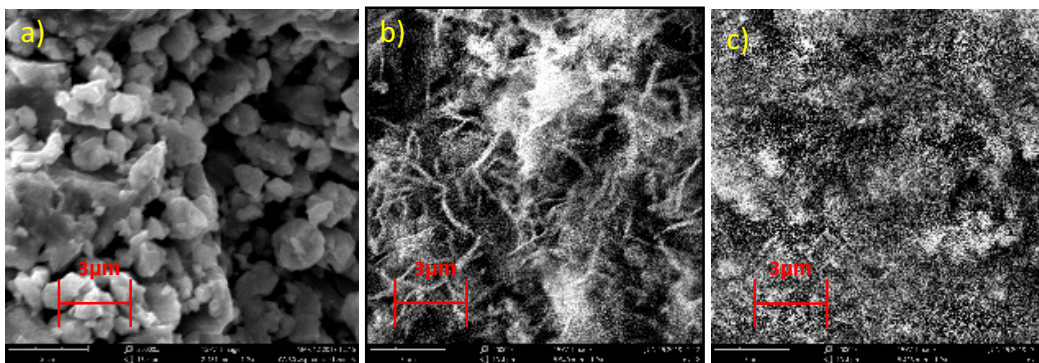
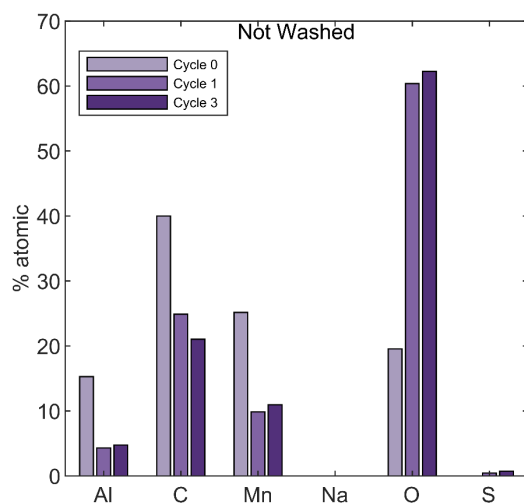


Figure 4-6-18. Morphology of the $Mn_{70}Al_{30}$ particles before using them (a), after the first decolorization cycle and washed with distilled water with pH 3 (b) and after the third cycle and the same washing (c).

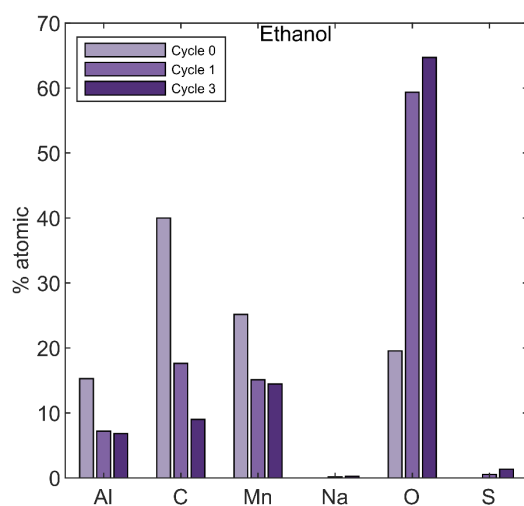
These visible layers may be formed by the degradation products of the colourant, a part of which could remain adhered to the surface, may be also due to the corrosion products

of the MPs in aqueous medium or by precipitations from the MPs reaction with the products used for washing. To check it, the atomic percentage of the elements present on the surface of MPs (Figure 4-6-19, Figure 4-6-20, Figure 4-6-21 and Figure 4-6-22) was analysed.



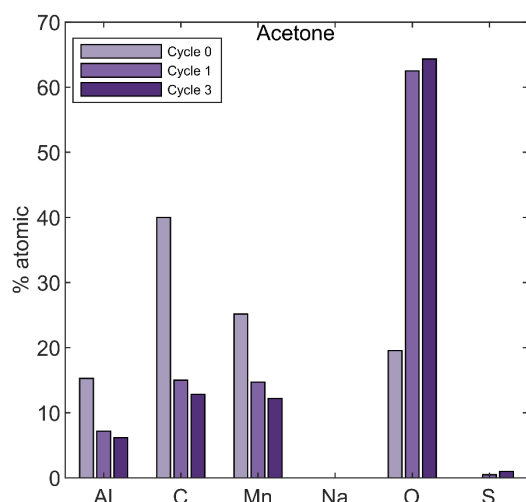
Element	Cycle 0	Cycle 1	Cycle 3
O	19.5	60.4	62.3
Mn	25.1	9.8	11.0
C	40.0	24.9	21.0
Al	15.3	4.3	4.8
S	0.00	0.4	0.7
Na	0.00	0.1	0.2

Figure 4-6-19. Atomic percentage of the elements present in the samples of MPs before using them, after the first cycle of decolourization and after the third.



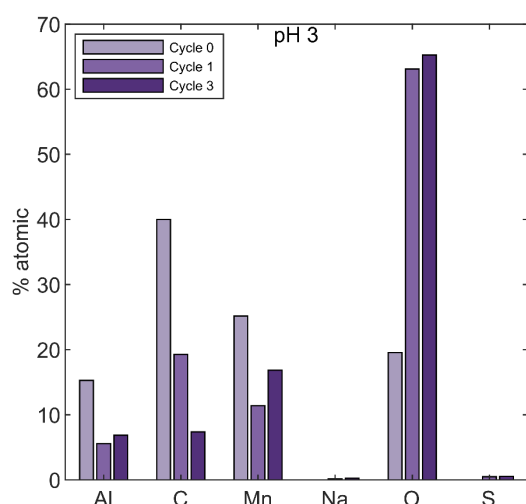
Element	Cycle 0	Cycle 1	Cycle 3
O	19.5	59.4	64.7
Mn	25.2	15.1	14.5
C	40.0	17.6	9.0
Al	15.3	7.2	6.8
S	0.00	0.5	1.4
Na	0.00	0.2	0.2

Figure 4-6-20. Atomic percentage of the elements present in the samples of MPs before using them, after the first cycle of decolourization and washing with ethanol, and after the third cycle and the same washing.



Element	Cycle 0	Cycle 1	Cycle 3
O	19.6	62.5	64.3
Mn	25.2	14.3	12.2
C	40.0	15.0	12.8
Al	15.3	7.2	6.2
S	0.00	0.5	1.0
Na	0.00	0.1	0.2

Figure 4-6-21. Atomic percentage of the elements present in the samples of MPs before using them, after the first cycle and washed with acetone and after the third cycle and same washing.



Element	Cycle 0	Cycle 1	Cycle 3
O	19.6	63.1	65.3
Mn	25.2	11.4	16.8
C	40.0	19.3	7.4
Al	15.3	5.6	6.9
S	0.00	0.5	0.5
Na	0.00	0.1	0.2
Cl	0.00	0.00	0.1

Figure 4-6-22. Atomic percentage of the elements present in the samples of MPS before using them, after the first decolorization cycle and washed with distilled water at pH 3 and after the third cycle and the same washing.

In all four cases an increase in the atomic percentage of oxygen was observed. This indicates that after each cycle the degree of oxidation of the particles or the presence of compounds with oxygen content adsorbed on their surface increased. There were not found significant differences between the atomic percentage of oxygen between the washed and the non-washed particles. Therefore, it can be concluded that the washings were not successful in diminishing the oxidation of the surface of the particles, oxidation that was mainly produced during the decolorization reaction.

Although it has been shown that the main decolorizing mechanism is the breakage of the azo bond of the dye molecule and not the adsorption of it by the particle, it was expected that part of the colouring or their degradation products remained adsorbed on

the surface of the particles. The increase in the presence of sodium and sulphur, elements that form part of the Orange II molecule, confirmed this. In the case of MPs washed with distilled water at pH3 (Figure 4-6-22), chlorine was found after the third cycle, a consequence of the hydrochloric acid used to lower the pH of the distilled water.

The analysis of the surface of the particles did not show significant differences, from the point of view of morphology or composition, which may explain the differences in efficiency between the different types of washing tested in this study. In fact, the comparison with the recovered particles without washing, indicates that the different types of washing protocols tested in this work did not manage to significantly modify the surface of the particles in order to reactivate their decolourizing properties. The different types of washing methods studied here had been reported to work in other types of zero-valent particles. Therefore, it is worth noting here that although Mn-Al particles show outstanding fast decolourizing reactions in some colourants, their reuse is not efficient. This may be solved by finding a proper washing solution that could reactivate the Mn-Al particles, but for the moment it remains an important drawback in comparison to other types of zero-valent metallic particles.

4.7 Comparison with bacterial treatment

Bacterial treatment is a simple method of decolourizing and degrading synthetic dyes [119]. Within the bioreactor, the decolourisation and degradation processes can take place either sequentially or concurrently. Bioreactors face the unfortunate problem that many dye compounds are chemically stable and resistant to microbiological attack [120]. This also proved to be the case with the Azo dyes used within the experiments, as they were found to be resistant to decolourisation and degradation by the biofilms and willow chips in the employed bioreactor. The key reason for choosing wood chips was due to them being commonly accessible by-products in most agronomical regions [121].

By doubling the number of reactors, from one to two, the potential performance of the system supposed to be enhanced but residence time was roughly doubled. This step was seen as somewhat vital as the wastewater employed by the system was not that dissimilar from genuine wastewater.

To utilise microorganisms with organic dye decolourization abilities the system made use of a solution obtained from the soaking of forest residue. Specifically forest residue in the form of willow chips, of weight 652 g, was soaked with 400 mL of 0.9 % NaCl for 48 h. The system employed a feed flow rate of 0.39 mL / min.

Aromatic compounds possess a large negative resonance energy, resulting in thermodynamic stability[122]. Microorganisms, particularly bacteria, have evolved

enzyme systems that degrade the benzene structure under aerobic and anoxic conditions. A group of aromatic amines difficult to degrade even under aerobic conditions are represented by aryl sulfonates, amino benzene (ABS) and aminonaphthyl sulfonates (ANS), which are the constituents of many azo dyes[123].

Two size ranges of willow chips, employed as the support media, were used for conducting the experiments, these being 2.8 cm - 4 cm and 5.6 cm - 8 cm. Meanwhile feed flow rate was altered from a minimum of 0.7 cm / min to a maximum of 8.5 cm / min. Base concentration on the other hand was altered from a minimum of 0.0211 mg / L to a maximum of 0.39 mg / L.

Raw feed concentration, in a commercial trickling filter operation, is normally diluted by recycling a percentage of the effluent back into the raw feed [124][125]. Furthermore, as the microorganisms are directly involved in the dye removal process[126], it is normal to sustain the health of the microorganisms in some manner and this is usually achieved by periodically providing nutrients to the raw feed. Following this, and prior to the release of the effluent, it is usual to separate the solid waste from the effluent by employing some form of sedimentation procedure. However, effluent re-cycling and nutrient addition scheduling were not utilised within the experiments conducted here.

Experiment one made use of the 2.8 cm – 4 cm diameter wood chips only; the wood chips being used to provide the support media for the microbiological build up. This diameter size range was chosen following best practices found in literature on the subject, which suggested a column diameter to particle diameter ratio. This experiment employed an acrylic column of internal diameter 20 cm (and height 100.33 cm), it therefore followed that 2.8 cm - 4 cm diameter wood chips would be a close-fit to the suggested ratio range. Secondary considerations that impacted the wood chip diameter choice were wood chip specific surface area as well as flow impediment issues. A greater total surface area presents more anchor site opportunities for the microorganisms. Surface area is increased by using smaller chip diameters. However, flow impediment issues increase in likelihood with decreasing diameter size. Therefore, total surface and impediment issues pull the diameter size decision in opposite directions.

Flow rate experiments exhibited a little wastewater dye removal at the lower 1.4 cm / min flow rate during the initial days. Later on in the experiment though, on day 9 at 3pm, the outlet effluent was found to contain willow chips which would imply that wastewater dye removal analysis should only be performed following outlet effluent filtering. This willow chips contamination of the outlet effluent was also noticed in samples outcomes taken on day 11 at 4pm and also on day 12 at 1pm which would again suggest that outlet effluent filtering should be performed prior to analysis. Flow rate was increased from 1.4

cm / min to 2.8 cm / min following day 14 of the experiment. This new flow rate was maintained for a period of 42 days. During this 42 day period the system at times removed up to 36.4% of the feed COD. However, during the same 42 day period, there were times when filtered outlet effluent COD was actually higher than the feed inlet COD resulting in a negative decolourisation efficiency. There was not a great deal of variation in the removal efficiency over this period.

Clogging was a recurring problem during this period as a result of willow chips overgrowth. During each clogging episode it was necessary to temporarily suspend the experiment in order to remedy the overgrowth before continuing. This remedial action took the form of removing the wood chips, cleaning them in a tap water filled beaker, then returning the wood chips to the reactor. The clogging episodes occurred on days 25, 35, 47, and 56. The remedial action previously mentioned took place following each clogging episode with the exception of day 56 where instead the experiment was finally stopped. Interestingly, it was noticed that removal efficiency would increase during the run-up to a clogging episode. Note that the larger 5.6 cm to 8 cm sized wood chips were far less susceptible to clogging than the 2.8 cm to 4 cm sized wood chips. Factors that influenced the decolourization rate, as discerned from the results, were residence time, concentration, and active surface area. However, it could not be determined which of these factors was the key factor.

The increased flow rate experimental results established that active surface area was increased at the cost of a reduction in residence time. It was determined that a column of length 100.33 cm would be required to allow approximately 90 % decolourization while using an ideal flow rate of 7.1 cm / min. This determination made several assumptions. The first assumption was that the feed mass transfer to the biofilm did not decrease as a result of decreasing pollutant concentration. The second was that the decolourisation rate was $10 \text{ kg COD} / \text{m}^3_{\text{bed}} \text{ day}$ in conjunction with a load rate of $53.3 \text{ kg COD} / \text{m}^3 \text{ day}$. Results collated from a set of experiments revealed that the trickling filter system employing willow chips as a support medium was unable to treat azo dye contaminated wastewater. The result also showed there was no preference to the removal of Azo dyes (Orange G). From the 0% removal between the inlet and the outlet Orange G concentration, there seemed to be no preference. The removal percentage of Orange G based on the GC results were both around less than 1%. For this set of experiments, loading rate was altered from experiment to experiment, by modifying feed concentration and/or feed flow rate. Both variations were done in separate columns. In the experiment that carried out using willow chip with a diameter of 5.6 – 8 cm, it was found that increasing the loading by increasing the flow rate and feed concentration resulted in increased removal rate. Higher feed concentration provided an increased driving force

mass transfer, while higher flow rate provided a larger active surface area on the medium that increased removal rate. However, in this experiment, the advantage of high flow rate was offset by the reduction in residence time.

4.8 Discussion of the decolourization reactions

One of the main results of the study of the degradation kinetics of an aqueous solution of Orange II is that the $Mn_{70}Al_{30}$ particles are much more efficient than the $Mn_{50}Al_{50}$ particles or the pure Mn and Al powders. The results of this study also indicate that an increase of temperature accelerates the degradation reaction of the Orange II dye. The results obtained in different temperature conditions can be used to calculate the thermodynamic parameters [117][127]. For all the dyes, the adsorption capacities decrease slightly with increasing temperature, implying the exothermic nature of the adsorption process. This exothermic nature is beneficial to the practical application without the need of additional energy when used in the river or other natural systems.

Many researchers [128] have reported that pH play a key role in the degradation of azo dyes. In our case, the pH was observed to produce a rather complex effects due to the changes that occur during the application of the particles. The pH values greatly influence the adsorption and degradation due to surface properties of adsorbent and ionization/dissociation of the adsorbate molecule [129]. In this sense, the inactivity of MPs in alkaline conditions is often explained by the formation of a passivation layers on their surface [130]. Figure 4-8-1 shows a simple scheme of the degradation reaction. The MPs induce a decrease in the pH due to the increase in protons. This step is essential for the degradation of Orange II. The presence of Mn (which has less potential than Al) in Mn-Al systems does not only accelerates the evolution of hydrogen but also prevents the development of a homogeneous layer of oxide above the surface of aluminium. That is why the MPs with more Al content are unable to act against the changes in pH due to this effect of surface passivation.

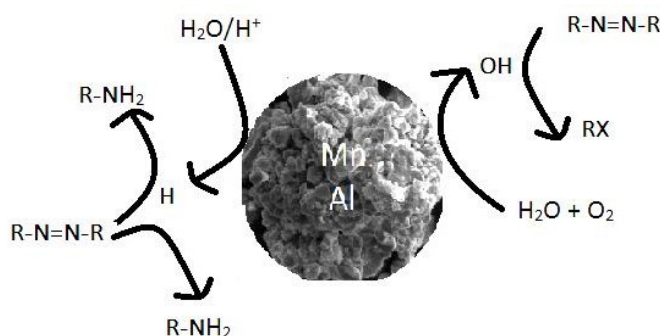
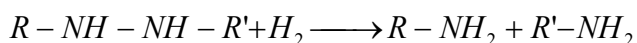
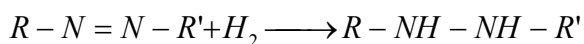
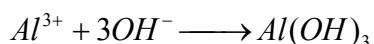
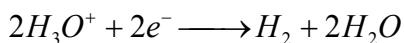
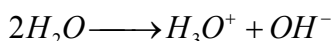
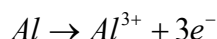


Figure 4-8-1. Representation of the extraction between the colourant and the metal particle and the resulting reactions.

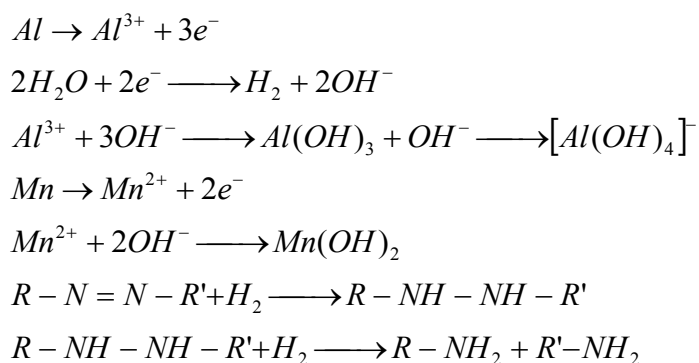
The decolourization reaction of Orange II has been proven to develop through the breakage of the azo bond, forming two amines as seen in the chromatography results discussed in this work [131]. Dye adsorption on the surface of nanoparticles was also detected, and could be an effective process as it increases the contact between dye molecules and the surface of MPs. This is governed by adsorption [106].

Metallic particles, both $Mn_{70}Al_{30}$ and $Mn_{50}Al_{50}$, lose metallic ions due to corrosion effects, and are covered by layers of reaction products during their corrosion. That is why in the EDX analyses there was, proportionally, less amount of Mn and Al in the final state than at the beginning. A certain amount of metal ions is released into the water and, as seen by atomic absorption spectrometry, this effect is more important for Mn, which is the most active element. After the treatment, the particles have a more homogeneous distribution of elements on the surface, more oxygen due to oxidation and more carbon and sulphur due to the colourant.

Both Al and Mn ions have different solubility dependent on the pH conditions. In aqueous media, Al oxidizes for $pH < 3$ but it forms $Al(OH)_3$ for $pH > 5$. On the other hand, Mn^{2+} forms soluble salts at $pH < 3$ but its solubility decreases with increasing pH until becoming completely insoluble at $pH = 9$. The ICP-MS measurements at initial $pH = 4$ conditions shown above confirmed this difference in solubility. Therefore, it is expected that the oxidation and dissolution of Mn permits that non-oxidized Al atoms, originally inside the metallic matrix, become exposed to the dyed solution thus participating also in the redox process in acidic conditions. Therefore, in acidic conditions the mechanism proposed for the degradation of Orange II is the same as the one proposed for RB5 degradation:



On the other hand, at high pH, Mn form insoluble hydroxides while the Al hydroxides become soluble, this becoming the main mechanism of the particles degradation reaction. In basic conditions we propose the following mechanism:



In other studies, Al-based alloys in metastable form showed good performance in alkaline conditions [132], the good performance under a wide range of pH is then a possible indication of the active role of Al in the reaction. It should be highlighted, however, that the mechanisms of the reaction proposed here would need further experimental confirmation.

In the study of Acid Black 58 we extracted as main results that it is susceptible of being degraded by the Mn-Al MPs. However, decolourization did not happen through the progressive degradation of the Azo link, but mainly by adsorption of the dye molecules on the particles surface. This colourant is known to form complexes with metals and this could be on reason for its facility to adhere on the MPs. The analysis by SEM and EDX of the particles indicated that there was a strong interaction between the dye and the MPs and, in addition, the washing of the particles corroborated the major adsorption of the dye molecules on the surface of the MPs.

As for the Orange G, the behaviour under pH and temperature changes is similar of Orange II despite the Mn-Al MPs did not achieve the same efficiency as for Orange II. In some conditions the decolourization was remarkable, but the process stabilized without being completed in all the studied cases. The acid pH and the higher temperatures were shown to increase the reaction rate. In this case, however, the absence of important adsorption, indicates the reaction should proceed with similar mechanisms as the ones proposed before for Orange II. Why this dye is more resistant to the treatments with Mn-Al particles is an important issue, both concerning the understanding of the decolourization reaction as well as in order to assess the efficiency of the treatment in real textile wastewaters with presence of different types of dyes. However, we do not have, at this stage of the research, enough experimental evidences to enlight this point.

5. Conclusions

The goal of this thesis was the study of the decolourization of textile wastewater by using micro-particles of Mn-Al alloys. The alloys were produced by mechanical alloying techniques resulting in nanostructured compounds. The water decolourization ability of the particles was tested for different commercially available azo dyes. The objective of the work was to find the optimal material and microstructure of the micro-particles for a given set of process conditions like temperature, pH, pollutant type, and concentration.

Efficacy and cost are key factors in deciding the best option. The Mn-Al metallic particles were found to have a high efficiency in catalysing the reaction that breaks the azoic linkage of the Orange II dye, achieving better performance than in the case of zero-valent iron metallic particles. Orange II colourant is one of the most used in this kind of studies, and it is often chosen as a benchmark to test the efficiency of decolourizing materials. Therefore, the high decolourization efficiency of the Mn-Al alloys reported in this work makes them potential candidates as materials for this kind of application.

The effects of different factors (temperature, pH, dosage, and milling time) were studied, permitting to define optimal working conditions. The reaction rate increased as the temperature increased and pH decreased. The activation energy of the reaction was found to be 43.9 kJ mol^{-1} . The low activation energy and the rapid degradation kinetics observed in this system makes it promising as a low-cost, efficient material for textile-waters decolourization. Although the effect of temperature is evident, the low activation energy does not justify the energy and economic costs in maintaining a temperature at values higher than $40 \text{ }^\circ\text{C}$. With respect to the pH, obvious changes were observed but were not significant enough to justify the cost that would entail maintaining a constant pH adjustment. Contrary of Fe-based materials, the high decolourizing efficiency was not severely decreased in alkaline conditions. An important feature of the MPs employed was the milling time, the reaction speed was found to increase significantly with this production parameter. Of the three types of particles that were studied (milled during 20h, 30h, and 60h), MPs with a milling time of 60 hours were those that catalysed faster the reaction. The characterization of the MPs determined that the MPs produced with the longest milling time were formed by particles of smaller size resulting, therefore, in a larger specific surface area. It was also determined that the minimum amount of MPs necessary to carry out a complete decolourization in less than one hour at room temperature and without pH modification is $12.5 \text{ mg} / 100 \text{ ml}$ for Orange II solution

All the compositions studied (Al, $\text{Mn}_{50}\text{Al}_{50}$, $\text{Mn}_{70}\text{Al}_{30}$, and Mn) were found to degrade the azo link of the Orange II dye, but the $\text{Mn}_{70}\text{Al}_{30}$ alloy was the most efficient. The

morphology and size of the MPs determines the specific area available to interact with the colourant. It was observed that, after being mechanically milled with the same protocols, the particles that presented a greater specific surface area were the aluminium particles while those that presented a smaller specific surface area were the $Mn_{70}Al_{30}$ particles. The fact that the $Mn_{70}Al_{30}$ particles produced a shorter reaction time, despite having the smallest specific surface area, remarks the high reactivity shown by this composition. The high reactivity of Mn is somewhat enhanced by the presence of Al. The latter, which is easily passivated and protected by an oxide layer, needs also the presence of Mn to remain active as a decolourizing element. The water and particle analyses revealed that MPs not only break the azo bonds producing amines but that some part of the dye is also adsorbed to the MPs surface. From the decolourization kinetics at different conditions and the particles and water analyses, a degradation mechanism of Orange II molecules by Mn-Al particles is proposed in this work, as detailed in section 4.8.

We next used the $Mn_{70}Al_{30}$ MPs to explore their effectiveness in the decolourization of other azo dyes such as Orange G and Acid Black 58. Kinetic studies demonstrated their efficacy in the decolourization of Acid Black 58. However, the experimental data indicated the role of additional decolourization mechanisms, in addition to the breakdown of the azo link, being responsible for the decolourization of Acid Black 58. Adsorption of dye on MPs or the breakage of other chemical bonds seems likely to play a significant role. It should be noted that the procedure used in this study demonstrates a limited effectiveness in the decolourization of Orange G, which only showed a partial decolourization, this indicating that the efficiency of the reaction is altered in different types of azo-dyes.

Regarding the toxicity, the toxicity tests concluded that the treatment using Mn-Al particles reduces the toxicity of the coloured solutions, even though the decolourized water contains a significant amount of Mn ions after the process. The significance of this Mn dissolution should be taken into account in case of implementing the Mn-Al as a decolourizing material in real world applications.

Another main objective of this study was to determine whether MPs of $Mn_{70}Al_{30}$ are reusable, and how their degradation efficiency decreases with each cycle. The obtained results showed that the particles can be recovered and reused up to four times; the decolourization capacities gradually decreasing in each cycle. This can be explained by the fact that more adsorption sites are occupied after each cycle and the formation of a layer of precipitates that decreases the roughness, causing a decrease in contact area between the zero metals and the coloured solution. Washings with ethanol, acetone and distilled water with pH 3, were not capable of removing the layer formed after each cycle. On the contrary, they cause a decrease in the efficiency of decolourization, in comparison

with the treatment with particles recovered but not washed. So the reuse without washing is the best option. However, the difference is not very pronounced between the various particle recuperation methods studied in this work, nor there are notable differences between washing with and without agitation.

The general experiment to determine whether willow chips could be used as a bed medium to remove organic pollutants was unsuccessful. Using artificial wastewater based on the dominant contaminants, the willow chips were not able to remove organic contaminants. In order to increase the removal rate of the treatment, flow rate was increased. Increasing the flow rate provided a more active surface area for mass transfer between the feed and the biofilm. Removal efficiency could be increased by using a longer column, as a longer column would give a longer residence time at the same flow rate compared to a shorter column. Aside from the treatment system factors, there were additional factors that could explain the low removal rate. First, there was no addition of nutrients during the experiment, since it was thought that the microorganisms were able to use nutrients present in the support medium. The bioreactor technology was shown to be unusable in the bio-decolourization of all of the types of dyes used in this work. However, when willow chips were used, the bio process exhibited lower efficiency and lower detoxification, and the wastewater did not fully decolourise all of the tested dyes. The repeated batch mode experiment showed that it was impossible to decolourise different dyes in a short period of time. After five cycles, loss of decolourisation capacity was observed. The use of the whole trickling filter is not fully applicable in cases where there is a complex compound to oxidize.

Many aspects must still be solved. Investigations with other commercially available dyes and additional tests to demonstrate the reliability of the results should be performed to better understand the mechanisms of degradation and the products obtained in each case. Also, it would be necessary to adjust the dosage of particles to avoid the release of metal ions into the environment in harmful concentrations. and to optimise the control of MPs during the decolourisation processes carried out in the industrial field. However, the results presented in this work, support the effectiveness of the Mn-Al MPs method for the decolourization of dye-contaminated water.

References

- [1] O. L. Rosi, M. Casarci, D. Mattioli, and L. De Florio, "Best available technique for water reuse in textile SMEs (BATTLE LIFE Project)," *Desalination*, vol. 206, no. 1–3, pp. 614–619, Feb. 2007.
- [2] "Integrated Pollution Prevention and Control (IPPC) Reference Document on Best Available Techniques for the Textiles Industry," 2003.
- [3] T. Robinson, G. McMullan, R. Marchant, and P. Nigam, "Remediation of dyes in textile effluent: a critical review on current treatment technologies with a proposed alternative," *Bioresour. Technol.*, vol. 77, no. 3, pp. 247–255, May 2001.
- [4] S. Asad and M. A. Amoozegar, "Decolorization of textile azo dyes by newly isolated halophilic and halotolerant bacteria," vol. 98, pp. 2082–2088, 2007.
- [5] R. S. Gandhi, "Chemical processing of synthetics and blends - Impact on environment and solutions," *Indian J. Fibre Text. Res.*, vol. 26, no. 1–2, pp. 125–135, 2001.
- [6] A. Conneely, W. F. Smyth, and G. McMullan, "Study of the white-rot fungal degradation of selected phthalocyanine dyes by capillary electrophoresis and liquid chromatography," *Anal. Chim. Acta*, vol. 451, no. 2, pp. 259–270, Jan. 2002.
- [7] A. Pandey, P. Singh, and L. Iyengar, "Bacterial decolorization and degradation of azo dyes," *Int. Biodeterior. Biodegradation*, vol. 59, no. 2, pp. 73–84, Mar. 2007.
- [8] P. Nigam, G. Armour, I. Banat, D. Singh, and R. Marchant, "Physical removal of textile dyes from effluents and solid-state fermentation of dye-adsorbed agricultural residues," *Bioresour. Technol.*, vol. 72, no. 3, pp. 219–226, May 2000.
- [9] M.-C. Chang, C.-P. Huang, H.-Y. Shu, and Y.-C. Chang, "A New Photocatalytic System Using Steel Mesh and Cold Cathode Fluorescent Light for the Decolorization of Azo Dye Orange G," *Int. J. Photoenergy*, vol. 2012, no. August, pp. 1–9, 2012.
- [10] N. Casas, P. Blázquez, X. Gabarrell, T. Vicent, G. Caminal, and M. Sarrà, "Degradation of Orange G by Laccase: Fungal Versus Enzymatic Process," *Environ. Technol.*, vol. 28, no. 10, pp. 1103–1110, Oct. 2007.
- [11] V. M. Correia, T. Stephenson, and S. J. Judd, "Characterisation of textile wastewaters - a review," *Environ. Technol.*, vol. 15, no. 10, pp. 917–929, Oct. 1994.
- [12] I. Holme, "Sir William Henry Perkin: a review of his life, work and legacy," *Color. Technol.*, vol. 122, no. 5, pp. 235–251, Oct. 2006.
- [13] R. Christie, *Colour Chemistry*. Cambridge: Royal Society of Chemistry, 2007.
- [14] K. Hunger, *Industrial dyes: chemistry, properties, applications*. Wiley-VCH, 2003.
- [15] D. Jacquemin, C. Peltier, and I. Ciofini, "On the Absorption Spectra of Recently Synthesized Carbonyl Dyes: TD-DFT Insights," *J. Phys. Chem. A*, vol. 114, no. 35, pp. 9579–9582, Sep. 2010.
- [16] Y. Zhang et al., "Cyanation of aryl bromides catalyzed by N-heterocyclic carbene / Pd(OAc)₂," vol. 8, pp. 41–45, 2009.
- [17] R. Kant, "Textile dyeing industry an environmental hazard," *Nat. Sci.*, vol. 04, no. 01, pp. 22–26, 2012.
- [18] R. M. Christie, *Colour chemistry*. Royal Society of Chemistry, 2001.
- [19] R. Raue and J. F. Corbett, "Nitro and Nitroso Dyes," in *Ullmann's Encyclopedia of Industrial Chemistry*, Weinheim, Germany: Wiley-VCH Verlag GmbH & Co. KGaA, 2000.
- [20] H. Zollinger, *Color chemistry: syntheses, properties, and applications of organic*

- dyes and pigments. Verlag Helvetica Chimica Acta, 2003.
- [21] M. Joshi, R. Bansal, and R. Purwar, "Colour removal from textile effluents," *Indian J. Fibre Text. Res.*, vol. 29, no. 2, pp. 239–259, 2004.
- [22] S. K. Sharma and R. Sanghi, "Advances in water treatment and pollution prevention," *Adv. Water Treat. Pollut. Prev.*, vol. 9789400742, no. June 2015, pp. 1–457, 2012.
- [23] M. Pérez, F. Torrades, X. Domènech, and J. Peral, "Fenton and photo-Fenton oxidation of textile effluents," *Water Res.*, vol. 36, no. 11, pp. 2703–2710, Jun. 2002.
- [24] T. Robinson, G. McMullan, R. Marchant, and P. Nigam, "Remediation of dyes in textile effluent: a critical review on current treatment technologies with a proposed alternative," vol. 77, pp. 247–255, 2001.
- [25] J. J. Pignatello, E. Oliveros, and A. MacKay, "Advanced Oxidation Processes for Organic Contaminant Destruction Based on the Fenton Reaction and Related Chemistry," *Crit. Rev. Environ. Sci. Technol.*, vol. 36, no. 1, pp. 1–84, Jan. 2006.
- [26] K. Wu, Y. Xie, J. Zhao, and H. Hidaka, "Photo-Fenton degradation of a dye under visible light irradiation," *J. Mol. Catal. A Chem.*, vol. 144, no. 1, pp. 77–84, Jul. 1999.
- [27] J. García-Montaña et al., "Environmental assessment of different photo-Fenton approaches for commercial reactive dye removal," *J. Hazard. Mater.*, vol. 138, no. 2, pp. 218–225, Nov. 2006.
- [28] A. Galadi and M. Julliard, "Photosensitized oxidative degradation of pesticides," *Chemosphere*, vol. 33, no. 1, pp. 1–15, Jul. 1996.
- [29] J. Kiwi, J. Fernández, H. D. Mansilla, C. Lizama, J. Freer, and J. Baeza, "Orange II photocatalysis on immobilised TiO₂," *Appl. Catal. B Environ.*, vol. 48, no. 3, pp. 205–211, 2004.
- [30] R. J. Davis, J. L. Gainer, G. O'Neal, and I.-W. Wu, "Photocatalytic Decolorization of Wastewater Dyes," *Water Environment Research*, vol. 66, pp. 50–53.
- [31] P. Peralta-Zamora et al., "Degradation of reactive dyes I. A comparative study of ozonation, enzymatic and photochemical processes," *Chemosphere*, vol. 38, no. 4, pp. 835–852, Feb. 1999.
- [32] E. Oguz and B. Keskinler, "Comparison among O₃, PAC adsorption, O₃/HCO₃⁻, O₃/H₂O₂ and O₃/PAC processes for the removal of Bomaplex Red CR-L dye from aqueous solution," *Dye. Pigment.*, vol. 74, no. 2, pp. 329–334, Jan. 2007.
- [33] C. A. Martínez-Huitle and E. Brillias, "Decontamination of wastewaters containing synthetic organic dyes by electrochemical methods: A general review," *Appl. Catal. B Environ.*, vol. 87, no. 3–4, pp. 105–145, Apr. 2009.
- [34] Ü. B. Ögütveren and S. Koparal, "Color removal from textile effluents by electrochemical destruction," *J. Environ. Sci. Heal. . Part A Environ. Sci. Eng. Toxicol.*, vol. 29, no. 1, pp. 1–16, Jan. 1994.
- [35] R. Pelegrini, P. Peralta-Zamora, A. R. de Andrade, J. Reyes, and N. Durán, "Electrochemically assisted photocatalytic degradation of reactive dyes," *Appl. Catal. B Environ.*, vol. 22, no. 2, pp. 83–90, Sep. 1999.
- [36] M. E. Karim, K. Dhar, and M. T. Hossain, "Physico-Chemical and Microbiological Analysis of Textile Dyeing Effluents," *IOSR J. Environ. Sci. Ver. II*, vol. 9, no. 7, pp. 2319–2399, 2015.
- [37] G. Crini, "Non-conventional low-cost adsorbents for dye removal: A review," *Bioresour. Technol.*, vol. 97, no. 9, pp. 1061–1085, Jun. 2006.
- [38] A. B. dos Santos, F. J. Cervantes, and J. B. van Lier, "Review paper on current technologies for decolourisation of textile wastewaters: Perspectives for anaerobic

- biotechnology,” *Bioresour. Technol.*, vol. 98, no. 12, pp. 2369–2385, Sep. 2007.
- [39] S. Sandhya, “Biodegradation of Azo Dyes Under Anaerobic Condition: Role of Azoreductase,” Springer, Berlin, Heidelberg, 2010, pp. 39–57.
- [40] I. M. Banat, P. Nigam, D. Singh, and R. Marchant, “Microbial decolorization of textile-dyecontaining effluents: A review,” *Bioresour. Technol.*, vol. 58, no. 3, pp. 217–227, Dec. 1996.
- [41] V. G. R. Babu, “Colour Removal From Dye House Effluent Using Zero Valent Iron And Fenton Oxidation,” no. December 2003, pp. 1–604, 2003.
- [42] C. O’Neill, A. Lopez, S. Esteves, F. R. Hawkes, D. L. Hawkes, and S. Wilcox, “Azo-dye degradation in an anaerobic-aerobic treatment system operating on simulated textile effluent,” *Appl. Microbiol. Biotechnol.*, vol. 53, no. 2, pp. 249–254, Feb. 2000.
- [43] H. O. Mndez-Acosta, R. Femat, V. Gonzlez-Ivarez, and J. P. Steyer, “Substrate regulation in an anaerobic digester based on geometric control,” *Ifacclca*, no. July 2016, 2002.
- [44] C. . Shaw, C. . Carliell, and A. . Wheatley, “Anaerobic/aerobic treatment of coloured textile effluents using sequencing batch reactors,” *Water Res.*, vol. 36, no. 8, pp. 1993–2001, Apr. 2002.
- [45] K. Paździor, A. Klepacz-Smółka, S. Ledakowicz, J. Sójka-Ledakowicz, Z. Mrozińska, and R. Żyła, “Integration of nanofiltration and biological degradation of textile wastewater containing azo dye,” *Chemosphere*, vol. 75, no. 2, pp. 250–255, Apr. 2009.
- [46] Ö. Çınar, S. Yaşar, M. Kertmen, K. Demiröz, N. Ö. Yigit, and M. Kitis, “Effect of cycle time on biodegradation of azo dye in sequencing batch reactor,” *Process Saf. Environ. Prot.*, vol. 86, no. 6, pp. 455–460, Nov. 2008.
- [47] H. Lade, A. Kadam, D. Paul, and S. Govindwar, “Biodegradation and detoxification of textile azo dyes by bacterial consortium under sequential microaerophilic/aerobic processes,” *EXCLI J.*, vol. 14, pp. 158–74, 2015.
- [48] L. Berthier and G. Biroli, “Theoretical perspective on the glass transition and amorphous materials,” *Rev. Mod. Phys.*, vol. 83, no. 2, pp. 587–645, 2011.
- [49] C. Suryanarayana and A. Inoue, “Iron-based bulk metallic glasses,” *Int. Mater. Rev.*, vol. 58, no. 3, pp. 131–166, 2012.
- [50] D. B. Miracle, “A structural model for metallic glasses,” *Microsc. Microanal.*, vol. 10, no. SUPPL. 2, pp. 786–787, 2004.
- [51] W. H. Wang, C. Dong, and C. H. Shek, “Bulk metallic glasses,” *Mater. Sci. Eng. R Reports*, vol. 44, no. 2–3, pp. 45–89, Jun. 2004.
- [52] A. L. Greer, “Metallic glasses,” *Science*, vol. 267, no. 5206, pp. 1947–53, Mar. 1995.
- [53] A. Inoue, “Stabilization of metallic supercooled liquid and bulk amorphous alloys,” *Acta Mater.*, vol. 48, no. 1, pp. 279–306, Jan. 2000.
- [54] H. S. Chen and C. E. Miller, “A Rapid Quenching Technique for the Preparation of Thin Uniform Films of Amorphous Solids,” *Rev. Sci. Instrum.*, vol. 41, no. 8, pp. 1237–1238, Aug. 1970.
- [55] H. W. Kui, A. L. Greer, and D. Turnbull, “Formation of bulk metallic glass by fluxing,” *Appl. Phys. Lett.*, vol. 45, no. 6, pp. 615–616, Sep. 1984.
- [56] J. Yu, Y. Ding, C. Xu, A. Inoue, T. Sakurai, and M. Chen, “Nanoporous Metals by Dealloying Multicomponent Metallic Glasses,” *Chem. Mater.*, vol. 20, no. 14, pp. 4548–4550, Jul. 2008.
- [57] R. . Schwarz, R. . Petrich, and C. . Saw, “The synthesis of amorphous Ni Ti alloy powders by mechanical alloying,” *J. Non. Cryst. Solids*, vol. 76, no. 2–3, pp. 281–

- 302, Dec. 1985.
- [58] H. Schröder, K. Samwer, and U. Köster, "Micromechanism for Metallic-Glass Formation by Solid-State Reactions," *Phys. Rev. Lett.*, vol. 54, no. 3, pp. 197–200, Jan. 1985.
- [59] R. E. Somekh, Z. H. Barber, C. S. Baxter, P. E. Donovan, and J. E. Evetts, "Low temperature diffusion measurements on d.c. sputtered multilayers of Nb/Ta," *J. Mater. Sci. Lett.*, vol. 3, no. 3, pp. 217–220, 1984.
- [60] A. Inoue, T. Zhang, and T. Masumoto, "Al–La–Ni Amorphous Alloys with a Wide Supercooled Liquid Region," *Mater. Trans. JIM*, vol. 30, no. 12, pp. 965–972, 1989.
- [61] A. Inoue, Y. Shinohara, and J. S. Gook, "Thermal and Magnetic Properties of Bulk Fe-Based Glassy Alloys Prepared by Copper Mold Casting," *Mater. Trans. JIM*, vol. 36, no. 12, pp. 1427–1433, 2014.
- [62] C. Q. Zhang, Z. W. Zhu, H. F. Zhang, and Z. Q. Hu, "Rapid reductive degradation of azo dyes by a unique structure of amorphous alloys," *Chinese Sci. Bull.*, vol. 56, no. 36, pp. 3988–3992, 2011.
- [63] J. Cao, L. Wei, Q. Huang, L. Wang, and S. Han, "Reducing degradation of azo dye by zero-valent iron in aqueous solution," *Chemosphere*, vol. 38, no. 3, pp. 565–571, Feb. 1999.
- [64] Wei-xian Zhang, "Nanoscale iron particles for environmental remediation: An overview," *J. Nanoparticle Res.*, vol. 5, pp. 323–332, 2003.
- [65] K. Petcharoen and A. Sirivat, "Synthesis and characterization of magnetite nanoparticles via the chemical co-precipitation method," *Mater. Sci. Eng. B*, vol. 177, no. 5, pp. 421–427, Mar. 2012.
- [66] C. P. Devatha, A. K. Thalla, and S. Y. Katte, "Green synthesis of iron nanoparticles using different leaf extracts for treatment of domestic waste water," *J. Clean. Prod.*, vol. 139, pp. 1425–1435, Dec. 2016.
- [67] J.-Q. Wang et al., "Rapid Degradation of Azo Dye by Fe-Based Metallic Glass Powder," *Adv. Funct. Mater.*, vol. 22, no. 12, pp. 2567–2570, Jun. 2012.
- [68] K. Sarayu and S. Sandhya, "Current Technologies for Biological Treatment of Textile Wastewater—A Review," *Appl. Biochem. Biotechnol.*, vol. 167, no. 3, pp. 645–661, Jun. 2012.
- [69] N. Rahman, Z. Abedin, and M. A. Hossain, "Rapid degradation of azo dyes using nano-scale zero valent iron," *Am. J. Environ. Sci.*, vol. 10, no. 2, pp. 157–163, 2014.
- [70] Jiyun Feng, * and Xijun Hu, P. L. Yue, H. Y. Z. and, and G. Q. Lu, "Degradation of Azo-dye Orange II by a Photoassisted Fenton Reaction Using a Novel Composite of Iron Oxide and Silicate Nanoparticles as a Catalyst," 2003.
- [71] A. R. Rahmani, M. Zarrabi, M. R. Samarghandi, A. Afkhami, and H. R. Ghaffari, "Degradation of Azo Dye Reactive Black 5 and Acid Orange 7 by Fenton-Like Mechanism," *Iran. J. Chem. Eng.*, vol. 7, no. 1, pp. 87–94, 2010.
- [72] J. Sun, X. Wang, J. Sun, R. Sun, S. Sun, and L. Qiao, "Photocatalytic degradation and kinetics of Orange G using nano-sized Sn(IV)/TiO₂/AC photocatalyst," *J. Mol. Catal. A Chem.*, vol. 260, no. 1–2, pp. 241–246, Dec. 2006.
- [73] C. (Universidad de S. de C. Lopez Díaz, "Departamento de Ingeniería Química Oxidación del tinte azo Orange II mediante MnP en reactores enzimáticos operados en continuo," 2005.
- [74] Z. Zhao, J. Liu, C. Tai, Q. Zhou, J. Hu, and G. Jiang, "Rapid decolorization of water soluble azo-dyes by nanosized zero-valent iron immobilized on the exchange resin," *Sci. China, Ser. B Chem.*, vol. 51, no. 2, pp. 186–192, 2008.

- [75] M. Hou, F. Li, X. Liu, X. Wang, and H. Wan, "The effect of substituent groups on the reductive degradation of azo dyes by zerovalent iron," *J. Hazard. Mater.*, vol. 145, no. 1–2, pp. 305–314, Jun. 2007.
- [76] S. C. D. Sharma et al., "Decolorization of azo dye methyl red by suspended and co-immobilized bacterial cells with mediators anthraquinone-2,6-disulfonate and Fe₃O₄ nanoparticles," *Int. Biodeterior. Biodegradation*, vol. 112, pp. 88–97, Aug. 2016.
- [77] K. Santhi, P. Manikandan, C. Rani, and S. Karuppuchamy, "Synthesis of nanocrystalline titanium dioxide for photodegradation treatment of remazol brown dye," *Appl. Nanosci.*, vol. 5, no. 3, pp. 373–378, Mar. 2015.
- [78] M. Darwish, A. Mohammadi, and N. Assi, "Microwave-assisted polyol synthesis and characterization of pvp-capped cds nanoparticles for the photocatalytic degradation of tartrazine," *Mater. Res. Bull.*, vol. 74, pp. 387–396, Feb. 2016.
- [79] P. Sathishkumar, N. Pugazhenthiran, R. V. Mangalaraja, A. M. Asiri, and S. Anandan, "ZnO supported CoFe₂O₄ nanophotocatalysts for the mineralization of Direct Blue 71 in aqueous environments," *J. Hazard. Mater.*, vol. 252–253, pp. 171–179, May 2013.
- [80] Q. Cao et al., "Gold nanoparticles decorated Ag(Cl,Br) micro-necklaces for efficient and stable SERS detection and visible-light photocatalytic degradation of Sudan I," *Appl. Catal. B Environ.*, vol. 201, pp. 607–616, Feb. 2017.
- [81] D. Ljubas, G. Smoljanić, and H. Juretić, "Degradation of Methyl Orange and Congo Red dyes by using TiO₂ nanoparticles activated by the solar and the solar-like radiation," *J. Environ. Manage.*, vol. 161, pp. 83–91, Sep. 2015.
- [82] T. H. Han, M. M. Khan, S. Kalathil, J. Lee, and M. H. Cho, "Simultaneous Enhancement of Methylene Blue Degradation and Power Generation in a Microbial Fuel Cell by Gold Nanoparticles," *Ind. Eng. Chem. Res.*, vol. 52, no. 24, pp. 8174–8181, Jun. 2013.
- [83] G. Ghodake, U. Jadhav, D. Tamboli, A. Kagalkar, and S. Govindwar, "Decolorization of Textile Dyes and Degradation of Mono-Azo Dye Amaranth by *Acinetobacter calcoaceticus* NCIM 2890," *Indian J. Microbiol.*, vol. 51, no. 4, pp. 501–8, Oct. 2011.
- [84] M. AboliGhasemabadi et al., "Application of mechanically alloyed MnAl particles to de-colorization of azo dyes," *J. Alloys Compd.*, vol. 741, pp. 240–245, Apr. 2018.
- [85] A. Chaturvedi, R. Yaqub, and I. Baker, "Microstructure and Magnetic Properties of Bulk Nanocrystalline MnAl," vol. 4, pp. 20–27, 2014.
- [86] H.-Y. Shu, M.-C. Chang, H.-H. Yu, and W.-H. Chen, "Reduction of an azo dye Acid Black 24 solution using synthesized nanoscale zerovalent iron particles," *J. Colloid Interface Sci.*, vol. 314, no. 1, pp. 89–97, Oct. 2007.
- [87] Y. Mu, H.-Q. Yu, S.-J. Zhang, and J.-C. Zheng, "Kinetics of reductive degradation of Orange II in aqueous solution by zero-valent iron," *J. Chem. Technol. Biotechnol.*, vol. 79, no. 12, pp. 1429–1431, Dec. 2004.
- [88] N. Ezzatahmedi et al., "Catalytic degradation of Orange II in aqueous solution using diatomite-supported bimetallic Fe/Ni nanoparticles," *RSC Adv.*, vol. 8, no. 14, pp. 7687–7696, 2018.
- [89] X. Qin et al., "Mechanism and kinetics of treatment of acid orange II by aged Fe-Si-B metallic glass powders," *J. Mater. Sci. Technol.*, vol. 33, no. 10, pp. 1147–1152, Oct. 2017.
- [90] H. Sarvari, E. K. Goharshadi, S. Samiee, and N. Ashraf, "Removal of Methyl Orange from Aqueous Solutions by Ferromagnetic Fe/Ni Nanoparticles," *Phys.*

- Chem. Res., vol. 6, no. 2, pp. 433–446, Jun. 2018.
- [91] F. S. Freyria, S. Esposito, M. Armandi, F. Deorsola, E. Garrone, and B. Bonelli, “Role of pH in the aqueous phase reactivity of zerovalent iron nanoparticles with acid orange 7, a model molecule of azo dyes,” *J. Nanomater.*, vol. 2017, 2017.
- [92] O. Casabella I Font, “Decoloració del tint tèxtil Orange II mitjançant materials metàl·lics amb alta superfície específica,” Jul. 2017.
- [93] H. Roca Bisbe, “Decoloració de tints tèxtils mitjançant partícules metàl·liques de manganès - alumini,” Sep. 2017.
- [94] J. Fan, Y. Guo, J. Wang, and M. Fan, “Rapid decolorization of azo dye methyl orange in aqueous solution by nanoscale zerovalent iron particles,” *J. Hazard. Mater.*, vol. 166, no. 2–3, pp. 904–910, Jul. 2009.
- [95] W. Feng, D. Nansheng, and H. Helin, “Degradation mechanism of azo dye C. I. reactive red 2 by iron powder reduction and photooxidation in aqueous solutions,” *Chemosphere*, vol. 41, no. 8, pp. 1233–1238, Oct. 2000.
- [96] W. S. Pereira and R. S. Freire, “Azo dye degradation by recycled waste zero-valent iron powder,” *J. Braz. Chem. Soc.*, vol. 17, no. 5, pp. 832–838, 2006.
- [97] J. Q. Wang, Y. H. Liu, M. W. Chen, V. L. L. Dmitri, A. Inoue, and J. H. Perepezko, “Excellent capability in degrading azo dyes by MgZn-based metallic glass powders,” *Sci. Rep.*, vol. 2, pp. 1–6, 2012.
- [98] C. Zhang, Z. Zhu, H. Zhang, and Z. Hu, “On the decolorization property of Fe–Mo–Si–B alloys with different structures,” *J. Non. Cryst. Solids*, vol. 358, no. 1, pp. 61–64, Jan. 2012.
- [99] C. Zhang, Z. Zhu, H. Zhang, and Z. Hu, “Rapid decolorization of Acid Orange II aqueous solution by amorphous zero-valent iron,” *J. Environ. Sci.*, vol. 24, no. 6, pp. 1021–1026, Jun. 2012.
- [100] S. Nam and P. G. Tratnyek, “Reduction of azo dyes with zero-valent iron,” *Water Res.*, vol. 34, no. 6, pp. 1837–1845, Apr. 2000.
- [101] A. M. Wang et al., “Ultrafast degradation of azo dyes catalyzed by cobalt-based metallic glass,” *Sci. Rep.*, vol. 5, no. 1, pp. 1–8, 2015.
- [102] M. Styliadi, D. I. Kondarides, and X. E. Verykios, “Mechanistic and kinetic study of solar-light induced photocatalytic degradation of Acid Orange 7 in aqueous TiO₂ suspensions,” *Int. J. Photoenergy*, vol. 5, no. 2, pp. 59–67, 2003.
- [103] F. Kielar, H. M. Talbot, and K. L. Johnson, “Oxidative Decolorization of Acid Azo Dyes by a Mn Oxide Containing Waste,” vol. 44, no. 3, pp. 1116–1122, 2010.
- [104] C. Li et al., “Fabrication of fine spongy nanoporous Ag-Au alloys with improved catalysis properties,” *Prog. Nat. Sci. Mater. Int.*, vol. 27, no. 6, pp. 658–663, 2017.
- [105] W. Ben Mbarek et al., “Rapid degradation of azo-dye using Mn-Al powders produced by ball-milling,” *RSC Adv.*, vol. 7, no. 21, pp. 12620–12628, 2017.
- [106] A. D. Bokare, R. C. Chikate, C. V. Rode, and K. M. Paknikar, “Iron-nickel bimetallic nanoparticles for reductive degradation of azo dye Orange G in aqueous solution,” *Appl. Catal. B Environ.*, vol. 79, no. 3, pp. 270–278, Mar. 2008.
- [107] S. Xie, P. Huang, J. J. Kruzic, X. Zeng, and H. Qian, “A highly efficient degradation mechanism of methyl orange using Fe-based metallic glass powders,” *Sci. Rep.*, vol. 6, no. December 2015, pp. 1–10, 2016.
- [108] a Khani, M. R. Sohrabi, M. Khosravi, and M. Davallo, “Decolorization of an Azo Dye from Aqueous Solution by Nano Zero-Valent Iron Immobilized on Perlite in Semi Batch Packed Bed Reactor,” *Fresenius Environ. Bull.*, vol. 21, no. 8A, pp. 2153–2159, 2012.
- [109] T. Bigg and S. J. Judd, “Kinetics of Reductive Degradation of Azo Dye by Zero-Valent Iron,” *Process Saf. Environ. Prot.*, vol. 79, no. 5, pp. 297–303, Sep. 2001.

- [110] H. Liu, G. Li, J. Qu, and H. Liu, "Degradation of azo dye Acid Orange 7 in water by Fe⁰/granular activated carbon system in the presence of ultrasound," *J. Hazard. Mater.*, vol. 144, no. 1–2, pp. 180–186, Jun. 2007.
- [111] M. Ghaffari, P. Y. Tan, M. E. Oruc, O. K. Tan, M. S. Tse, and M. Shannon, "Effect of ball milling on the characteristics of nano structure SrFeO₃ powder for photocatalytic degradation of methylene blue under visible light irradiation and its reaction kinetics," *Catal. Today*, vol. 161, no. 1, pp. 70–77, Mar. 2011.
- [112] C. C. Chou and S. S. Que Hee, "Microtox EC₅₀ values for drinking water by-products produced by ozonolysis," *Ecotoxicol. Environ. Saf.*, vol. 23, no. 3, pp. 355–363, Jun. 1992.
- [113] K. R. Beg and S. Ali, "Microtox toxicity assay for the sediment quality assessment of Ganga River," *Am. J. Environ. Sci.*, vol. 4, no. 4, pp. 382–387, 2008.
- [114] A. Franco, I. Hernández Pérez, E. García, R. Medina, M. Valero, and M. Lozano, "Adsorption of Azo-Dye Orange II from Aqueous Solutions Using a Metal-Organic Framework Material: Iron- Benzenetricarboxylate," *Materials (Basel)*, vol. 7, no. 12, pp. 8037–8057, 2014.
- [115] A. A. Atia, A. M. Donia, and W. A. Al-Amrani, "Adsorption/desorption behavior of acid orange 10 on magnetic silica modified with amine groups," *Chem. Eng. J.*, vol. 150, no. 1, pp. 55–62, Jul. 2009.
- [116] X.-R. Xu and X. Li, "Degradation of azo dye orange G in aqueous solution 4 by persulfate with ferrous ion." 2010.
- [117] F. Zhang, X. Chen, F. Wu, and Y. Ji, "High adsorption capability and selectivity of ZnO nanoparticles for dye removal," *Colloids Surfaces A Physicochem. Eng. Asp.*, vol. 509, pp. 474–483, Nov. 2016.
- [118] V. C. Nguyen, M. D. Luu Thi, and T. O. Nguyen, "Reusable Mn-Doped ZnS Magnetic Nanocomposite for Photodegradation of Textile Dyes," *J. Nano Res.*, vol. 33, pp. 72–82, Jun. 2015.
- [119] M. Jekel and T. Reemtsma, *Organic pollutants in the water cycle : properties, occurrence, analysis and environmental relevance of polar compounds*. Wiley-VCH, 2006.
- [120] M. Kornaros and G. Lyberatos, "Biological treatment of wastewaters from a dye manufacturing company using a trickling filter," *J. Hazard. Mater.*, vol. 136, no. 1, pp. 95–102, Aug. 2006.
- [121] A. Kristiono, "Wood Drying Condensate Treatment Using a Bio – Trickling Filter with Bark Chips as a Support Medium," 2009.
- [122] J. Dearden, G. Bresnen, J. C. Dearden, and G. M. Bresnen, "Thermodynamics of Water-octanol and Water-cyclohexane Partitioning of some Aromatic Compounds," *Int. J. Mol. Sci.*, vol. 6, no. 1, pp. 119–129, Jan. 2005.
- [123] C. Zaharia and D. Şuteu, "Textile Organic Dyes – Characteristics , Polluting Effects and Separation / Elimination Procedures from Industrial Effluents – A Critical Overview," *Org. Pollut. ten years after Stock. Conv. - Environ. Anal. Updat.*, pp. 55–86, 2010.
- [124] A. Pandey, P. Singh, and L. Iyengar, "Bacterial decolorization and degradation of azo dyes," *Int. Biodeterior. Biodegradation*, vol. 59, no. 2, pp. 73–84, Mar. 2007.
- [125] R. G. Saratale, G. D. Saratale, J. S. Chang, and S. P. Govindwar, "Bacterial decolorization and degradation of azo dyes: A review," *J. Taiwan Inst. Chem. Eng.*, vol. 42, no. 1, pp. 138–157, Jan. 2011.
- [126] R. G. Saratale, G. D. Saratale, J. S. Chang, and S. P. Govindwar, "Bacterial decolorization and degradation of azo dyes: A review," *J. Taiwan Inst. Chem. Eng.*, vol. 42, no. 1, pp. 138–157, 2011.

- [127] M. Ghaemi, G. Absalan, and L. Sheikhian, "Adsorption characteristics of Titan yellow and Congo red on CoFe₂O₄ magnetic nanoparticles," *J. Iran. Chem. Soc.*, vol. 11, no. 6, pp. 1759–1766, Dec. 2014.
- [128] L. Yosefi, M. Haghighi, and S. Allahyari, "Solvothermal synthesis of flowerlike p-BiOI/n-ZnFe₂O₄ with enhanced visible light driven nanophotocatalyst used in removal of acid orange 7 from wastewater," *Sep. Purif. Technol.*, vol. 178, pp. 18–28, May 2017.
- [129] X. Li et al., "Preparation of magnetically separable Fe₃O₄/BiOI nanocomposites and its visible photocatalytic activity," *Appl. Surf. Sci.*, vol. 286, pp. 40–46, Dec. 2013.
- [130] L. Lian, L. Guo, and C. Guo, "Adsorption of Congo red from aqueous solutions onto Ca-bentonite," *J. Hazard. Mater.*, vol. 161, no. 1, pp. 126–131, Jan. 2009.
- [131] H. M. Pinheiro, E. Touraud, and O. Thomas, "Aromatic amines from azo dye reduction: status review with emphasis on direct UV spectrophotometric detection in textile industry wastewaters," *Dye. Pigment.*, vol. 61, no. 2, pp. 121–139, May 2004.
- [132] P. Wang et al., "Fast decolorization of azo dyes in both alkaline and acidic solutions by Al-based metallic glasses," *J. Alloys Compd.*, vol. 701, pp. 759–767, Apr. 2017.

Additional bibliography

- [1] S. Larouk et al., "Catalytic ozonation of Orange-G through highly interactive contributions of hematite and SBA-16 – To better understand azo-dye oxidation in nature," *Chemosphere*, vol. 168, pp. 1648–1657, 2017.
- [2] H. Lee and M. Shoda, "Removal of COD and colour from livestock wastewater by the Fenton method," *J. Hazard. Mater.*, vol. 153, no. 3, pp. 1314–1319, 2008.
- [3] O. Türgay, G. Ersöz, S. Atalay, J. Forss, and U. Welander, "The treatment of azo dyes found in textile industry wastewater by anaerobic biological method and chemical oxidation," *Sep. Purif. Technol.*, vol. 79, no. 1, pp. 26–33, 2011.
- [4] S. Yi et al., "Removal of levofloxacin from aqueous solution using rice-husk and wood-chip biochars," *Chemosphere*, vol. 150, pp. 694–701, 2016.
- [5] I. M. Banat, P. Nigam, D. Singh, and R. Marchant, "Microbial decolourization of textile-dye-containing effluents: A review," *Bioresour. Technol.*, vol. 58, no. 3, pp. 217–227, 1996.
- [6] E. Forgacs, T. Cserhádi, and G. Oros, "Removal of synthetic dyes from wastewaters: A review," *Environ. Int.*, vol. 30, no. 7, pp. 953–971, 2004.
- [7] E. Brillas et al., "Decolourization and mineralization of Orange G azo dye solutions by anodic oxidation with a boron-doped diamond anode in divided and undivided tank reactors," *Electrochim. Acta*, vol. 130, pp. 568–576, 2014.
- [8] H. Liu, G. Li, J. Qu, and H. Liu, "Degradation of azo dye Acid Orange 7 in water by Fe₀/granular activated carbon system in the presence of ultrasound," *J. Hazard. Mater.*, vol. 144, no. 1–2, pp. 180–186, Jun. 2007.
- [9] S. Natarajan, H. C. Bajaj, and R. J. Tayade, "Recent advances based on the synergetic effect of adsorption for removal of dyes from waste water using photocatalytic process," *J. Environ. Sci. (China)*, vol. 65, pp. 201–222, 2018.
- [10] A. Loukanov, V. Blaskov, S. Vassilev, M. Shipochka, and I. Stambolova, "Sprayed nanostructured TiO₂ films for efficient photocatalytic degradation of textile azo dye," *J. Photochem. Photobiol. B Biol.*, vol. 117, pp. 19–26, 2012.

- [11] Z. Deng, X. H. Zhang, K. C. Chan, L. Liu, and T. Li, "Fe-based metallic glass catalyst with nanoporous surface for azo dye degradation," *Chemosphere*, vol. 174, pp. 76–81, 2017.
- [12] Y. Zhang, F. Gao, B. Wanjala, Z. Li, G. Cernigliaro, and Z. Gu, "High efficiency reductive degradation of a wide range of azo dyes by SiO₂-Co core-shell nanoparticles," *Appl. Catal. B Environ.*, vol. 199, pp. 504–513, 2016.
- [13] D. Ağaoğulları, Ö. Balcı, and M. L. Öveçoğlu, "Effect of milling type on the microstructural and mechanical properties of W-Ni-ZrC-Y₂O₃ composites," *Ceram. Int.*, vol. 43, no. 9, pp. 7106–7114, 2017.
- [14] P. Blánquez et al., "Mechanism of textile metal dye biotransformation by *Trametes versicolour*," *Water Res.*, vol. 38, no. 8, pp. 2166–2172, 2004.
- [15] Č. Novotný, K. Svobodová, O. Benada, O. Kofroňová, A. Heissenberger, and W. Fuchs, "Potential of combined fungal and bacterial treatment for colour removal in textile wastewater," *Bioresour. Technol.*, vol. 102, no. 2, pp. 879–888, Jan. 2011.
- [16] S. Yang, H. He, C. Sun, J. Zheng, and Z. Gao, "Efficient degradation of Acid Orange 7 in aqueous solution by iron ore tailing Fenton-like process," *Chemosphere*, vol. 150, pp. 40–48, 2016.
- [17] W. Guo, F. Hao, X. Yue, A. Wang, and Y. Leng, "Degradation of Acid Orange 7 in aqueous solution by zero-valent aluminum under ultrasonic irradiation," *Ultrason. Sonochem.*, vol. 21, no. 2, pp. 572–575, 2013.
- [18] G. Boczkaj and A. Fernandes, "Wastewater treatment by means of advanced oxidation processes at basic pH conditions: A review," *Chem. Eng. J.*, vol. 320, pp. 608–633, 2017.
- [19] C. Chompuchan, T. Satapanajaru, P. Suntornchot, and P. Pengthamkeerati, "Decolourization of Reactive Black 5 and Reactive Red 198 using Nanoscale Zerovalent Iron," *World Acad. Sci. Eng. Technol. Int. J. Chem. Mol. Nucl. Mater. Metall. Eng.*, vol. 3, no. 1, pp. 7–11, 2009.
- [20] A. George and B. Stephen Brunauer, "Adsorption of gases in multimolecular layers 300 (Contribution from the Bureau of chemistry and Adsorption of Gases in Multimolecular Layers)," vol. 407, no. 1, pp. 309–319, 1938.
- [21] L. S. Hundal, J. Singh, E. L. Bier, P. J. Shea, S. D. Comfort, and W. L. Powers, "Removal of TNT and RDX from water and soil using iron metal," *Environ. Pollut.*, vol. 97, no. 1–2, pp. 55–64, Jan. 1997.
- [22] H. Park and W. Choi, "Visible light and Fe(III)-mediated degradation of Acid Orange 7 in the absence of H₂O₂," *J. Photochem. Photobiol. A Chem.*, vol. 159, no. 3, pp. 241–247, Jul. 2003.
- [23] R. Patel and S. Suresh, "Decolourization of azo dyes using magnesium–palladium system," *J. Hazard. Mater.*, vol. 137, no. 3, pp. 1729–1741, Oct. 2006.
- [24] N. Supaka, K. Juntongjin, S. Damronglerd, M.-L. Delia, and P. Strehaiano, "Microbial decolourization of reactive azo dyes in a sequential anaerobic–aerobic system," *Chem. Eng. J.*, vol. 99, no. 2, pp. 169–176, Jun. 2004.
- [25] F. P. van der Zee and S. Villaverde, "Combined anaerobic–aerobic treatment of azo dyes—A short review of bioreactor studies," *Water Res.*, vol. 39, no. 8, pp. 1425–1440, Apr. 2005.